Studies in Molecular Recognition:

Self-Assembling Molecular Host-Guest Systems

by

Robert M. Grotzfeld
Diplomchemiker
Universität Hamburg
Germany

submitted to the Department of Chemistry in partial fulfillment of the requirements for the degree of
Doctor of Philosophy

at the
Massachusetts Institute of Technology
June 1996

Signature of Author .....
Department of Chemistry
May 14, 1996

Certified by .....
Professor Julius Rebek, Jr.
Thesis Supervisor

Accepted by .....
Professor Dietmar Seyferth
Chairman, Departmental Committee on Graduate Students

This doctoral thesis has been examined by a Committee of the Department of Chemistry as follows:

Professor Satoru Masamune . .....
Chairman

Professor Julius Rebek, Jr. ....
Thesis Supervisor

Professor Stephen J. Lippard .....

Studies in Molecular Recognition: Self-Assembling Molecular Host-Guest Systems

by

Robert M. Grotzfeld

Submitted to the Department of Chemistry on May 14, 1996 in partial fulfillment of the requirements for the degree of Doctor of Philosophy

Abstract

A series of glycoluril derivatives based on 4,4'-disubstituted benzils and diesters of dihydroxytartaric acid was synthesized with the goal to find a highly soluble building block for self-complementary molecules. The bis-(3-methyl-butyl)-ester glycoluril is the ideal derivative combining both high solubility and a distinctive ^{1}H NMR spectrum. It was successfully used together with a derivative of triphenylene for the construction of a self-complementary molecule. The synthesis of the triphenylene derivative and of the new C_{3v}-symmetric self-complementary bowl-shaped molecule is described. Two of these bowl-shaped molecules can form a dimeric assembly in organic solvents. The dimeric complex is held together by twelve hydrogen bonds and features an internal cavity which is filled by one solvent molecule in the case of CD_2Cl_2, $CDCl_3$, and 1,1,2,2-tetrachloroethane-d_2. The solvent molecule can be displaced by appropriate disc-shaped guest molecules. Encapsulation of benzene in $CDCl_3$ solution is demonstrated indirectly by ^{1}H NMR and directly by ^{13}C NMR experiments. The encapsulation is enthalpy driven by weak interactions of the guest with the interior of the host dimer. Encapsulation of cyclohexane from *p*-xylene-d_{10} solution is evidenced by the appearance of a ^{1}H NMR signal for encapsulated cyclohexane at -0.9 ppm. The exchange rate of guest molecules could be observed in the case of cyclohexane when an equal amount of cyclohexane-d_{12} was added. The decrease of the ^{1}H NMR signal for encapsulated cyclohexane being replaced by cyclohexane-d_{12} gave a half-life for the exchange process at 2.5 h.

The design and synthesis of an attempted functional model system for hemerythrin is described. A cleft-shaped ligand based on xanthene wall units and a biphenyl spacer was synthesized. The ligand features two imidazole nitrogen functions and two carboxy groups which were supposed to bind two μ-oxo-bridged iron ions.

Thesis Supervisor: Dr. Julius Rebek, Jr.
Title: Camille Dreyfus Professor of Chemistry

to

my parents

Acknowledgments

First, I wish to thank my advisor, Professor Julius Rebek, for accepting me into his group, and giving me the freedom to explore and develop as a researcher. His visionary thinking will always be a source of inspiration for me. I am also indebted to him for having given me the opportunity to represent our group at the NATO Advanced Research Workshop on Supramolecular Chemistry in Iceland in 1994.

Furthermore, I wish to thank my former advisor at the Universität Hamburg, Professor Walter Kaminsky, for supporting my application to M.I.T.

The members of the Rebek Group, past and present, are to thank for scientific advice, tips, and tricks, and good times in the lab and outside. Listing everyone's contribution would fill pages, but three brave ones who endured next to me at the fume hood will be mentioned. Neil deserves special credit for initiating me in the self-assembly project, the design of the "Jelly-Doughnut", and for handing over his project to me after his graduation. In Takashi I found a wonderful friend who taught me many things about his native Japan. Tomas introduced many new ideas in the self-assembly field and I regret that there was no time to initiate a collaboration.

I would also like to thank Jean Harrington for lifting many a bureaucratic burden from my shoulder, and Jeanne Owens for helpful hints regarding the NMR.

The crew of 206 Charles Street was fantastic and made "our house" a terrific place to come home to after long hours in the lab.

I am grateful to my parents for their constant love and support.

And above all, I want to thank Eva for making me happy, and forgiving my broken promises and occasional moodiness while I was writing this thesis.

Chapter 5
Towards a More Effective Synthesis of Self-Assembled Systems Based on the Glycoluril Moiety

Chapter 6
A Self-Complementary Monomer Forming a D_{3d}-Symmetric Dimeric Capsule

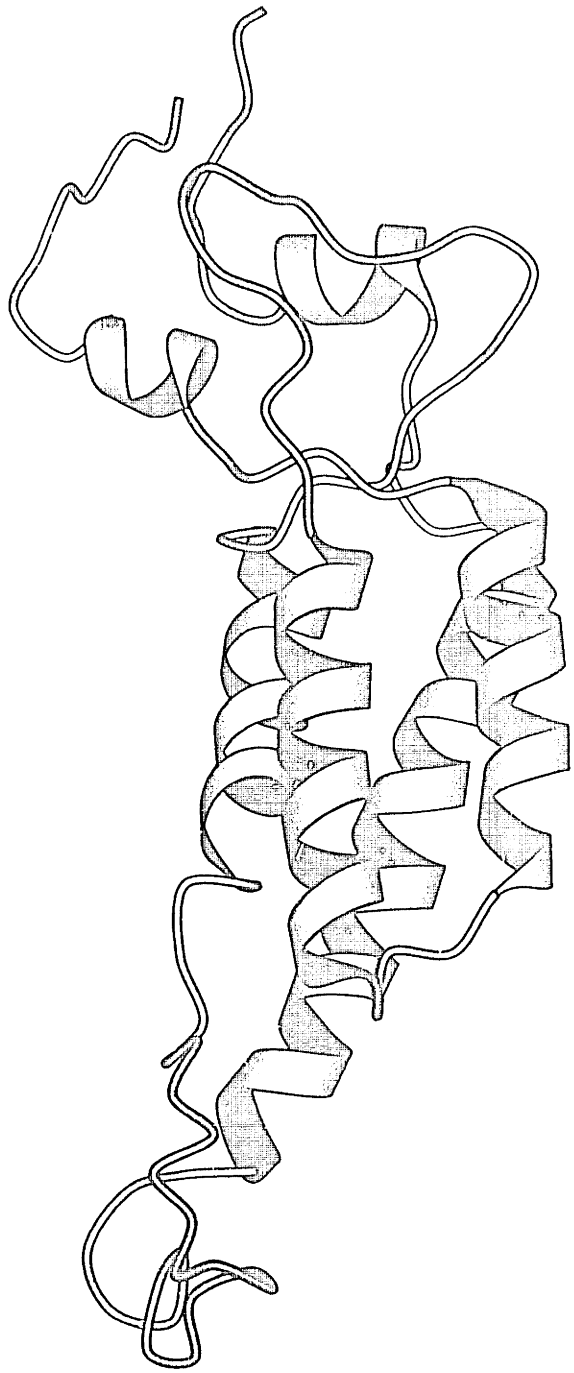

Schematic representation (Molscript[1]) of the tobacco mosaic virus coat protein[2], one of the smallest self-assembling units found in nature.

---

(1) Kraulis, P. J. *J. Appl. Cryst.* **1991**, *24*, 946-950.
(2) Namba, K.; Pattanayek, R.; Stubbs, G. *J. Mol. Biol.* **1989**, *208*, 307-325.

Part I

Three-Dimensional Self-Assembled Structures

The process of individual molecules aggregating into larger ordered structures is a fundamental one to all forms of life[1,2]. The aggregation of phospholipids to form cell membranes and the spontaneous assembly of coat proteins to form a closed shell about viral genetic material are prominent examples for the construction of long-range three-dimensional structures from small subunits[3,4]. Biological machinery in the cells also relies on self-assembled systems; the translation of mRNA into protein in self-assembled ribosomes, oxygen transport in self-assembled hemoglobin, and oxidation of methane to methanol in the multicomponent assembly of bacterial methane monooxygenase are just a few examples[2,3,5,6]. Research in the area of natural and synthetic self-assembling systems has opened up the field of *Supramolecular Chemistry*, i.e. chemistry of molecular assemblies and intermolecular bonds[7-19]. The importance of this emerging interdisciplinary field has been demonstrated by awarding the 1987 Nobel Prize in chemistry to pioneering work in supramolecular chemistry[8,20,21].

Chapter 1

Natural Systems: Viruses[3,4,22-29]

1.1
One-Component Assembly: Tobacco Mosaic Virus

The tobacco mosaic virus (TMV)[30-32] provides a famous illustration for the economical aspects of self-assembly[3,33,34]. Its protein coat contains about 50 times more amino acids than there are nucleotides in the viral RNA. It is therefore impossible to encode a complete viral coat in the RNA, unless the coat is composed of many identical copies of only a few building blocks. By employing over 2000 copies of a coat protein of

158 amino acids, the complete RNA can be encapsulated using only 10% of the genetic information of the viral RNA. Stability of the viral assemblies arises from the formation of the maximum surface contacts by repeated use of the same intermolecular interactions between the self-complementary building blocks. Limitation to one or only very few building blocks imparts geometrical constraints on the entire assembly. As a result, all small viruses (mainly plant viruses) adopt either a cylindrical or spherical shell with helical or icosahedral symmetries, respectively. The current model for the RNA encapsulation process in the case of TMV is shown in figure ***1-1***.

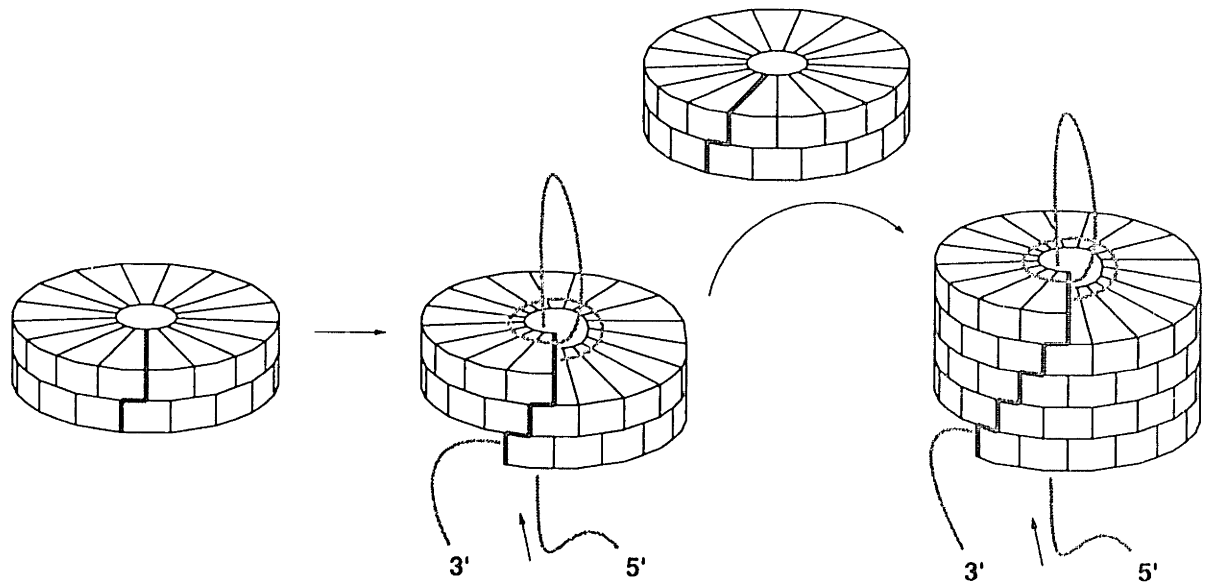

Figure 1-1: Schematic model for the assembly of the tobacco mosaic virus.

The assembly of the coat proteins around the viral RNA begins with spontaneously assembled two-layer discs of 34 subunits[30]. Upon binding the initiation region of the RNA, the protein disc changes into a lock-washer configuration, RNA is embedded in a helical form, and more discs are added on top as the RNA 5' tail is pulled through the central tunnel[35]. Employing pre-formed protein discs for construction of the virus as opposed to adding the coat proteins one by one has two major advantages: **1.** Rapid initiation of the assembly is ensured since adding a rigid ring structure to the flexible RNA provides stability in a single step. Otherwise, the RNA would have to interact with 17 individual subunits before a stable geometry can be formed. **2.** Specificity is enhanced since an assembled disc binds to 102 nucleotides instead of only three in the case of an individual

coat protein. This guarantees that TMV RNA is discriminated from surrounding host mRNA and selectively encapsulated. The reconstitution of an active virus *in vitro* from its inactive protein and RNA components has been demonstrated in a classic experiment[36].

1.2
Multicomponent Assembly: Spherical Viruses

Another geometry that small viruses can adopt is a spherical shape of icosahedral symmetry. As indicated in figure ***1-2a***, an icosahedron can be constructed from 60 strictly equivalent subunits.

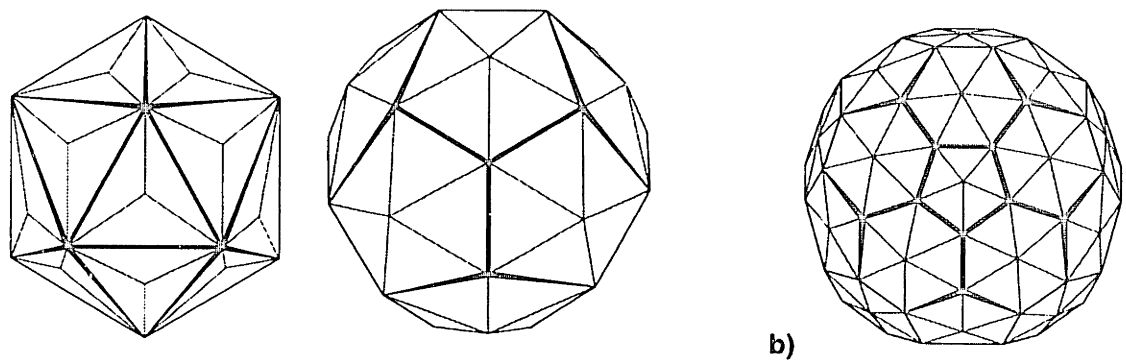

Figure 1-2: Spherical structures of icosahedral symmetry. **a)** An icosahedron built from 60 identical and strictly equivalent subunits. **b)** 180 quasi-equivalent building blocks giving rise to a soccer ball type structure. 60 building blocks each belong to one of the following three groups: **i)** located within a five-membered ring, **ii)** located within a six-membered ring and bordering to a five-membered ring, and **iii)** located within a six-membered ring and bordering to a six-membered ring. The structures are not drawn to scale.

One of the smallest known viruses is the satellite tobacco necrosis virus (STNV) which uses the minimal number of 60 copies of an asymmetric subunit for building its icosahedral shell. The tomato bushy stunt virus (TBSV)[37,38] and the southern bean mosaic virus (SBMV)[39] each use 180 chemically identical subunits to construct their protein shell. The building blocks belong to different groups, depending on their environment in the capsid shell (the protein subunits are arranged similar to the pattern of triangles in the stencil shown in figure ***1-2b***). In order for a capsid protein to be used universally in the three different environments, it has to be able to accommodate slight variations in geometry.

This is achieved by flexible linkages acting as hinges between the domains within the capsid protein[3], "structural diversity has been achieved without sacrificing genetic economy"[4]. Other examples for spherical viruses are the picornaviruses, e.g. the common cold virus human rhinovirus 14[40,41] and the poliovirus[42,43]. Both have a capsid containing 60 copies each of four proteins. Since these viruses rely on eucaryotic hosts, the viral genes are expressed as a single large polyprotein. Sequential cleavage of this protein generates the coat proteins[44]. Table ***1-1*** shows a comparison between the viruses discussed above.

Virus	*Length*	*Outer Ø*	*Subunits*	*Copies*	*aa/subunit*
TMV	3000 Å	180 Å	1	2130	158
STNV	n/a	190 Å	1	60	195
TBSV	n/a	350 Å	1	180	386
SBMV	n/a	350 Å	1	180	260
PV	n/a	300 Å	3+1	60 each	306, 272, 238
HRV14	n/a	300 Å	3+1	60 each	289, 262, 236

Table 1-1: Comparison of some viral capsids. TMV = Tobacco Mosaic Virus; STNV = Satellite Tobacco Necrosis Virus; TBSV = Tomato Bushy Stunt Virus; SBMV = Southern Bean Mosaic Virus; PV= Poliovirus; HRV14 = Human Rhinovirus 14, the common cold virus. In the case of PV and HRV14, 60 copies each of three proteins form the outer capsid surface (the fourth protein is located beneath the surface). Only the amino acid count of the surface proteins is given.

1.3
Implications for Artificial Self-Assembling Systems

From the study of biological systems, especially protein denaturation and viral capsid disassembly and reconstitution into the original superstructures, it became clear that self assembly processes have advantages over single-molecule syntheses[2,45]:

- *Information*: The genetic information required is drastically reduced if only one or a few repeating building blocks are used for the formation of a large structure.

- *Control*: Different states of assembly are allowed if the building blocks are associated by merely weak bonds. This also allows for facilitated release of material contained within the assembly since only weak bonds have to be broken.
- *Error-Checking*: The information for building the superstructure is inscribed in the periphery of the building blocks. In the case of reversible assembly processes, defective building blocks are excluded from the assembly since they cannot compete with the proper building blocks in the formation of the best arrangement of bonds.
- *Efficiency*: Direct piece-by-piece construction of a large structure can never be as effective as a self-assembly process, which corresponds to a convergent synthesis with self-purifying intermediates. Cooperative effects can be utilized in self-assembly situations, so that the formation of several bonds actually becomes easier than formation of only one bond.

Following these principles, a variety of artificial systems have been prepared, some of which are shown to spontaneously self-assemble and form three-dimensional aggregates with defined geometries in solution.

1.4
References

(1) Alberts, B.; Bray, D.; Lewis, J.; Raff, M.; Roberts, K.; Watson, J. D. *Molecular Biology of the Cell;* 3rd ed.; Garland Publishers: New York, NY, 1994.

(2) Watson, J. D.; Hopkins, N. H.; Roberts, J. W.; Steitz, J. A.; Weiner, A. M. *Molecular Biology of the Gene*; Benjamin/Cummings: Menlo Park, CA, 1988.

(3) Stryer, L. *Biochemistry;* 3rd. ed.; Freeman: New York, NY, 1988.

(4) Branden, C.; Tooze, J. *Introduction to Protein Structure*; Garland Publishers: New York, NY, 1991.

(5) Nomura, M. *Science* **1973**, *179*, 864-873.

(6) Lippard, S.; Berg, J. *Principles of Bioinorganic Chemistry*; University Science Books: Mill Valley, CA, 1994.

(7) Lehn, J.-M. *Science* **1985**, *227*, 849-856.

(8) Lehn, J.-M. *Angew. Chem. Int. Ed. Engl.* **1988**, *27*, 89-112.

(9) Rebek, J., Jr. *Angew. Chem. Int. Ed. Engl.* **1990**, *29*, 245-255.

(10) Lehn, J.-M. *Angew. Chem. Int. Ed. Engl.* **1990**, *29*, 1304-1319.

(11) *Frontiers in Supramolecular Organic Chemistry and Photochemistry*; Schneider, H.-J.; Dürr, H., Ed.; VCH Publishers: Weinheim, 1991.

(12) Schneider, H.-J. *Angew. Chem. Int. Ed. Engl.* **1991**, *30*, 1417-1436.

(13) Whitesides, G. M.; Mathias, J. P.; Seto, C. T. *Science* **1991**, *254*, 1312-1319.

(14) Vögtle, F. *Supramolecular Chemistry. An Introduction*; John Wiley & Sons: Chichester, 1991.

(15) Lehn, J.-M. *Science* **1993**, *260*, 1752-1763.

(16) *Top. Curr. Chem.* **1993**, *165*

(17) *Top. Curr. Chem.* **1995**, *175*

(18) Lehn, J.-M. *Supramolecular Chemistry. Concepts and Perspectives*; VCH Publishers: Weinheim, 1995.

(19) Lawrence, D. S.; Jiang, T.; Levett, M. *Chem. Rev.* **1995**, *95*, 2229-2260.

(20) Cram, D. J. *Angew. Chem. Int. Ed. Engl.* **1988**, *27*, 1009-1020.

(21) Pedersen, C. J. *Angew. Chem. Int. Ed. Engl.* **1988**, *27*, 1021-1027.

(22) Caspar, D. L. D.; Klug, A. *Cold Spring Harbor Symp. Quant. Biol.* **1962**, *27*, 1-24.

(23) Harrison, S. C. *Trends Biochem. Sci.* **1984**, *9*, 345-351.

(24) *Biological Macromolecules and Assemblies. Volume 1: Virus Structures*; Jurnak, F. A.; McPherson, A., Ed.; John Wiley & Sons: New York, NY, 1984.

(25) Kihara, T. *Acta Cryst.* **1985**, *A41*, 556-559.

(26) Baltimore, D. *Science* **1985**, *229*, 1366-1367.

(27) Rossmann, M. G.; Johnson, J. E. *Annu. Rev. Biochem.* **1989**, *58*, 533-573.

(28) Harrison, S. C. In *Virology*; 2nd ed.; B. N. Fields, Ed.; Raven Press: New York, 1990; Vol. 1; pp 37-61.

(29) Zlotnik, A. *J. Mol. Biol.* **1994**, *241*, 59-67.

(30) Bloomer, A. C.; Champness, J. N.; Bricogne, G.; Staden, R.; Klug, A. *Nature* **1978**, *276*, 362-368.

(31) Namba, K.; Pattanayek, R.; Stubbs, G. *J. Mol. Biol.* **1989**, *208*, 307-325.

(32) Pattanayek, R.; Stubbes, G. *J. Mol. Biol.* **1992**, *228*, 516-528.

(33) Namba, K.; Caspar, D. L. D.; Stubbs, G. J. *Science* **1985**, *227*, 773-776.

(34) Klug, A. *Angew. Chem. Int. Ed. Engl.* **1983**, *22*, 565-582.

(35) Lebeurier, G.; Nicolaieff, A.; Richards, K. E. *Proc. Natl. Acad. Sci. USA* **1977**, *74*, 149-153.

(36) Fraenkel-Conrat, H.; Williams, R. C. *Proc. Natl. Acad. Sci. USA* **1955**, *41*, 690-698.

(37) Harrison, S. C.; A.J., O.; Schutt, C. E.; Winkler, F. K.; Bricogne, G. *Nature* **1978**, *276*, 368-373.

(38) Olson, A. J.; Bricogne, G.; Harrison, S. C. *J. Mol. Biol.* **1983**, *171*, 61-93.

(39) Abad-Zapatero, C.; Abdel-Meguid, S. S.; Johnson, J. E.; Leslie, A. G. W.; Rayment, I.; Rossmann, M. G.; Suck, D.; Tsukihara, T. *Nature* **1980**, *286*, 33-39.

(40) Rossmann, M. G.; Arnold, E.; Erickson, J. W.; Frankenberger, E. A.; Griffith, J. P.; Hecht, H.-J.; Johnson, J. E.; Kamer, G.; Luo, M.; Mosser, A. G.; Rueckert, R. R.; Sherry, B.; Vriend, G. *Nature* **1985**, *317*, 145-153.

(41) Rossmann, M. G.; Arnold, E.; Griffith, J. E.; Kamer, G.; Luo, M.; Smith, T. J.; Vriend, G.; Rueckert, R. R.; Sherry, B.; McKinlay, M. A.; Diana, G.; Otto, M. *Trends Biochem. Sci.* **1987**, *12*, 131-318.

(42) Hogle, J. M.; Chow, M.; Filman, D. J. *Science* **1985**, *229*, 1358-1365.

(43) Hogle, J. M.; Chow, M.; Filman, D. J. *Sci. Am.* **1987**, 42-48.

(44) Arnold, E.; Luo, M.; Vriend, G.; Rossmann, M. G.; Palmenberg, A. C.; Parks, G. D.; Nicklin, M. J. H.; Wimmer, E. *Proc. Natl. Acad. Sci. USA* **1987**, *84*, 21-25.

(45) Lindsey, J. S. *New J. Chem.* **1991**, *15*, 153-181.

Chapter 2

Artificial Systems: Three-Dimensional Molecular Aggregates in Solution

Various ways can be imagined to achieve attractive interactions between the subunits of a molecular assembly. For self-assembly coupled with molecular recognition[1-4], the use of hydrogen bonding or metal coordination has proven to be very effective[5].

2.1
Self-Assembly via Metal Coordination

Metal coordination as the driving force for self-assembly has been widely used to generate supramolecular structures. A variety of macrocyclic systems has been prepared in this way, some of which can act as host compounds and will be discussed below. A particularly intriguing family of three-dimensional cavities assembled via metal coordination has been introduced by Lehn et al.[6,7].

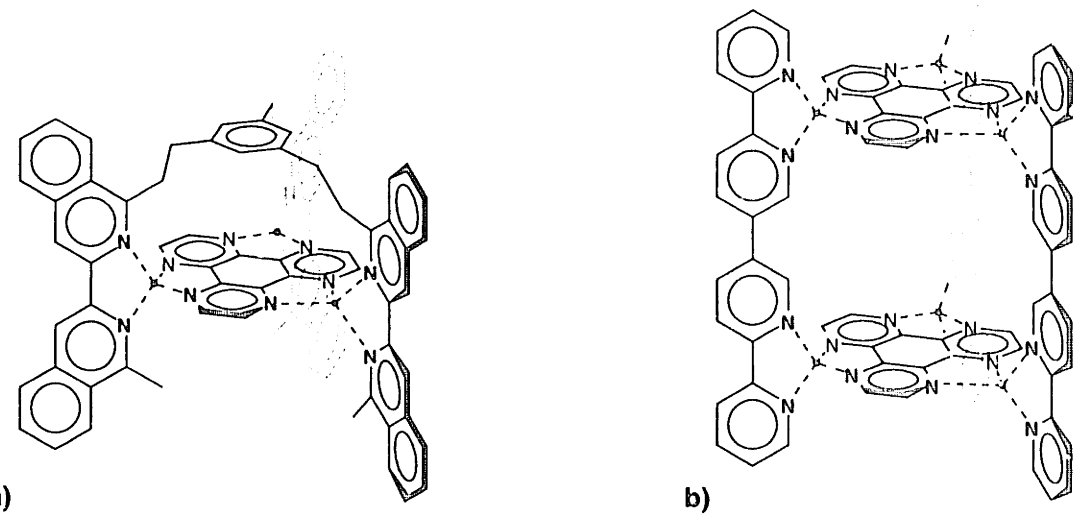

a) b)

Figure 2-1: Three-dimensional structures assembled through metal coordination, M=Cu^+. **a)** 1:1 complex linked by three metal ions[6], **b)** 3:2 complex linked by six metal ions[7].

The complexes form spontaneously upon addition of $[Cu^I(CH_3CN)_4]BF_4$ to a solution of the organic ligands. In the case of the "double-decker" complex in figure ***2-1b***, a cylindrical internal cavity is formed with a height of 4 Å and an approximate diameter of 8 Å, taking the van der Waals radii into account. However, no substrate binding experiments have been reported.

2.2
Self-Assembly via Hydrogen Bonds

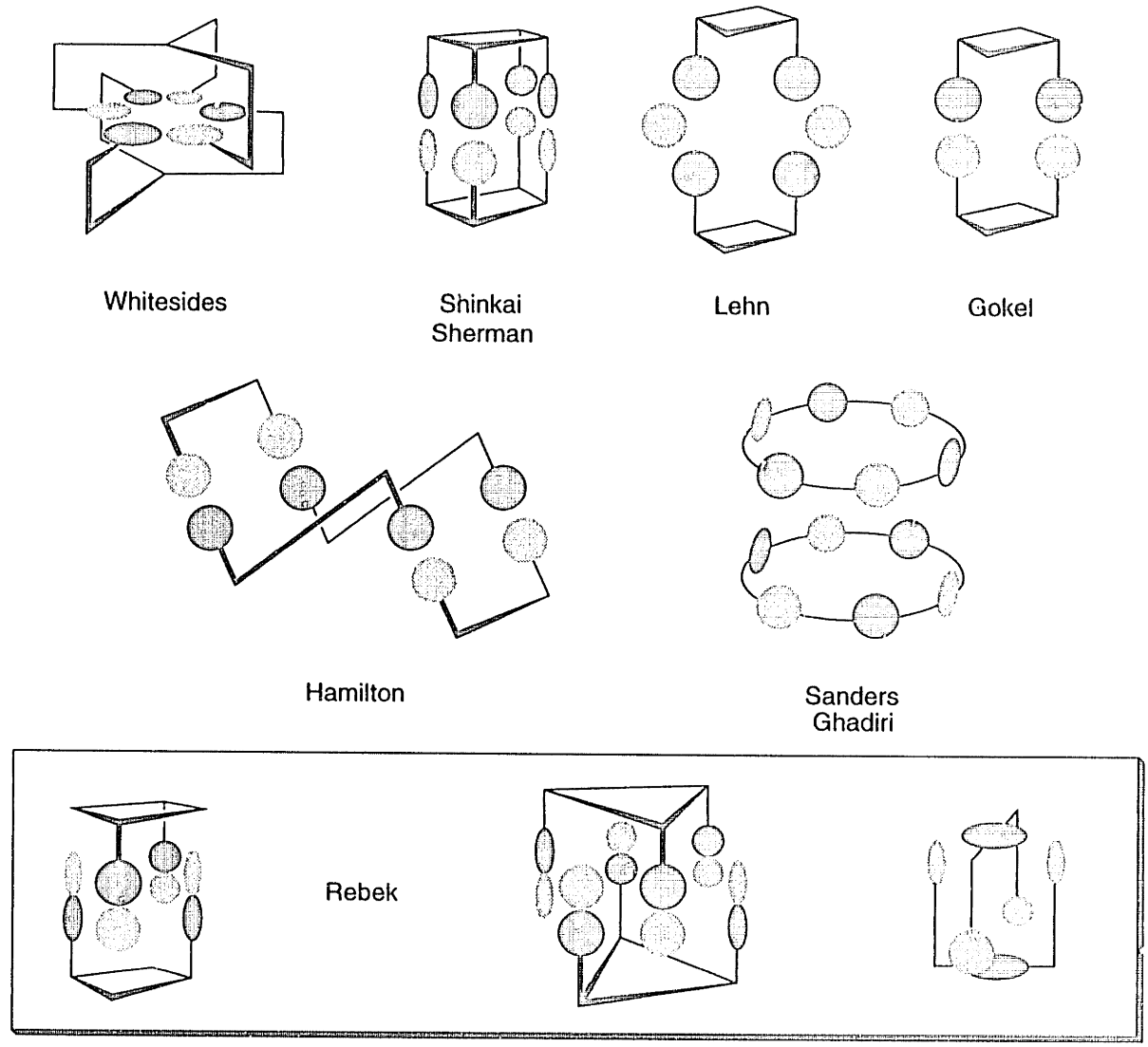

Figure 2-2: Geometries of three-dimensional self-assemblies that have been explored by the research groups indicated. The gray and black structure elements represent the mutually recognizing counterparts (molecular recognition moieties). The stencils are not drawn to scale.

The design of building blocks for self-assembly via hydrogen bonds has to combine donor and acceptor sites with appropriate scaffolds. Assemblies resulting in three-dimensional structures require a certain degree of curvature within the building blocks.

Various geometries for three-dimensional aggregates can be envisioned, some which are represented in figure ***2-2***.

The following overview will first highlight aspects of assemblies in solution with special focus on the hydrogen bonding interactions. The second part of the introduction will discuss hydrogen bonded and metal-coordinated assemblies which can act as hosts for smaller guests, with special attention on the host-guest characteristics.

The first example for a self-assembling host system dates back to 1987 and was synthesized in the research group of G. Gokel[8]. Mimicking the binding between the two strands of DNA, adenine and thymine groups were used for hydrogen bonding in the synthetic system (figure ***2-3***). Two differently functionalized diaza-18-crown-6 scaffolds, one with thymine sidearms, the other one with adenine sidearms, form four hydrogen bonds upon assembly of the "molecular box".

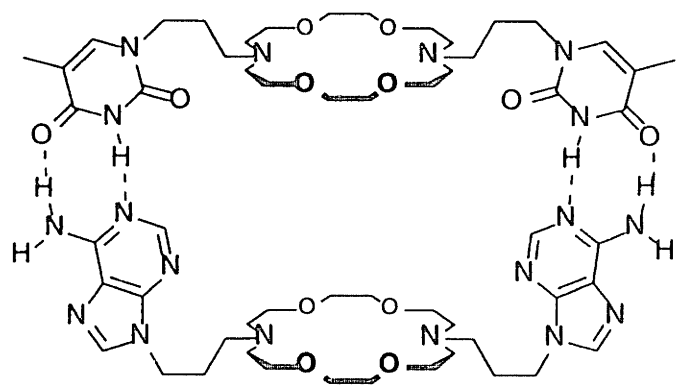

Figure 2-3: Hydrogen bonds between thymine and adenine contribute to the stability of the first self-assembled host system[8].

Vapor phase osmometry indicates that the system forms a labile assembly (K_a = 2 M^{-1}) in water. The association can be favored by adding appropriate cationic guests which can from additional hydrogen bonds to the crown ethers. Stabilization of the assembly is achieved by addition of $[H_3N–(CH_2)_{12}–NH_3]Cl_2$, where the dication can from a hydrogen bonded tether across the molecular box between the two crown ethers. In chloroform, which in contrast to water does not compete in the hydrogen bonding, a much higher degree of association is observed (K_a = 860 M^{-1}). Several different equilibria exist in

solution, including Hoogsteen-type bonding and intramolecular interactions between bases linked to the same crown ether scaffold[9].

The interaction between carboxylic acids and 2-acylaminopyridines has been exploited for the assembly of multicomponent systems by Hamilton et al. Two carboxyl groups on a biphenylene spacer represent a C-shaped component. The other component contains two acylaminopyridine moieties in an overall S-shaped geometry (figure *2-4*).

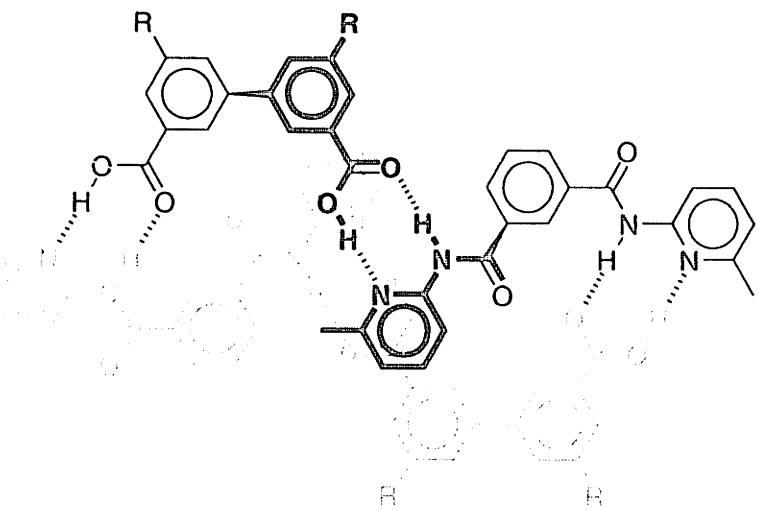

Figure 2-4: Tetrameric C_2S_2 assembly of two C-shaped and S-shaped components each.

A labile tetrameric complex is formed in methylene chloride and chloroform as evidenced by gel permeation chromatography, vapor phase osmometry, and ^1H NMR spectroscopy. The figure-of-eight shaped assembly is observed in the solid state, the N–O distances in the eight hydrogen bonds ranging between 2.7 and 2.9 Å. Encapsulation of guest molecules within the assembly is prohibited due to the short stacking distance of 3.5 Å, i.e. the space is filled.

Porphyrins have been used as rigid spacers for a self-assembling system introduced by Lehn et al.[10] The acceptor–donor–acceptor hydrogen bonding motif on the uracil substituents finds its complementary motif in the trimethylpyrimidine units, two of which serve as chain links between the two larger subunits.

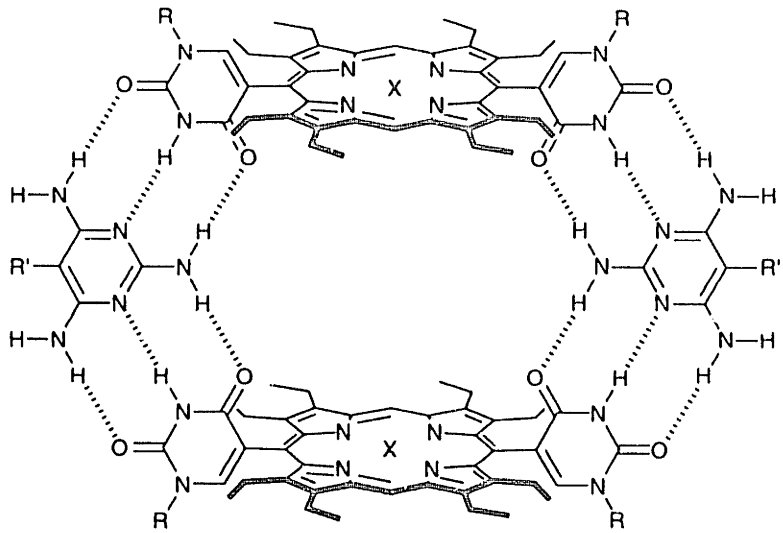

Figure 2-5: Tetrameric assembly of *syn*-bis(uracil) components and trimethylpyrimidine units.

Formation of a 2+2 tetrameric open-sided cage-like complex is observed in organic solvents. It acts as a host for 4,4'-bipyridine: The assembly with M = Zn^{II} coordinates 4,4'-bipyridine stronger than Zn^{II}-porphyrin alone, which indicates a cooperative effect of the appropriately spaced porphyrin rings in the assembled host.

The same triangular donor-acceptor pattern as in the previous example is found in the building blocks used by Whitesides et al[11-18]. Through appropriate functionalization of cyanuric acid and melamine, one of the hydrogen bonding edges in each subunit is blocked, so that assembly can only occur in a circular or zig-zag fashion.

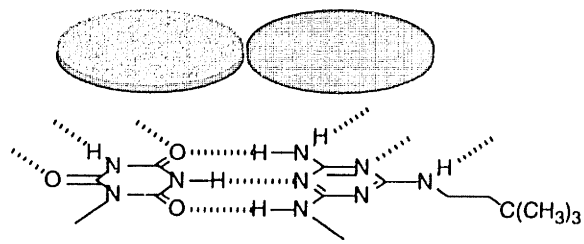

The circular assembly is facilitated if some preorganization has been provided, e.g. three subunits of the same type are tethered to a centerpiece. The first assembly of this sort was reported in 1990[11].

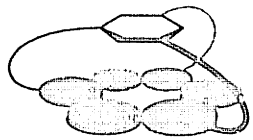

The ^{1}H NMR spectrum of the C_3-symmetric tris(melamine) unit is very broad but becomes completely sharp upon titration with the cyanuric acid derivative once a 1:3 stoichiometry has been reached. While the resulting 3+1 complex is stable even to chromatography, no encapsulation studies were reported. Apparently, the large open spaces between the "spokes" of the tethered building block permit rapid entry and exit of solvent molecules.

An enlarged version was later presented, a 2:3 complex comprised of two tris-melamine units and three bis-cyanuric acid units[12]. With its five components the assembly is entropically disfavored, but the enthalpy gained from the 36 hydrogen bonds within the complex more than compensates the entropy loss and drives the self-assembly process.

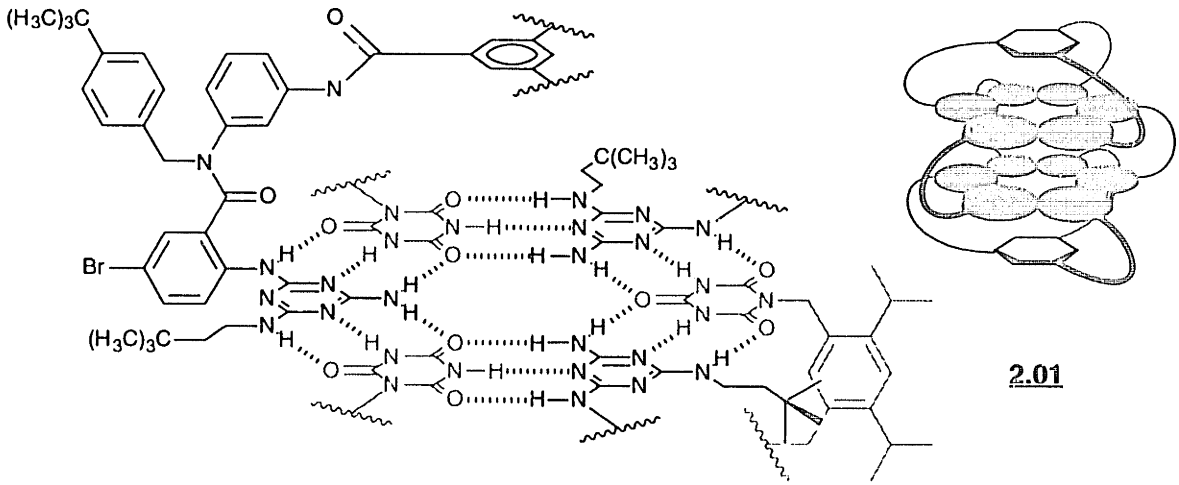

2.01

The assembly shows some stability against disruption of the hydrogen bonding network by polar solvents. A chloroform solution containing up to 15% v/v methanol-d_4 leaves the assembly intact as determined from the broadness of the ^{1}H NMR signals[13]. The "double decker" system **2.01** should in principle act as a host for flat molecules. However, given the fairly short *m*-xylylene spacer between the cyanuric acid moieties, the distance between the two disc-shaped hydrogen bonded arrays is too small for intercalation of guest

compounds. Twisting the two hydrogen bonded planes against each other can further shorten the distance and thus allows the complex to adopt a conformation most suitable for stacking interactions.

In addition to linking the individual components by tethers, another strategy was used to maximize formation of specific assemblies. The use of very bulky terminal substituents on the components disfavors infinite zig-zag arrays because of steric hindrance[17]. The subunits can arrange only in a circular pattern in which their bulky residues are facing away from each other.

A self-assembling calixarene-derived dimeric system has been presented by Shinkai et al.[19] The monomers are substituted with different mutually recognizing functionalities, so that the assembly resembles a molecular pot topped off by a molecular lid. The simplified structure is shown below.

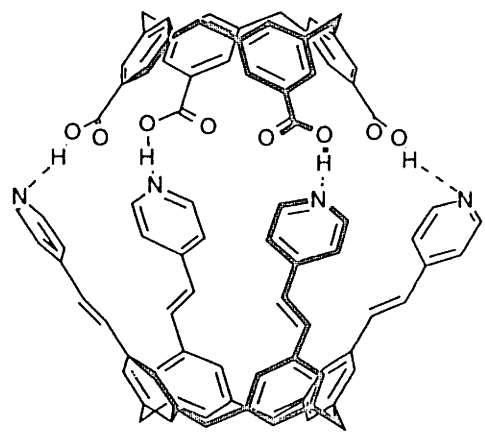

The recognition between the two monomers relies on four hydrogen bonding interactions between carboxyl groups and pyridine moieties. Formation of a 1:1 complex is observed in chloroform and tetrahydrofuran but no encapsulation studies have been reported. The large holes in the capsule walls presumably allow rapid access of the slovent so that the inner cavity is constantly flushed by solvent molecules.

Self-assembly relying solely on cis-amides has been demonstrated by Sanders et al.[20] Cholic acid derivatives featuring solubilizing esters were cyclotrimerized and the degree of self-association was measured in carbon tetrachloride.

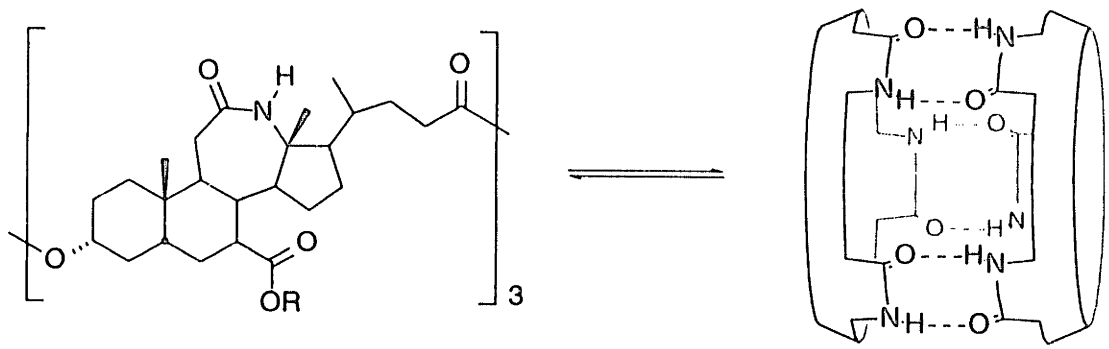

The amide proton signal in an overall broad ^{1}H NMR spectrum undergoes a 2.3 ppm downfield shift depending on the concentration, indicating dimer formation on the NMR time scale. Evaluation of IR data for the NH absorptions confirmed the interpretation of the NMR experiments ($K_a = 10^3$ M^{-1} in carbon tetrachloride).

Another approach to directed self-assembly via hydrogen bonds is based on peptide amide groups as hydrogen bond donors and acceptors. DeSantis et al.[21] realized that in cyclic peptides composed of alternating D- and L- amino acids the plane of the backbone amide groups is approximately perpendicular to the ring plane. If the amide nitrogens are alternatingly alkylated, only one face of the ring is able to undergo hydrogen bonding interactions with its counterpart to form a dimeric assembly. Appropriately *N*-methylated cyclic peptides have been prepared and investigated by Ghadiri et al[22-24] and Loren[illegible] al.[25] It was shown that the eight-residue peptide *cyclo*[(—L-Phe—D-*N*-MeAla—)$_4$] assembles in nonpolar solvents ($K_a = 10^3$ M^{-1} in chloroform) to form a dimeric complex in which each hydrogen bond contributes 0.5-0.7 kcal mol^{-1} for the self-assembly process[22].

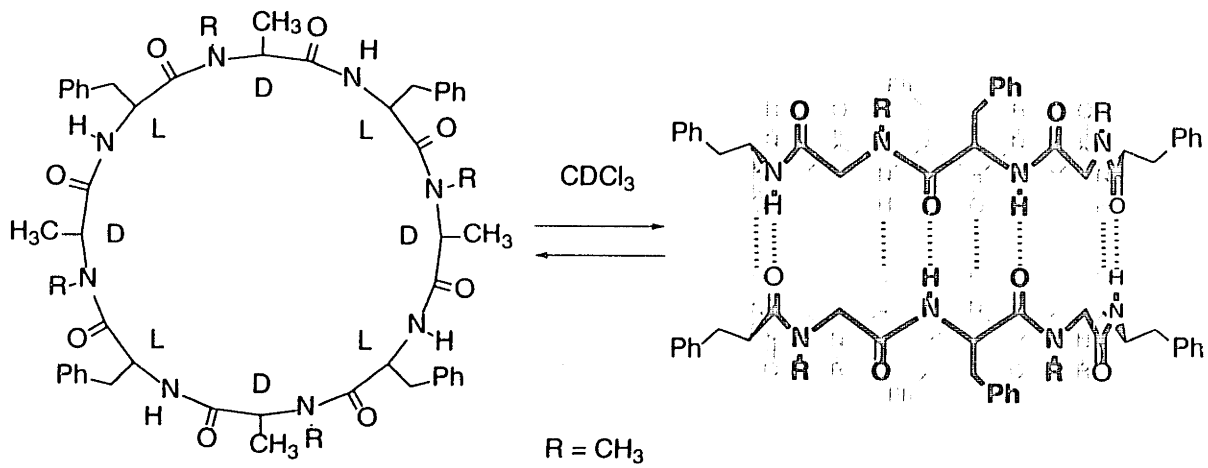

More recently, a different cyclic peptide has been synthesized. Two L-homoallylglycine residues are incorporated into the cyclic peptide, furnishing the ring with a functionality that allows coupling by means of olefin metathesis. The kinetically labile dimeric assembly (K_a = 10^2 M^{-1} in chloroform-*d*) is exposed to Grubbs' ruthenium carbene catalyst and the three diastereomers (*cis-cis*; *cis-trans*; *trans-trans*) of the covalently linked structure **2.02** are obtained in high yields.

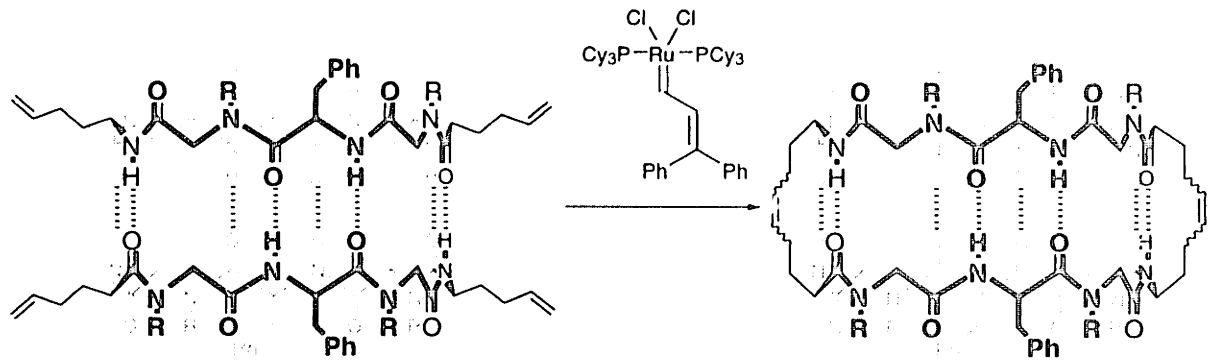

2.02

Compound **2.02** represents an open-sided cavity suitable to encapsulate guest compounds, in addition it shows the feasibility of covalently linking two large subunits together after some of the activation entropy has been overcome during the hydrogen bond formation.

The importance of cooperativity and directionality is demonstrated in the attempted self-assembly of a cyclic hexamer from six units of the enantiomerically pure diaza-bicyclooctane derivative **2.03**[26]. (Racemic **2.03** has been shown to crystallize in extended hydrogen-bonded ribbons.[26,27])

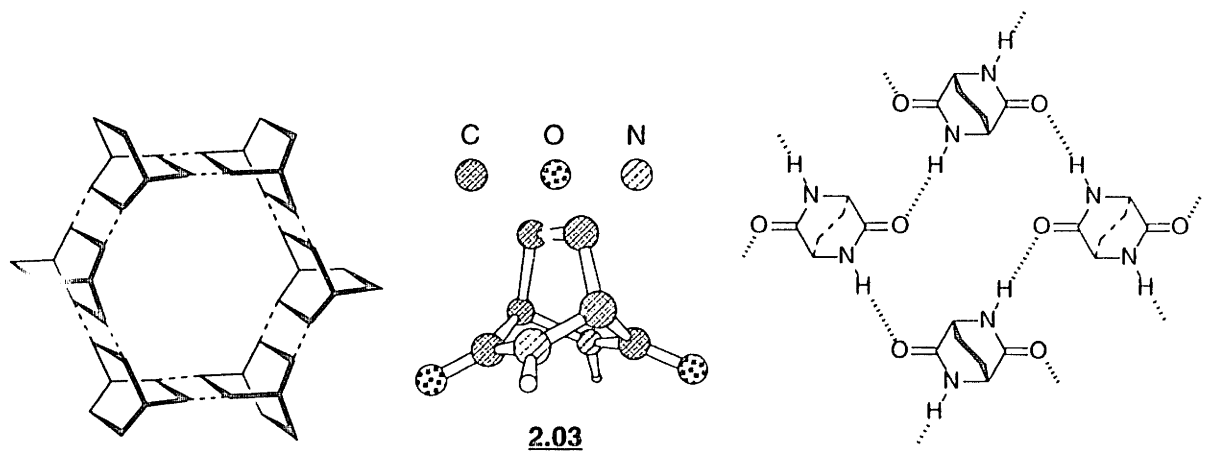

2.03

In the solid state the diamides pack under formation of infinite hydrogen bonded planes composed of alternating upward and downward facing molecules. A defined multicomponent assembly such as the cyclic hexamer might be favored if for example three molecules were linked together and preorganized by a tether or spacer, thereby decreasing the entropic cost of assembly in solution.

2.3
Host-Guest Chemistry in Self-Assembled Systems

In the case of the metal-coordinated assembly of Fujita et al.[28] it was found that various methoxy- and methoxymethylsubstituted derivatives of benzene were bound in the cavity with binding constants between 10^2 and 10^3 M^{-1} in water.

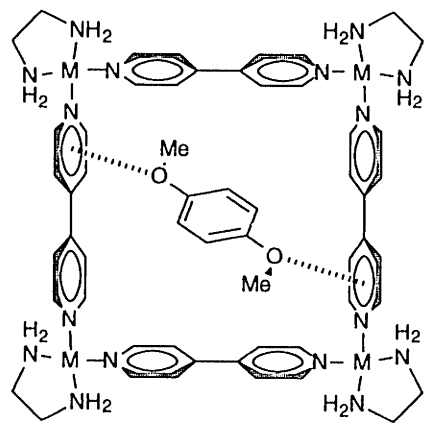

M = Pd^{2+}, Pt^{2+}

Complexation is attributed to hydrophobic effects and to charge transfer interactions between the electron-deficient dipyridyl cavity walls and the electron-rich guests. An upfield shift of ^1H NMR signals is observed for bound species ($\Delta\delta$ = 1-2 ppm for aromatic and 0.25 ppm for alicyclic guests). Recent work on a related system[29] based on tris(pyridylmethyl)benzene led to the cage-like complex shown below.

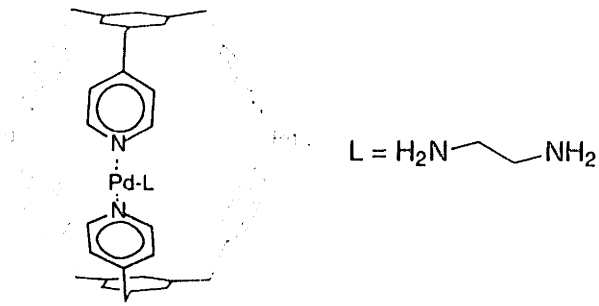

Assembly is nucleated by a guest and the formation of the cage structure depends strongly on the fit of the guest. Anionic guests with a large hydrophobic moiety such as adamantyl or phenylethyl groups have a shape complementary to the cavity and give rise to high yields in the formation of the complex. Ion pairing is not essential for the formation of a complex between the guest and the assembled host: The fact that an uncharged guest such as *p*-xylene induces organization of the host but *p*-dimethoxybenzene does not, shows that hydrophobicity of the guest is crucial. Again, an upfield shift of 2-3 ppm is observed for the ^{1}H NMR signals of guest protons located inside the cavity.

Another binary system that self-assembles through metal coordination has been worked out by Hunter et al.[30] and is based on a porphyrin platform linked to a pyridine donor moiety. The linkage features two amide-pyridine hydrogen bonds and therefore reduces the expected 120° angle to an approximately 96° bend, thus making the monomer highly self-complementary. The high cooperativity of the self-assembly process is reflected in the association constant of more than 10^8 M^{-1} in methylene chloride. Vapor phase osmometry data indicates that the assembly is a dimer. The resulting macrocycle features inwardly directed amide protons which can serve as recognition sites for carbonyl functions.

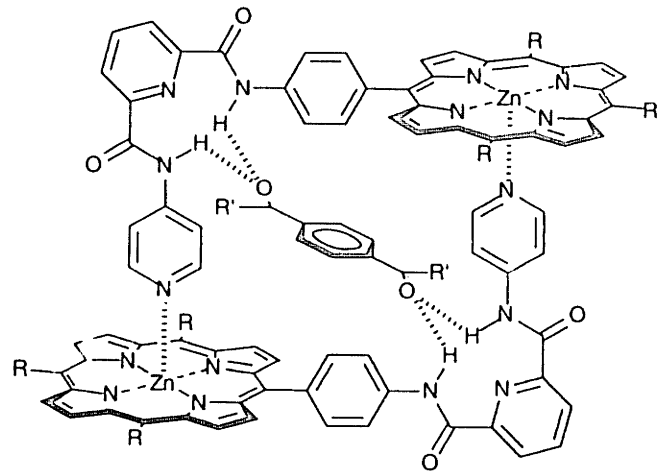

^{1}H NMR titrations demonstrate that terephthalic acid derivatives are bound preferentially to derivatives of isophthalic acid. Only 1,4-dicarbonyl benzene derivatives can reach across the macrocycle to form hydrogen bonds to all four amide protons of the host. Upon guest complexation the amide proton signals are shifted downfield. The signals for the guest protons are shifted upfield, indicating that the guest is experiencing the ring current from the host's phenyl and porphyrin rings.

An example of self-assembling molecular bowls in which the assembly can be controlled by the pH of the surrounding medium had been introduced by Sherman et al.[31] Upon partial deprotonation of the cyclic tetraphenol **2.04**, it selects the most suitable guest molecule (pyrazine) from a mixture of several candidates and forms a dimeric assembly via four charged hydrogen bonds. Exchange of encapsulated pyrazine is observed to be slow (within hours) or fast (within minutes), depending on the medium. The fact that complex formation is observed even in dimethyl sulfoxide indicates that the charge of the hydrogen bonds is a contributing factor for the self-assembly process. Electrostatic and van der Waals interactions between the guest and the interior of the cavity account for the discrimination between guests and the selectivity of the capsule.

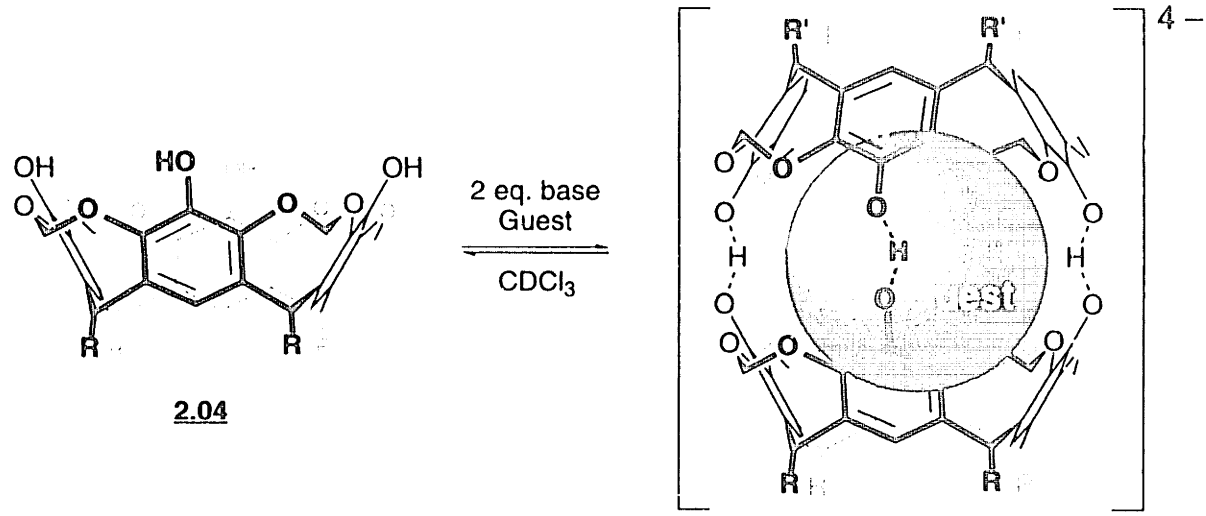

2.04

It is also noteworthy that the encapsulated pyrazine is restricted in its mobility. The rotational barrier of the guest pyrazine around the pseudo C_2 axis is 18 kcal/mol, similar to the barrier observed in the covalently linked carceplex host-guest complex[32].

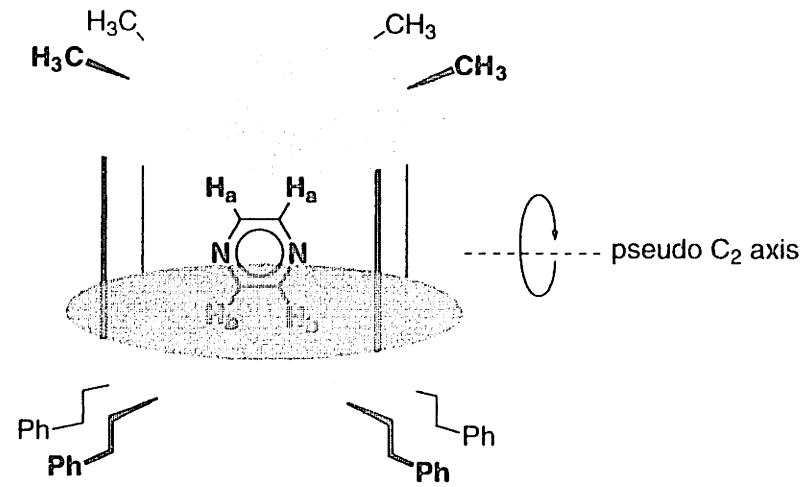

A mixture of methyl- and benzyl-derivatives of **2.04** and an appropriate guest contains three different host-guest species: A dimeric assembly of the methyl- and phenyl-substituted monomers and a mixed dimer composed of one methyl- and one phenyl-substituted monomer. In the case of the mixed assembly, the magnetic inequivalence of the guest protons can be observed by NMR at room temperature.

From the examples mentioned so far, one can learn some requirements for the design of self-assembling systems for effective guest complexation:

- Complementarity of the hydrogen bonding perimeter of the monomers so that the enthalpic contribution of the hydrogen bonds formed upon assembly is maximized.
- The use of few components so that the entropic cost upon assembly is minimized.
- Structural rigidity and conformational preorganization of the monomers so that the entropic cost prior to assembly is minimized.
- Design of the monomers in such a way that "gaps" or "holes" in the assembly are closed, so that the release of an encapsulated guest is disfavored.

A versatile method for making various self-assembled host molecules was found in the combination of glycoluril derivatives with rigid aromatic spacers[33]. The result is a self-complementary compound with the information for molecular recognition encrypted in the amide functionalities on the perimeter of the molecule.

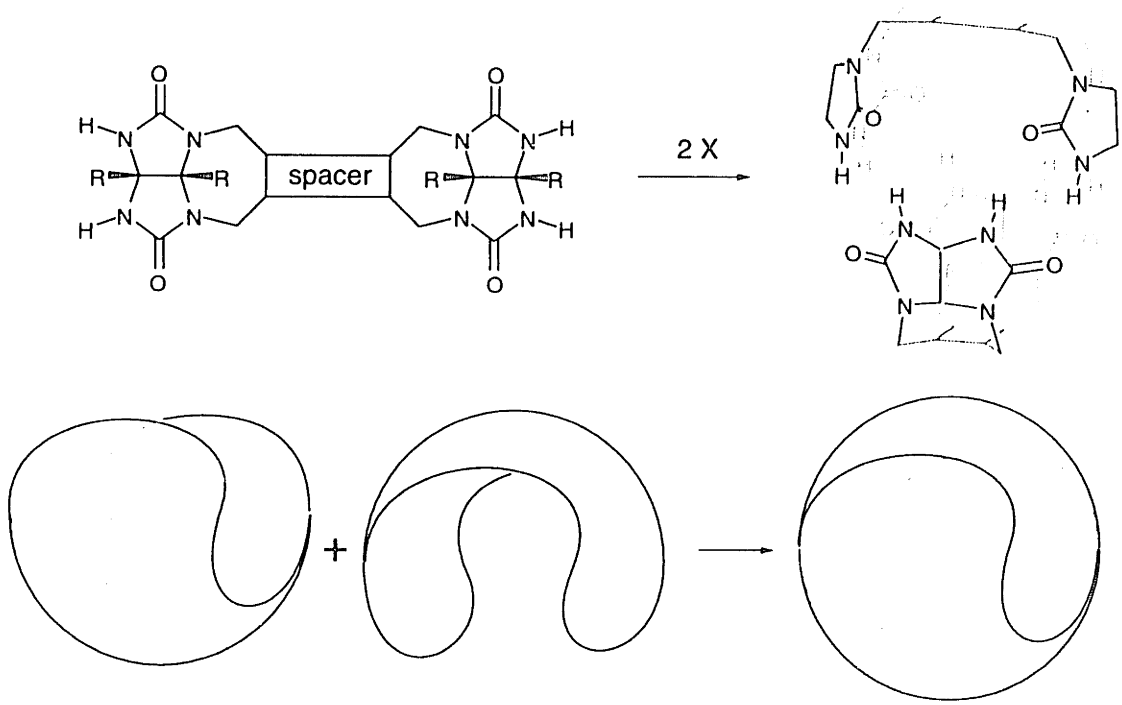

Figure *2-6* (previous page): Schematic diagram of a self-assembling three-dimensional structure. The assembly has a S_4 symmetry axis, and the same geometry as a tennis ball. For clarity, substituents R have been omitted in the representation of the dimeric assembly.

The substituents on the glycoluril moieties can be varied, allowing for special characteristics of the assemblies, and the spacers can be chosen from various shapes and sizes allowing access to different geometries of the assemblies[4,34-40]. Reversible encapsulation of guest compounds within the cavity has been demonstrated in all cases.

The high tendency of these compounds to form specific aggregates is a result of structural rigidity and curvature. Curvature along the "latitude" of the pseudospherical dimeric assembly is due to the intrinsic bend within the glycoluril moieties[41,42]. The "longitudinal" curvature of the monomeric subunits arises from the bent seven-membered rings fusing the glycoluril moieties to the spacers (figure *2-6*). Structural rigidity is ensured by the substituents (R) on the glycoluril groups. Figure *2-7* illustrates the steric requirements due to inversion of the seven-membered ring.

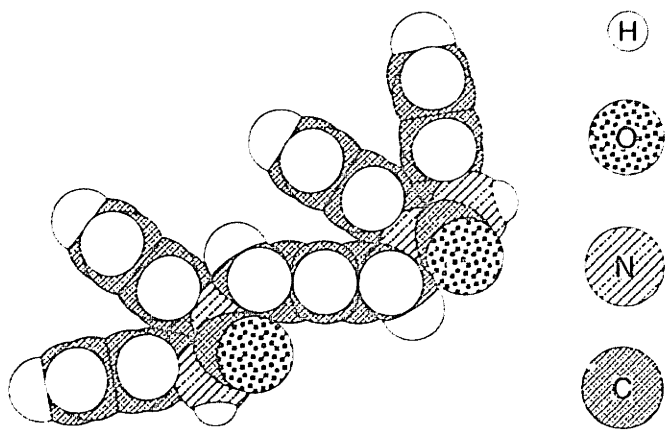

Figure *2-7*: Interconversion of the glycoluril-spacer linkage brings the glycoluril substituents (phenyl groups in this case) close to the spacer and is therefore disfavored.

The importance of rigidity and preorganization within the building blocks for multicomponent assemblies has been demonstrated by work in our group. A suggested assembly **2.06** arising from four molecules **2.05** coming together in an alternating head-to-tail fashion resulted in an extended hydrogen bonded network in the solid state[43].

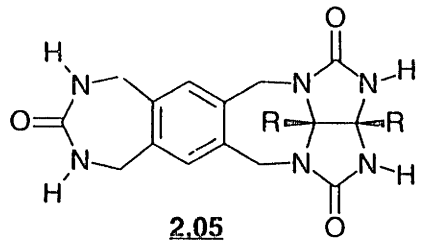

2.05

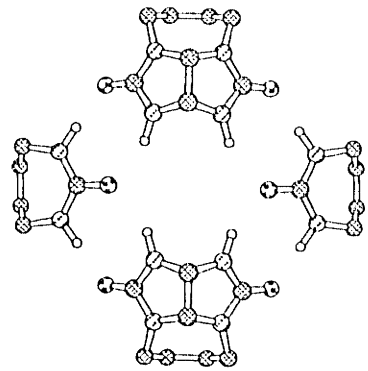

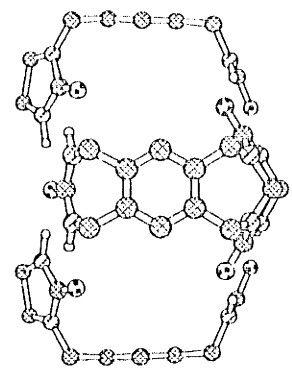

2.06

The problem in this case was the flexibility of the seven membered rings in which the benzylic carbons act as hinges allowing two conformations. While the ring containing the glycoluril group is locked in one conformation due to the bulk of the glycoluril–R groups, the seven membered cyclic urea can adopt both a Z- and E- conformation relative to the glycoluril. Only in the Z-conformation four molecules can form an assembly resulting in a barrel shaped structure, whereas in the E-conformation various scenarios of extended hydrogen bonding networks are possible, one of which is favored in the crystalline state. Even in solution there is no evidence for a four-molecule assembly.

The extent to which molecular modeling can be trusted is illustrated for the suggested assembly of six molecules **2.07** to form a cube-like assembly[44].

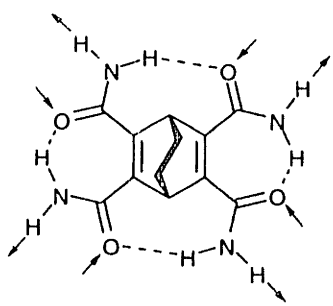

2.07

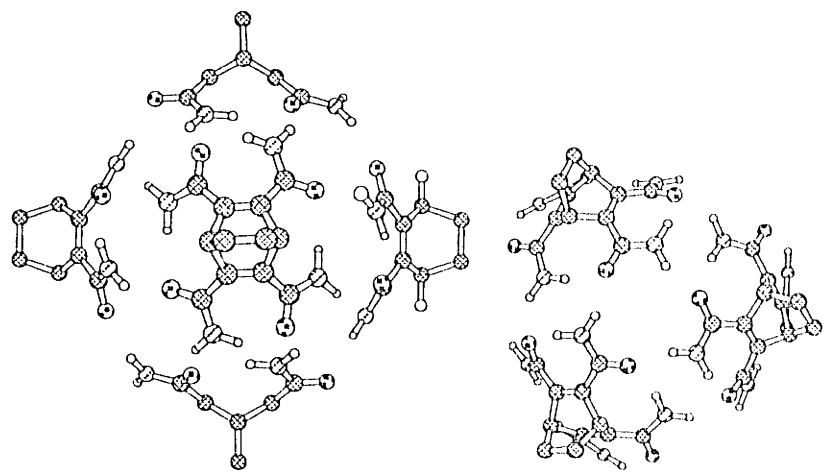

According to the calculations[45] four intramolecular hydrogen bonds are formed around the bicyclic frame of the monomer furnishing rigidity. Furthermore, six molecules stabilized in this way would represent selfcomplementary monomers and could form a

hexameric assembly resembling a cube. Solution studies of N-monobenzylated **2.07** in chloroform-*d* indicated the existence of intramolecular hydrogen bonds but this derivative can of course not form any multicomponent assemblies. In dimethyl formamide d_7 (the least polar solvent in which **2.07** is sufficiently soluble) the intramolecular hydrogen bonds are broken and no indications for any self-assembly is found. With its symmetry and rigidity this system resembles Lehn's bicyclic diamide[26] discussed above. This example again illustrates the importance of structural preorganization so that "undesired" modes of assembly are excluded.

2.4
References

(1) Rebek, J., Jr. *Angew. Chem. Int. Ed. Engl.* **1990**, *29*, 245-255.

(2) Rebek, J., Jr. *Acc. Chem. Res.* **1990**, *23*, 399-404.

(3) Schneider, H.-J. *Angew. Chem. Int. Ed. Engl.* **1991**, *30*, 1417-1436.

(4) Rebek, J., Jr. *Acta Chem. Scand.* **1996**, *50*, in press.

(5) Lawrence, D. S.; Jiang, T.; Levett, M. *Chem. Rev.* **1995**, *95*, 2229-2260.

(6) Leize, E.; VanDorsselaer, A.; Krämer, R.; Lehn, J.-M. *J. Chem. Soc., Chem. Commun.* **1993**, 990-993.

(7) Baxter, P.; Lehn, J. M.; DeCian, A.; Fischer, J. *Angew. Chem. Int. Ed. Engl.* **1993**, *32*, 69-72.

(8) Kim, M.; Gokel, G. W. *J. Chem. Soc., Chem. Commun.* **1987**, 1686-1688.

(9) Schall, O.; Gokel, G. W. *J. Am. Chem. Soc.* **1994**, *116*, 6089-6100.

(10) Drain, C. M.; Fischer, R.; Nolen, E. G.; Lehn, J.-M. *J. chem. Soc., Chem. Commun.* **1993**, 243-245.

(11) Seto, C. T.; Whitesides, G. M. *J. Am. Chem. Soc.* **1990**, *112*, 6409-6411.

(12) Seto, C. T.; Whitesides, G. M. *J. Am. Chem. Soc.* **1991**, *113*, 712-713.

(13) Seto, C. T.; MAthias, J. P.; Whitesides, G. M. *J. Am. Chem. Soc.* **1993**, *115*, 1321-1329.

(14) Seto, C. T.; Whitesides, G. M. *J. Am. Chem. Soc.* **1993**, *115*, 1320-1340.

(15) Mathias, J. P.; Seto, C. T.; Simanek, E. E.; Whitesides, G. M. *J. Am. Chem. Soc.* **1994**, *116*, 1725-1736.

(16) Mathias, J. P.; Simanek, E. E.; Zerkowski, J. A.; Seto, C. T.; Whitesides, G. M. *J. Am. Chem. Soc.* **1994**, *116*, 4316-4325.

(17) Mathias, J. P.; Simanek, E. E.; Whitesides, G. M. *J. Am. Chem. Soc.* **1994**, *116*, 4326-4340.

(18) Cheng, X.; Gao, Q.; Smith, R. D.; Simanek, E. E.; Mammen, M.; Whitesides, G. M. *J. Org. Chem.* **1996**, *61*, 2204-2206.

(19) Koh, K.; Araki, K.; Shinkai, S. *Tetrahedron Lett.* **1994**, *35*, 8255-8258.

(20) Bonar-Law, R. P.; Sanders, J. K. M. *Tetrahedron Lett.* **1993**, *34*, 1677-1680.

(21) DeSantis, P.; Morosetti, S.; Rizzo, R. *Macromolecules* **1974**, *7*, 52-58.

(22) Ghadiri, R. M.; Kobayashi, K.; Granja, J. R.; Chadha, R. K.; McRee, D. E. *Angew. Chem. Int. Ed. Engl.* **1995**, *34*, 93-95.

(23) Kobayashi, K.; Granja, J. R.; Ghadiri, M. R. *Angew. Chem. Int. Ed. Engl.* **1995**, *34*, 95-98.

(24) Clark, T. D.; Ghadiri, M. R. *J. Am. Chem. Soc.* **1995**, *117*, 12364-12365.

(25) Sun, X.; Lorenzi, G. P. *Helv. Chim. Acta* **1994**, *77*, 1520-1526.

(26) Brienne, M.-J.; Gabard, J.; Leclerq, M.; Lehn, J.-M.; Cesario, M.; Pascard, C.; Chevé, M.; Dutruc-Rosset, G. *Tetrahedron Lett.* **1994**, *35*, 8157-8160.

(27) Branda, N. R. Ph.D. Thesis, Massachusetts Institute of Technology, 1994.

(28) Fujita, M.; Yazaki, J.; Ogura, K. *Tetrahedron Lett.* **1991**, *32*, 5589-5592.

(29) Fujita, M.; Nagao, S.; Ogura, K. *J. Am. Chem. Soc.* **1995**, *117*, 1649-1650.

(30) Hunter, C. A.; Sarson, L. D. *Angew. Chem. Int. Ed. Engl.* **1994**, *33*, 2313-2316.

(31) Chapman, R. G.; Sherman, J. C. *J. Am. Chem. Soc.* **1995**, *117*, 9081-9082.

(32) Fraser, J. R.; Borecka, B.; Trotter, J.; Sherman, J. C. *J. Org. Chem.* **1995**, *60*, 1207-1213.

(33) Wyler, R.; de Mendoza, J.; Rebek, J., Jr. *Angew. Chem. Int. Ed. Engl.* **1993**, *32*, 1699-1701.

(34) Branda, N.; Wyler, R.; Rebek, J., Jr. *Science* **1994**, *263*, 1267-1268.

(35) Branda, N.; Grotzfeld, R. M.; Valdés, C.; Rebek, J., Jr. *J. Am. Chem. Soc.* **1995**, *117*, 85-88.

(36) Grotzfeld, R. M.; Branda, N. R.; Valdés, C.; Rebek, J. J. *NATO ASI Series, Series C: Mathematical and Physical Sciences* **1995**, *473*, *Supramolecular Stereochemistry;* Siegel, J.S. Ed., 195-198.

(37) Valdés, C.; Spitz, U. P.; Kubik, S. W.; Rebek, J., Jr. *Angew. Chem. Int. Ed.* **1995**, *34*, 1885-1887.

(38) Valdés, C.; Spitz, U. P.; Toledo, L. M.; Kubik, S. W.; Rebek, J., Jr. *J. Am. Chem. Soc.* **1995**, *117*, 12733-12745.

(39) Meissner, R. S.; Rebek, J., Jr.; de Mendoza, J. *Science* **1995**, *270*, 1485-1488.

(40) Grotzfeld, R. M.; Branda, N.; Rebek, J., Jr. *Science* **1996**, *271*, 487-489.

(41) Akyev, D.; Lebedev, O. V.; Pivina, T. S.; Khmel'nitskii, L. I. *Bull. Acad. Sci. U.S.S.R., Div. Chem. Sci.* **1989**, 1860-1863.

(42) Dekaprilevich, M. O.; Suvorova, L. I.; Khmelnitskii, L. I.; Struchkov, Y. T. *Acta Cryst.* **1994**, *C50*, 2056-2058.

(43) Garcías, X.; Toledo, L. M.; Rebek, J., Jr. *Tetrahedron Lett.* **1995**, *36*, 8535-8538.

(44) Beerli, R.; Rebek, J., Jr. *Tetrahedron Lett.* **1995**, *36*, 1813-1816.

(45) Mohamadi, F.; Richards, N. G.; Guida, W. C.; Liskamp, R.; Lipton, M.; Caufield, C.; Chang, G.; Hendrickson, T.; Still, W. C. *J. Comput. Chem.* **1990**, *11*, 440-467.

Chapter 3

Glycoluril Derivatives with Enhanced Solubility: Improving Established Building Blocks for Self-Assembled Structures

3.1
Introduction

In the initial self-assembled "tennis ball"-type structure synthesized by our group, diphenyl glycoluril **3.01** was employed for simplicity[1,2].

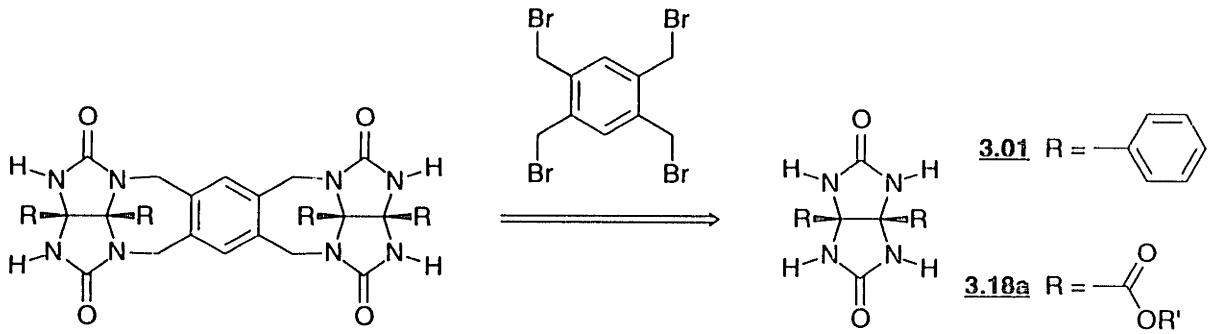

The first studies soon revealed a major drawback of simple diphenyl substituents on the glycolurils: Low solubility of both dimeric assemblies and monomers in chloroorganic solvents. Therefore, more soluble derivatives of the glycoluril scaffold were sought.

Many glycoluril derivatives had been published in the past[3]. One of the most promising candidates for rendering soluble derivatives upon alkylation (i.e. soluble "tennis balls") was the ethyl ester derivative **3.18a** Because the original synthesis[4] for the ethyl ester derivative could not be reproduced, an effective synthesis had to be developed. Dr. Carlos Valdés found that a stepwise synthesis gave good yields of **3.18a**[5]. The ester derivative also required anhydrous conditions in the final alkylation step with tetrakis(bromomethyl)benzene which led to general improvements of the alkylation step. The expected increase in solubility was indeed observed as Dr. Valdés' derivative **3.18a** was used in the synthesis of the self-assembling structures. It was my goal to synthesize an even more soluble glycoluril building block which still has a simple ^{1}H NMR spectrum, thereby facilitating interpretation of ^{1}H NMR spectra of the assemblies.

The glycoluril core is obtained from condensation of two equivalents of urea with one equivalent of a diketone. For many diketones, the condensation can be achieved under either acidic or basic conditions.

Many of the earlier glycoluril derivatives known from the literature had been prepared under basic conditions. Usually a hydantoin side product **3.02** was obtained due to rearrangement of a phenyl group under the reaction conditions[6-8].

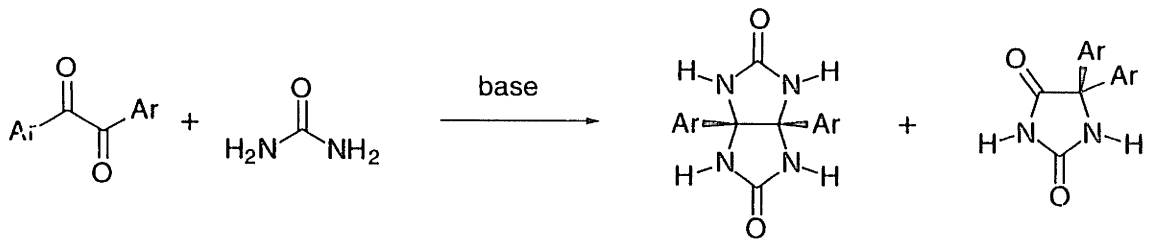

3.02

The most successful route used in our laboratory is based on the work of Butler et al.[9], i.e. the condensation with trifluoroacetic acid in benzene under azeotropic removal of water. Butler's reaction conditions give the best results for the condensation of non-enolizable diketones, specifically benzil derivatives. Therefore, I used various diphenylsubstituted 1,2-diketones to synthesize different glycolurils as potential building blocks with good solubility properties.

3.2
Increased solubility in the diphenylglycoluril series

In the search for soluble glycolurils derived from diphenyldiketones, two strategies were followed:

- increase the solvent accessible area on what would become the R residues on the glycoluril so that more solvent molecules are required to interact with the solute;
- introduce a dipole moment into the R groups to allow for stronger interactions between the solvent and the solute.

Only few benzil derivatives are available commercially. Since halogenated derivatives were not deemed very suitable for further modifications, 4,4'-dimetylbenzil **3.03** and 4,4'-dimethoxybenzil **3.04** were investigated instead.

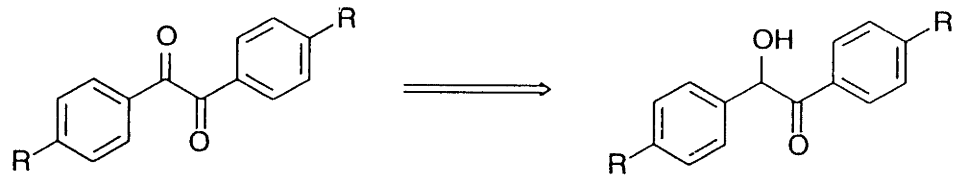

3.03 R = Me

3.04 R = OMe

3.05 R = Me

3.06 R = OMe

Since the corresponding benzoin derivatives **3.05** and **3.06** were much cheaper than the diketones **3.03** and **3.04** , an effective oxidation method was required. The reaction of benzoins with copper(II)sulfate pentahydrate in aqueous pyridine[10] was found to be very general and gave the corresponding diketones in virtually quantitative yields.

Having found an easy and cheap access to anisil, I could obtain a variety of 4,4'-dialkoxy substituted benzil derivatives and their corresponding glycolurils. The generality of this approach relied on the facile quantitative demethylation of 4,4'-dimethoxybenzil **3.04** in refluxing pyridine hydrochloride[11]. Alkylation of the resulting 4,4'-dihydroxybenzil **3.07** with appropriate alkyl halides was the final step in the diketone synthesis.

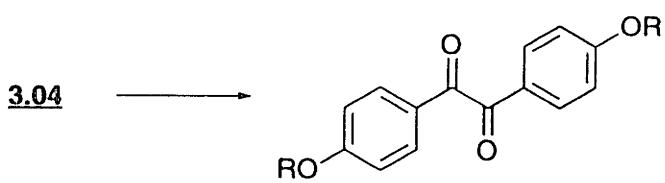

3.07 R = H

3.08 R = CH_2CO_2Et

3.09 R = Ac

3.10 R = 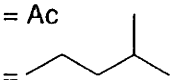

The versatility of 4,4'-dimethylbenzil **3.03** is due to the facile functionalization of the methyl groups. Bromination with NBS proceeds in acceptable yields and the resulting 4,4'-bis(bromomethyl)benzil **3.11** [12,13] can be reacted with appropriate nucleophiles.

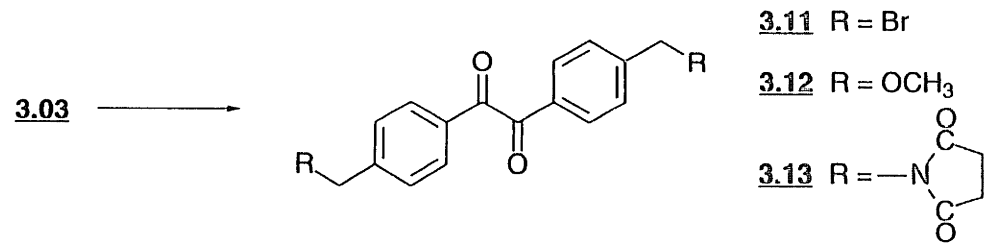

The condensation of the diketones under the acidic conditions mentioned above afforded the corresponding glycoluril derivatives.

3.3
Increased solubility in the esterglycoluril series

The synthesis of the diester substituted glycolurils is based on the disodiumsalt of dihydroxytartrate **3.16** a synthon for a non-enolizable diketone. I prepared the starting material **3.16** from L–tartaric acid **3.14** by oxidation with nitric acid[14,15].

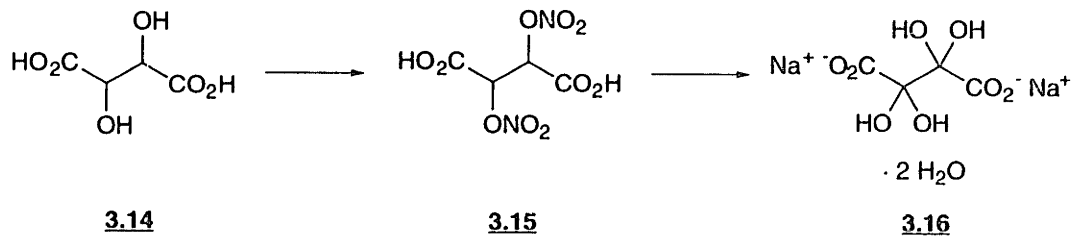

3.14 **3.15** **3.16**

The improved synthesis of the diethyl ester glycoluril **3.18a** found by Dr. Carlos Valdés is a two step procedure[5]. First, the crude diethyl ester **3.17a** of dihydroxytartaric acid is prepared which is then subjected to the condensation with urea without prior purification.

In analogy to Dr. Valdés' procedure, I used several alcohols, including the secondary alcohol cyclohexanol, for the synthesis of a series of glycolurils[16]. The glycoluril **3.18d** derived from the 2-methoxy-ethanol could only be isolated in a slightly gummy modification. In the case of the 3-methyl-butanol derivative **3.18e** a crystalline product was obtained which even was soluble in a 20% (v/v) chloroform/methanol mixture.

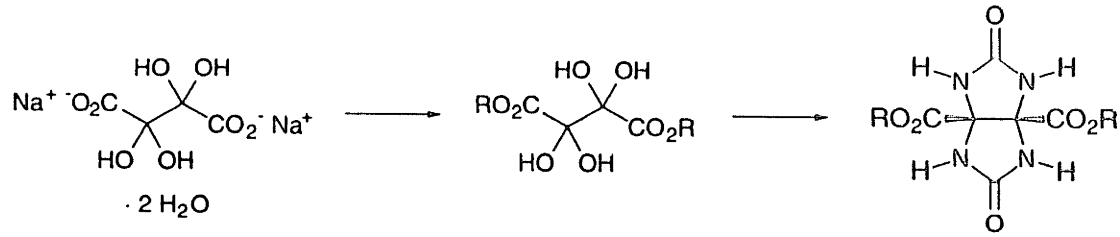

3.16 **3.17** **3.18**

a R = ethyl; b R = isopropyl; c R = cyclohexyl;

d R = 2-methoxy-ethyl; e R = 3-methyl-butyl

Compound **3.18e** therefore was a promising candidate for more complex self-assembling systems because of its high solubility and the simple and diagnostic ^{1}H NMR spectrum. These hopes were later confirmed by the successful use of **3.18e** for larger dimeric hosts[17,18].

The procedure allows the use of a wide range of alcohols, which could become important in future studies on asymmetric assemblies. Chiral glycoluril building blocks derived from chiral alcohols would allow the synthesis of asymmetric self-assembled "tennis ball"-type systems with a chiral periphery. Cram *et al.* have shown that a hemicarceplex with a chiral periphery discriminates between enantiomeric guests, probably due to steric repulsions in the diastereomeric transition states of guest release[19].

The first demonstration of the high solubility of "tennis balls" based on ester glycolurils was for the encapsulation of xenon in chloroform solution[5]. Due to the high solubility of **3.19** prepared by Carlos Valdés the concentration of xenon-filled capsules was high enough to permit ^{129}Xe NMR studies.

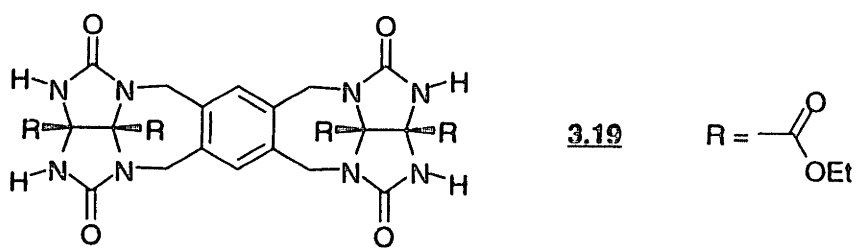

3.19

Upon saturation of a chloroform solution of **3.19** with xenon, virtually all the **(3.19)$_2$** dimers contained the guest xenon. The ^{129}Xe NMR[20-22] spectra obtained by Neil

Branda show the signal for the encapsulated xenon at ~19 ppm upfield from the solvated xenon signal (figure *3-1*).

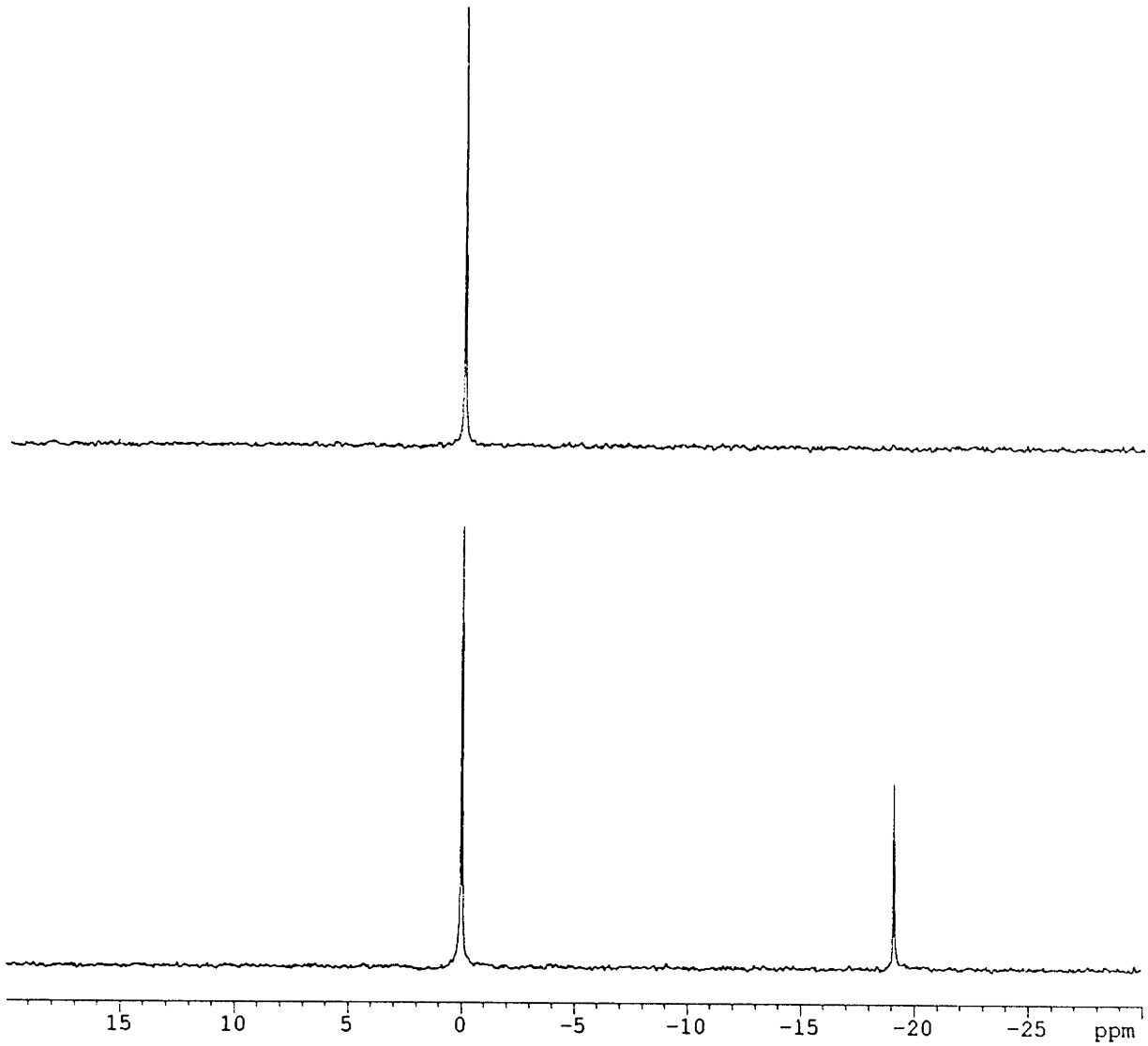

Figure *3-1*: ^{129}Xe NMR ($CDCl_3$, 138 MHz, 23°C). *Top*: Reference spectrum of a solution of xenon in $CDCl_3$. The xenon resonance is arbitrarily set to 0 ppm. *Bottom*: A solution of xenon and the host compound **3.19** in $CDCl_3$. The scale is referenced to the solvated xenon at 0 ppm. The signal for the encapsulated xenon appears approximately 19 ppm upfield of the solvated xenon. All spectra are taken from Neil Branda's PhD thesis[23].

3.4
Experimental

3.4.1
Apparatus:

^{1}H NMR spectra were obtained on Bruker AC-250 and Varian XL-300, UN-300, and VXR-500 MHz spectrometers in the solvents indicated as internal lock compounds. ^{1}H and ^{13}C NMR chemical shifts are listed as parts per million (δ) relative to either tetramethylsilane or to residual solvent peak (^{1}H NMR: $CDCl_3$, 7.26 ppm; DMSO-d_6, 2.50 ppm; toluene-d_8, xylene-d_{10}, 2.09 ppm; DMF-d_7, 2.91 ppm; ^{13}C NMR: $CDCl_3$, 77.23 ppm; DMSO-d_6, 39.51 ppm). Melting points were determined on a Thomas/Hoover capillary melting point apparatus or an Electrothermal IA9100 digital melting point apparatus and are all uncorrected. IR spectra were recorded on a Perkin-Elmer 1600 Series FT-IR spectrometer. Mass spectra were obtained on a Finnigan MAT System 8200, double focusing, magnetic sector, Mass Spectrometer.

3.4.2
Materials and Methods:

All chemicals were purchased from Aldrich, Mallinckrodt, or EM Science unless otherwise indicated. Unless stated expressively, commercially available chemicals were used without further purification. Deuterated solvents were obtained from Cambridge Isotope Labs and used from freshly opened ampoules or stored over actvated molecular sieves. Anhydrous tetrahydrofuran and ether was obtained by distillation from sodium-benzophenone ketyl. Dimethyl sulfoxide (DMSO) was dried by storing over avtivated molecular sieves (4 Å), or distillation from calcium hydride at 20 Torr. Column chromatography (flash chromatography[24]) was performed on E. Merck Silica Gel 60 (230-400 mesh) or ICN SiliTech 32-63 D 60 A. Thin Layer Chromatography (TLC) was carried out on E. Merck Silica Gel 60 F_{254} precoated glass plates. The preparative procedures described gave all compounds pure by ^{1}H NMR and TLC (single spot).

General procedure for the oxidation of benzoins to benzils

A solution of $CuSO_4 \cdot 5H_2O$ (0.21 mol, 52.4 g) in 120 ml water was added to a solution of the α-hydroxyketone (0.10 mol) in 120 ml pyridine. The mixture was placed in a steam bath and heated while stirring over night. After completion of reaction (checked by TLC: hexanes, EtOAc 1/1) the mixture was poured in 1000 ml ice water, and the precipitate was collected by filtration. The crystalline material was suspended in 500 ml 10% aq. HCl, stirred vigorously 30 minutes, filtered off, washed with water, and dried on a steam bath.

4,4'–Dimethylbenzil (Tolil), 3.03

Yield: 23.3 g (98%)

^{1}H NMR ($CDCl_3$, 250 MHz): δ 7.86 (d, $4H_{ar}$, J=8.2 Hz); 7.30 (d, $4H_{ar}$ J=8.1 Hz); 2.43 (s, 6H) ppm

^{13}C NMR ($CDCl_3$, 75 MHz): δ 194.7; 146.3; 130.9; 130.2; 129.9; 22.1 ppm

4,4'–Dimethoxybenzil (Anisil), 3.04

Yield: 26.0 g (96 %)

^{1}H NMR ($CDCl_3$, 250 MHz): δ 7.95 (d, $4H_{ar}$, J=8.9 Hz); 6.97 (d, $4H_{ar}$ J=9.0 Hz); 3.88 (s, 6H) ppm

^{13}C NMR ($CDCl_3$, 75 MHz): δ 193.6; 165.0; 132.5; 126.5; 114.5; 55.8 ppm

4,4'-Dihydroxybenzil, 3.07

was prepared according to a modified procedure[11].

A mixture of 4,4'-dimethoxybenzil **3.04** (0.05 mol, 13.51 g) and pyridine hydrochloride (0.13 mol, 15 g) was heated to reflux in a 250°C oil bath for 6h. After completion of reaction (checked by TLC: hexanes, EtOAc 1/1) the mixture was allowed to cool somewhat and 30 ml water was slowly added through the reflux condenser followed by 20 ml 10% aq. HCl. The resulting suspension was poured in 100 ml 10% aq. HCl. The precipitate was collected by filtration, washed with 10% aq. HCl and water, and dried.

Yield: 11.7 g (97 %)

^{1}H NMR (DMSO-d_6, 250 MHz): δ 10.83 (s, $2H_{OH}$); 7.72 (d, $4H_{ar}$, J=8.7 Hz); 6.91 (d, $4H_{ar}$ J=8.8 Hz) ppm

^{13}C NMR (DMSO-d_6, 75 MHz): δ 193.6; 163.9; 132.2; 124.2; 116.1 ppm

4,4'-Bis(ethoxycarbonylmethoxy)benzil, 3.08

A mixture of 4,4'-dihydroxybenzil **3.07** (0.032 mol, 9.87 g), K_2CO_3 (0.071 mol, 9.87 g, 2.2 eq.), ethyl bromoacetate (0.81 mol, 13.55 g, 9 ml, d=1.506, 2.5 eq.), and 50 ml acetone was heated to reflux over night. The reaction was quenched by pouring in a mixture of 100 ml HCl conc. with 700 ml icewater. The precipitate was collected by filtration, washed with water, dried, and recrystallized from EtOH.

Yield: 10.41 g (77 %)

^{1}H NMR ($CDCl_3$, 300 MHz): δ 7.95 (d, $4H_{ar}$, J=9.0 Hz); 6.97 (d, $4H_{ar}$, J=9.0 Hz); 4.70 (s, 4H); 4.28 (q, $4H_{Et}$, J=7.2 Hz); 1.30 (t, J=7.2 Hz, $6H_{Et}$) ppm

^{13}C NMR ($CDCl_3$, 75 MHz): δ 193.1; 167.9; 162.9; 132.4; 127.1; 114.9; 65.2; 61.7; 14.1 ppm

MS (EI) *m/z* 414 (M, 1%); 341 (M – COOEt, 5%); 207 (diketone cleavage, 100%)

HRMS calcd for M^+ $C_{22}H_{22}O_8$ 414.1355, found 414.1315

4,4'-Diacetoxybenzil, 3.09

4,4'-Dihydroxybenzil **3.07** (10 mmol, 2.42 g) was heated to reflux 4 h in 20 ml acetic anhydride in the presence of sodium acetate (0.5 mmol, 50 mg). Excess acetic anhydride was distilled off, the residue was taken up in ethyl ether and washed with water. The organic phase was dried over $MgSO_4$, stirred with charcoal, filtered through Celite, and evaporated. Crystallization was induced by adding 5 ml methanol and scratching the wall of the flask with a glass rod. The crystalline material was taken up in 10 ml methanol, sonicated, collected by filtration and washed with 10 ml methanol to afford a product clean by TLC (hexanes, EtOAc 1:1).

Yield: 1.98 g (61 %)

^{1}H NMR ($CDCl_3$, 300 MHz): δ 8.02 (d, $4H_{ar}$, J=7.8 Hz); 7.27 (d, $4H_{ar}$ J=8.7 Hz); 2.34 (s, 6H) ppm

^{13}C NMR ($CDCl_3$, 75 MHz): δ 193.0; 168.8; 156.0; 131.9; 130.6; 122.6; 21.4 ppm

4,4'-Bis(3-methyl-butoxy)benzil, 3.10

4,4'-Dihydroxybenzil **3.07** (5 mmol, 1.21 g) was dissolved in a suspension of powdered KOH (12 mmol, 670 mg) in 30 ml methanol. 1-Bromo-3-methylbutane (12 mmol, 1.8g, 1.43 ml) was added and the mixture was heated to reflux over night. The mixture was poured in 300 ml icewater, acidified with HCl, and extracted with ether. The

organic phase was washed with 1N NaOH and brine. The combined aqueous phases were back extracted with ether. The combined organic phases were dried over $MgSO_4$, stirred with charcoal, filtered through Celite, and evaporated. The resulting yellow oil (clean by TLC, hexanes/EtOAc, 4/1) was kept under vacuum over night.
Yield: 0.95 g (50 %)
^{1}H NMR ($CDCl_3$, 250 MHz): δ 7.78 (d, $4H_{ar}$, J=9.0 Hz); 6.95 (d, $4H_{ar}$ J=9.0 Hz); 6.60 (t, 4H J=6.6 Hz); 1.90-1.75 (m, 2H); 1.69 (q, 4H J=6.6 Hz); 0.96 (d, 12H J=6.4 Hz)ppm

4,4'–Bis(bromomethyl)benzil, 3.11

was prepared according to a modified published procedure[12,13]
A mixture of 4,4'-dimethylbenzil **3.03** (0.07 mol, 16.7 g), *N*-bromosuccinimide (0.161 mol, 28.6 g) and 1 g benzoylperoxide in 300 ml benzene was heated to reflux over night. The mixture was filtered while hot, the filtrate evaporated, and recrystallized from ethanol.
Yield: 15.3 g (55%)
^{1}H NMR ($CDCl_3$, 300 MHz): δ 7.95 (d, $4H_{ar}$, J=8.4 Hz); 7.54 (d, $4H_{ar}$, J=8.4 Hz); 4.50 (s, 4H) ppm

4,4'–Bis(methoxymethyl)benzil, 3.12

Sodium (0.50 mol, 11.5 g) was dissolved in a mixture of 300 ml dry methanol and 50 ml toluene. 4,4'–Bis(bromomethyl)benzil **3.11** (0.05 mol, 19.8 g) was added and the mixture was heated to reflux for 10 min until a dark suspension had formed. After stirring at room temperature for 1 h the mixture was diluted with 100 ml water, acidified with conc. HCl, and extracted with toluene (3x50 ml). The combined toluene extracts were washed with water, dried over $MgSO_4$, stirred with charcoal, filtered throough Celite, and evaporated.
Crude yield: 9.0 g (60%)
^{1}H NMR ($CDCl_3$, 300 MHz): δ 7.95 (d, $4H_{ar}$, J=8.1 Hz); 7.47 (d, $4H_{ar}$, J=8.1 Hz); 4.54 (s, 4H); 3.42 (s, 6H) ppm

4,4'–Bis(succinimidomethyl)benzil, 3.13

To a solution of succinimide (11 mmol, 1.09 g) in 40 ml DMF was added potassium tert-butoxide (12.5 mmol, 1.40 g). The slurry was heated to 100°C and a solution of bis(bromomethyl)benzil **3.11** (5 mmol, 1.98 g) in 10 ml DMF was added. After stirring 30

minutes, the dark mixture was poured in 500 ml 10% aq. HCl, the precipitate collected by filtration and dried.

Yield: 1.46 g (67%)

^{1}H NMR ($CDCl_3$, 300 MHz): δ 7.89 (d, $4H_{ar}$, J=8.7 Hz); 7.51 (d, $4H_{ar}$, J=8.4 Hz); 4.72 (s, 4H); 2.74 (s, 8H) ppm

^{13}C NMR ($CDCl_3$, 75 MHz): δ 193.6; 176.6; 142.7; 132.2; 130.1; 129.2; 41.8; 28.1 ppm

MS (EI) *m/z* 432 (M, 1%); 216 (diketone cleaveage, 100%);

HRMS calcd for M^+ $C_{24}H_{20}N_2O_6$ 432.1321, found 432.1322

General Procedure for the Preparation of Glycolurils

A mixture of benzil (5 -20 mmol), urea (12.5 - 50 mmol), and TFA (1 - 4 ml) in 50 - 100 ml benzene was heated to reflux over night using a Dean-Stark trap. The warm mixture was allowed to sit for 5 min, the supernatant was decanted and the solid material triturated with ethanol. The product was collected by filtration, washed with ethanol and acetone, and dried under vacuum.

3a,6a-Di(4-methoxyphenyl)glycoluril

Yield: 67 %

^{1}H NMR (DMSO-d_6, 500 MHz): δ 7.63 (s, $4H_{NH}$); 6.97 (d, $4H_{ar}$, J=9.0 Hz); 6.65 (d, $4H_{ar}$, J=9.0 Hz); 3.61 (s, 6H) ppm

^{13}C NMR (DMSO-d_6, 75 MHz): δ 160.7; 158.7; 134.4; 128.3; 112.7; 81.6; 55.0 ppm

3a,6a-Di[(4-ethoxycarbonylmethoxy)phenyl]glycoluril

Yield: 79%

^{1}H NMR (DMSO-d_6, 300 MHz): δ 7.65 (s, $2H_{NH}$); 6.95 (d, $4H_{ar}$, J=9.0 Hz); 6.64 (d, $4H_{ar}$, J=9.0 Hz); 4.63 (s, 4H); 4.11 (q, $4H_{Et}$, J=7.2 Hz); 1.17 (t, J=7.1 Hz, $6H_{Et}$) ppm

^{13}C NMR (DMSO-d_6, 75 MHz): δ 168.4; 160.5; 157.0; 131.1; 128.2; 113.3; 81.5; 64.5; 60.5; 13.9 ppm

3a,6a-Di(4-acetoxyphenyl)glycoluril

Yield: 46 %

^{1}H NMR (DMSO-d_6, 300 MHz): δ 7.83 (s, $4H_{NH}$); 7.06 (d, $4H_{ar}$, J=8.7 Hz); 6.84 (d, $4H_{ar}$, J=8.7 Hz); 2.18 (s, 6H) ppm

^{13}C NMR (DMSO-d_6, 75 MHz): δ 168.9; 160.6; 150.0; 135.7; 128.2; 120.9; 81.5; 20.8 ppm

3a,6a-Di(4-(3-methylbutoxy)phenyl)glycoluril

Yield: 60 %

^{1}H NMR (DMSO–d_6, 300 MHz): δ 7.61 (s, 4H_{NH}); 6.94 (d, 4H_{ar}, J=8.7 Hz); 6.63 (d, 4H_{ar}, J=9.6 Hz); 3.84 (t, 4H, J=6.3 Hz); 1.76–1.62 (m, 2H); 1.50 (m, 4H, J=6.7 Hz); 0.87 (d, 12H, J=6.3 Hz) ppm

^{13}C NMR (DMSO–d_6, 75 MHz): δ 160.6; 158.1; 130.3; 128.2; 113.3; 81.5; 65.8; 37.2; 24.5; 22.3 ppm

HRMS calcd for M^+ $C_{26}H_{34}N_4O_4$ 466.2580, found 466.2580

3a,6a-Di[4-(bromomethyl)phenyl]glycoluril

Yield: 46 %

^{1}H NMR (DMSO–d_6, 300 MHz): δ 7.80 (s, 4H_{NH}); 7.14 (d, 4H_{ar}, J=8.3 Hz); 7.04 (d, 4H_{ar}, J=8.3 Hz); 4.51 (s, 4H) ppm

^{13}C NMR (DMSO–d_6, 75 MHz): δ 160.4; 138.4; 137.5; 128.4; 127.4; 81.5; 33.7 ppm

Disodium dihydroxytartrate dihydrate, 3.16

was prepared by a modified published procedure[14,15].

100 ml conc. H_2SO_4 was added to a suspension of L-tartaric acid **3.14** (0.33 mol, 50 g) in 70 ml conc. HNO_3 and the mixture was stirred until a solution had formed. After addition of 120 ml conc. H_2SO_4 the mixture was allowed to sit at room temperature over night. The precipitate **3.15** was rapidly filtered off using a fritted glass filter (porosity 70-100 µm) and drained well. The filtercake was mixed with 150 ml chopped ice, stirred to a thin paste, and neutralized by addition of Na_2CO_3 in portions. The precipitate was collected by filtration, suspended in 400 ml water, stirred 5 min., filtered off, washed with water and allowed to dry.

Yield: 28-31 g (32-36 %)

3a, 6a-Diethylester-glycoluril, 3.18a[5]

A suspension of disodium dihydroxytartrate dihydrate **3.16** (0.19 mol, 50 g) in 500 ml ethanol was cooled in an ice bath and saturated with HCl gas. After stirring at room

temperature over night the solids were filtered off and washed with ethanol. Upon concentration of the filtrate the crude diester was obtained as a viscous orange liquid which was used without further purification. A mixture of the crude diester, urea (0.45 mol, 27 g), trifluoroacetic acid (35 ml), and 300 ml benzene was heated to reflux 20 h using a Dean-Stark trap. After cooling to room temperature the supernatant was decanted and the semisolid was shaken with ethanol (200 ml) on a vibrator until complete separation of solid material. The colorless product was collected by filtration, washed with ethanol, and dried under vacuum.

Yield: 25.7 g (51 %)

^{1}H NMR (DMSO-d_6 250 MHz): δ 8.02 (s, 4H$_{NH}$), 4.07 (q, 4H), 1.62 (t, 6H) ppm

3a, 6a-Diisopropylester-glycoluril, 3.18b

was prepared analogous to the diethylester derivative.

^{1}H NMR (DMSO-d_6, 300 MHz): d 7.98 (s, 4H$_{NH}$); 4.86 (hept., 2H, J=6.3 Hz); 1.18 (d, 12H, J=6.9 Hz) ppm

^{13}C NMR (DMSO-d_6, 75 MHz): δ 166.7; 159.6; 77.8; 69.8; 21.3 ppm

HRMS calcd for M$^+$ $C_{12}H_{18}N_4O_6$ 314.1226, found 314.1228

3a, 6a-Bis(3-methyl-butylester)glycoluril, 3.18e

A suspension of disodium dihydroxytartrate **3.16** (0.11-0.12 mol, 28-31 g) in 150 ml 3-methyl-1-butanol was saturated with HCl gas for 5 minutes. After stirring over night, precipitated NaCl was removed by filtration, the filtercake washed with xylenes, and the filtrate evaporated. The evaporation residue was taken up in xylenes, evaporated again, and diluted with 250 ml benzene. Urea (0.28-0.30 mol, 17-18 g) and 10 ml TFA was added and the mixture was heated to reflux over night using a Dean-Stark trap for water removal. After evaporation of the solvent, the semisolid residue was taken up in isopropyl alcohol and stirred until all the solids came free. The product was collected by filtration, the combined filtrates were concentrated to yield another crop.

Yield: 13-15 g (32-33 %; 11-12 %, based on L-tartaric acid)

^{1}H NMR (DMSO-d_6, 300 MHz): δ 8.0 (s, 4H$_{NH}$); 4.05 (t, 4H, J=6.8 Hz); 1.72–1.58 (m, 2H); 1.44 (m, 4H); 0.87 (d, 12H, J=6.6Hz) ppm

^{13}C NMR (DMSO-d_6, 75 MHz): δ 167.3; 159.5; 77.8; 64.3; 36.5; 24.2; 22.3 ppm

HRMS calcd for M$^+$ $C_{16}H_{26}N_4O_6$ 370.1852, found 370.1851

Diethylester "tennis ball" monomer, 3.19[2]

Diethylester-glycoluril **3.18a** (15.1 mmol, 4.58 g) was dissolved at room temperature in 50 ml anhydrous DMSO under argon. ^{t}BuOK (30.2 mmol, 3.3 g) was added in one portion. After stirring for 15 minutes tetrabromodurene (1.22 mmol, 564 mg) was added and stirring was continued for 75 minutes at room temperature. The mixture was poured in 0.1 N HCl (1000 ml) and extracted with ethyl acetate (3x400 ml). The organic layer was washed with brine (3x300 ml), dried over Na_2SO_4, and concentrated affording a white solid in which both isomers of the alkylation product could be identified by ^{1}H NMR. The solid was stirred with chloroform (150 mL) 30 minutes. The insoluble material—containing the *S*-shaped isomer—was separated by filtration. Upon evaporation of the filtrate a solid was obtained which was dissolved in boiling benzene. After cooling to room temperature the precipitate was collected by filtration.

Yield: 130 mg (15%)

^{1}H NMR ($CDCl_3$, 250 MHz): δ 9.08 (s, $4H_{NH}$); 7.30 (s, $2H_{ar}$); 4.68 (d, 4H, J=15.5 Hz); 4.4 - 4.2 (m, 12H); 1.31 (m, 12H) ppm.

^{13}C NMR ($CDCl_3$, 75 MHz): δ 165.9; 158.6; 135.6; 131.2; 82.2; 74.9; 62.8; 43.5; 30.9 ppm.

HRMS calcd for $[M + H]^+$ $C_{30}H_{35}N_8O_{12}$ 699.2374, found 699.2415

Diisoamylester "tennis ball" monomer

was prepared analogous to the diethylester derivative.

^{1}H NMR ($CDCl_3$, 300 MHz): δ 9.16 (s, $4H_{NH}$); 7.25 (s, $2H_{ar}$); 4.66 (d, 4H, J=15.6 Hz); 4.29 (d, 4H, J=15.4 Hz); 4.27 - 4.19 (m, 8H); 1.91 (hept, 2H, J=6.9 Hz); 1.75 - 1.51 (m, 10H); 0.99 (d, 12H, J=6.0 Hz); 0.92 (d, 12H, J=6.3 Hz) ppm.

3.5
References

(1) Wyler, R.; de Mendoza, J.; Rebek, J., Jr. *Angew. Chem. Int. Ed. Engl.* **1993**, *32*, 1699-1701.

(2) Branda, N.; Wyler, R.; Rebek, J., Jr. *Science* **1994**, *263*, 1267-1268.

(3) *Beilstein Handbuch der Organischen Chemie*; Vol. 26.

(4) Anschütz, R.; Geldermann, H. *Justus Liebigs Ann. Chem.* **1891**, *261*, 129-138.

(5) Branda, N.; Grotzfeld, R. M.; Valdés, C.; Rebek, J., Jr. *J. Am. Chem. Soc.* **1995**, *117*, 85-88.

(6) Dunnavant, W. R.; James, F. L. *J. Am. Chem. Soc.* **1956**, *78*, 2740-2743.

(7) Butler, A. R.; Leitch, E. *J. Chem. Soc., Perkin Trans. 2* **1977**, 1972-1976.

(8) Mergen, F.; Poupaert, J. H.; de Keyser, J.-L.; Dumont, P. *Parmazie* **1989**, *44*, 110-112.

(9) Butler, A. B.; Leitch, E. *J. Chem. Soc., Perkin Trans. 2* **1980**, 103-105.

(10) Gilman, H.; Broadbent, H. S. *J. Am. Chem. Soc.* **1948**, *70*, 2619-2621.

(11) Somin, I. N.; Kuznetsov, S. G. *Chem. Abstr.* **1960**, 10950i.

(12) Krieg, B. *Chem. Ber.* **1969**, *102*, 371-373.

(13) Wasserman, N. H.; Erlanger, B. F. *Chem.-Biol. Interact.* **1981**, *36*, 251-258.

(14) Lachman, A. *J. Am. Chem. Soc.* **1921**, *43*, 577-581.

(15) Lachman, A. *J. Am. Chem. Soc.* **1921**, *43*, 2091-2097.

(16) Grotzfeld, R. M.; Branda, N. R.; Valdés, C.; Rebek, J. J. *NATO ASI Series, Series C: Mathematical and Physical Sciences* **1995**, *473, Supramolecular Stereochemistry;* Siegel, J.S. Ed., 195-198.

(17) Meissner, R. S.; Rebek, J., Jr.; de Mendoza, J. *Science* **1995**, *270*, 1485-1488.

(18) Grotzfeld, R. M.; Branda, N.; Rebek, J., Jr. *Science* **1996**, *271*, 487-489.

(19) Judice, J. K.; Cram, D. C. *J. Am. Chem. Soc.* **1991**, *113*, 2790-2791.

(20) Schrobilgen, G. J. In *NMR and the Periodic Table*; R. K. Harris and B. E. Mann, Ed.; Academic Press: London, 1978; pp 439-454.

(21) Brevard, C.; Granger, P. *Handbook of High Resolution Multinuclear NMR*; John Wiley and Sons: New York, 1981, pp 176-177.

(22) Dybowski, C.; Bansal, N.; Duncan, T. M. *Annu. Rev. Phys. Chem.* **1991**, *42*, 433-464.

(23) Branda, N. R. Ph.D. Thesis, Massachusetts Institute of Technology, 1994.

(24) Still, W. C.; Kahn, M.; Mitra, A. *J. Org. Chem.* 1978, *43*, 2923-2925.

Chapter 4

Glycoluril Derivatives with Specific Functionalities: Building Blocks for Self-Assembled Structures with Specific Properties

4.1
Introduction

In analogy to the solubility considerations discussed in Chapter 3, substituents on the glycoluril moieties can be chosen in a way to render specific properties to the assembly as a whole. One could think, for example, of substituents for metal coordination or charge accumulation. The introduction of redox-responsive or pH-sensitive functionalities might present a way to control the state of assembly. Specifically, the buildup of charge on the periphery of the assembly, e.g. through protonation of basic groups, was considered suitable to control an assembly through the pH of the surrounding medium. The expected behavior is outlined in figure ***4-1***:

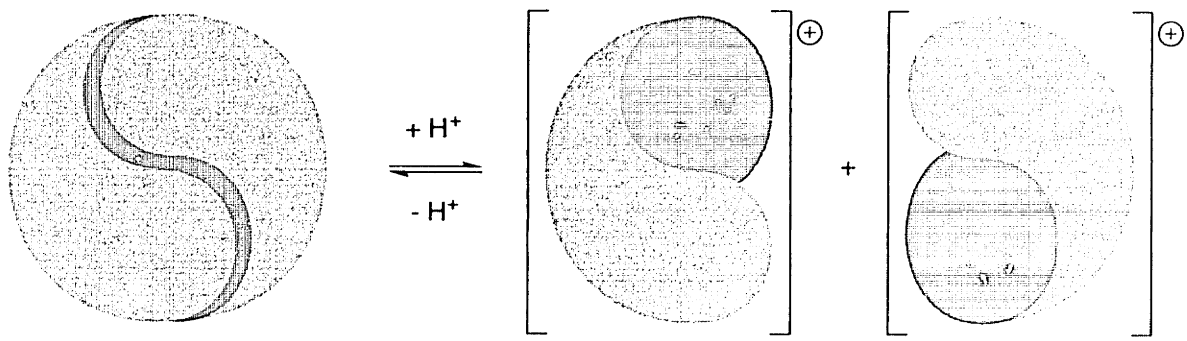

Figure *4-1*: Deliberate control of assembly and disassembly e.g. through protonation

A first attempt to effect this kind of behavior was suggested by Neil Branda. I synthesized a "tennis ball" based on dimethylamino substituted glycolurils, and Neil Branda performed the ^{1}H NMR studies[1-3].

4.2
Synthesis

The glycoluril candidate chosen was derived from 4,4'-*N*,*N*-dimethylamino-benzil **4.02**, and had been previously synthesized by condensation with urea under basic

conditions[4]. I found that even in this case, where the diketone features basic functions, a condensation under acidic conditions was more effective (see Chapter 3).

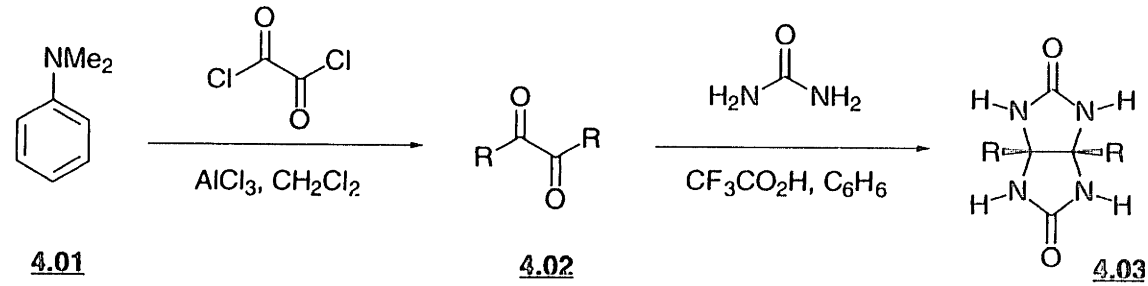

Figure 4-2: Improved synthesis of *N,N*-dimethylaminophenylglycoluril **4.03** R = *p*-Me_2N-C_6H_4 .

The alkylation of glycoluril **4.03** (R = *p*-Me_2N-C_6H_4) with tetrabromodurene was effected in the usual manner with potassium hydroxide in hot dimethyl sulfoxide. The amount of impurities due to side reactions was however much higher than in the synthesis of the previously known "tennis ball" derivatives based on the glycolurils **3.01** (R=Ph) and **3.18a** (R=CO_2Et). Presumably some alkylation took place on the dimethylamino groups as well, leading to polymeric quaternary ammonium salts which were insoluble in the water phase.

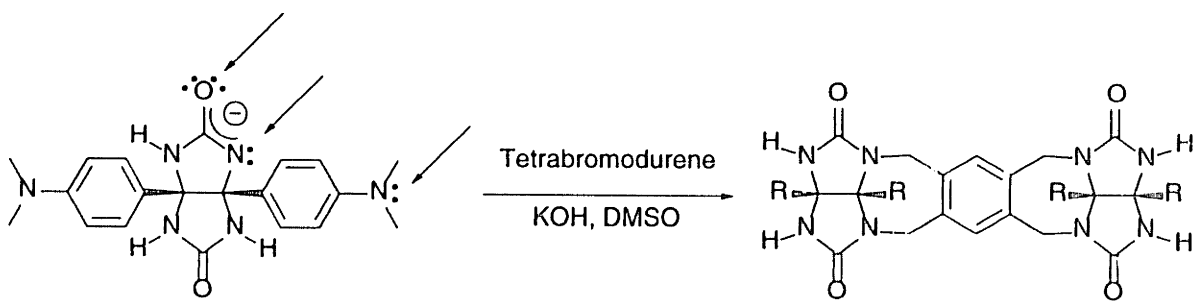

Figure 4-3: Alkylation of *N,N*-dimethylaminophenylglycoluril **4.03**. The arrows indicate possible alkylation sites after deprotonation, two out of three leading to undesired products.

4.3
Encapsulation Studies

The introduction of the polar dimethylamino groups increased the solubility of the "tennis ball" (**4.04**)$_2$ compared to (**4.05**)$_2$ (R=Ph). The NMR studies on the host-guest behavior of (**4.04**)$_2$ reported below were performed by Neil Branda. Small gaseous guest species were encapsulated in chloroform solution. The unusual properties of this particular "tennis ball" were observed in N,N-dimethylformamide-d_7 solution. Without the presence of a suitable guest, no assembly is observed. In the ^{1}H NMR spectrum all the glycoluril N-H protons appear in a region expected for non-hydrogen-bonded amide protons (figure *4-4*).

Once a suitable guest is added to the solution, a dynamic equilibrium between monomeric and dimeric species is observed. This indicates that an appropriate guest molecule induces enough favorable interactions to overcome the entropy decrease associated with the formation of a termolecular complex. If the dynamic assembly is now acidified with *p*-toluenesulfonic acid, the complex is gradually broken up and no more hydrogen-bonded N-H protons are observed in the ^{1}H NMR spectrum. Charge buildup on the presumably multiprotonated half-shells leads to electrostatic repulsion and drives the dimeric complex apart. Alternatively, protonation could induce a conformational change in the glycolurils which would distort the geometry of the dimer components and thereby prevent dimerization. Neutralization of the solution by addition of sodium carbonate removes the charges and allows the dimer to be formed again, as evidenced by the reappearance of a downfield N-H resonance in the ^{1}H NMR spectrum.

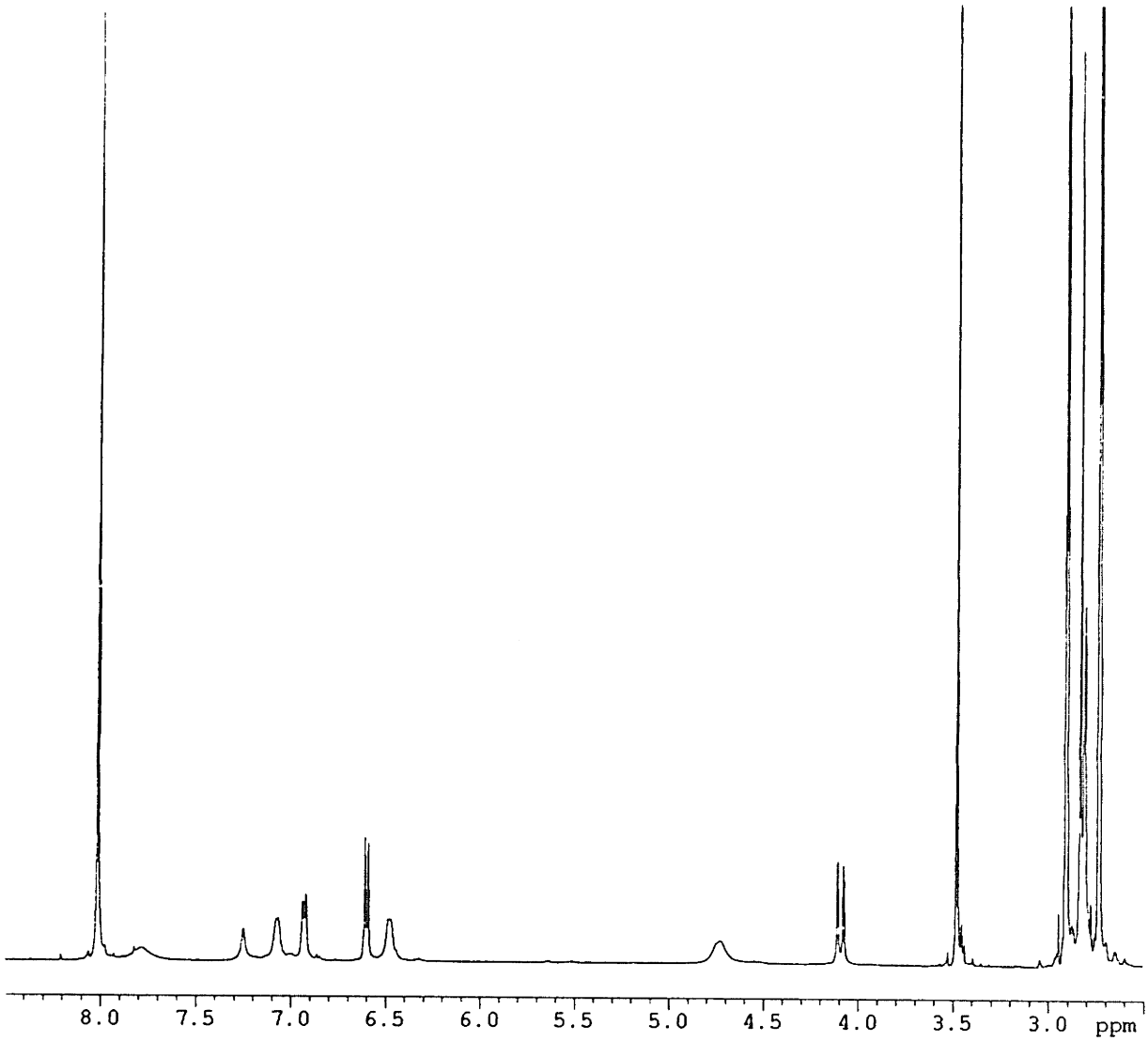

Figure *4-4*: ^{1}H NMR (DMF-d_7, 500 MHz, 23°C) spectrum of 4.04. In DMF-d_7 solution only the monomeric 4.04 is present. The signal for the non-hydrogen-bonded N-H can be seen at 7.8 ppm. Signals at 8.0, 2.9, and 2.7 ppm stem from DMF, at 3.5 ppm from water.

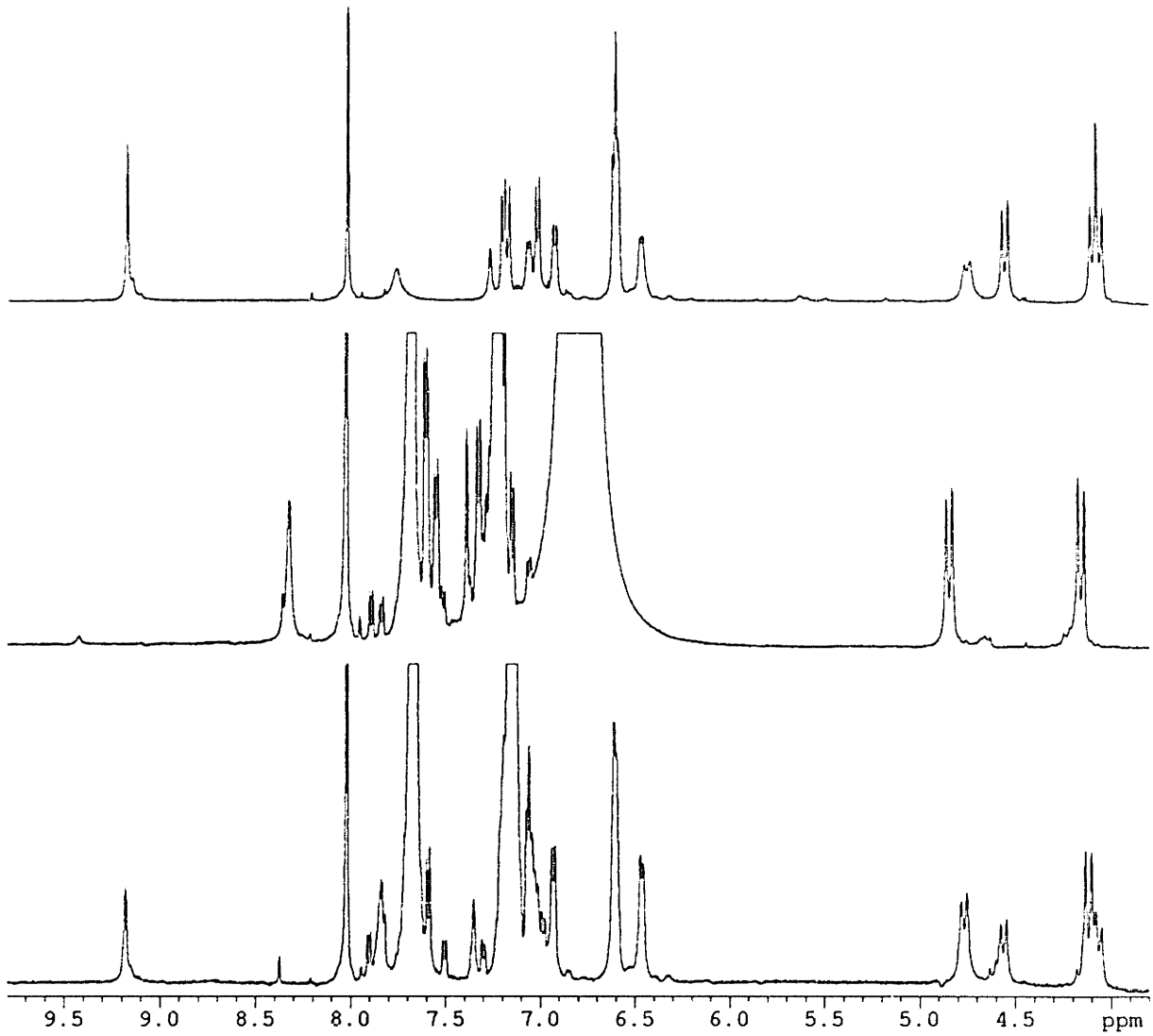

Figure *4-5*: ^{1}H NMR (DMF-d_7, 500 MHz, 23°C) spectra of 4.04. *Top*: After addition of xenon a mixture of monomeric and dimeric species is observed. The signal for the hydrogen-bonded N-H in the dimer appears at 9.2 ppm. *Center*: Addition of increasing amounts of *p*-toluenesulfonic acid breaks up the dimeric assembly as evidenced by the disappearance of the signal for hydrogen bound N-H. *Bottom*: Neutralization of the acid by addition of Na_2CO_3 allows the dimeric assembly to be formed again, nucleated by the residual xenon in solution, evidenced by the reappearance of the N-H signal at 9.2 ppm. Spectra taken from Neil Branda's Ph.D. thesis[1].

The overall scenario for the nucleation of assembly and pH-control of the assembly is depicted in figure *4-6*.

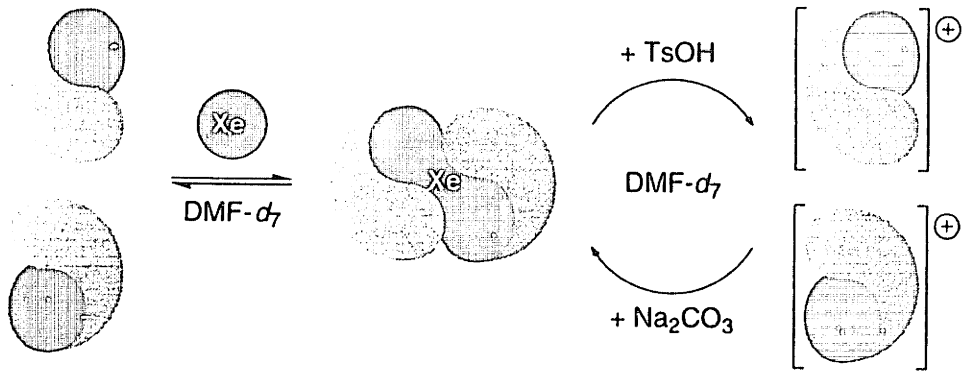

Figure *4-6*: Nucleation of the dimerization by xenon and reversible pH-dependent disassembly and assembly in DMF solution[1-3].

This experiment reveals a delicate balance between the entropic cost of a termolecular complex and the enthalpic profit of the weak intermolecular forces in the nucleated assembly. Even a solvent like N,N-dimethylformamide that can compete for the hydrogen bonds is released from the hydrogen bonding sites along the edge of the monomer provided the guest matches the size, shape and chemical linings in the cavity of the dimer. An additional factor favoring dimerization upon addition of xenon is the ethalpic gain from the release of solvent molecules from solvated xenon upon encapsulation by the host dimer.

4.4
Experimental

For general apparatus, methods, and materials information, see Chapter 3, page 53.

Bis(4-*N*,*N*-dimethylaminophenyl)benzil, 4.02

was prepared by a modified published procedure[5].

A 2000 ml flask equipped with a mechanical stirrer was charged with $AlCl_3$ (0.5 mol, 67 g) and flushed with argon. After addition of 100 ml dry CH_2Cl_2, a *N*,*N*-dimethylaniline (0.75 mol, 91 g, 95 ml) was added within 15 min. under external ice/water cooling. A solution of oxalyl chloride (0.125 mol, 15.9 g, 10.7 ml) in 100 ml dry CH_2Cl_2 was added, the intenal temperature being kept below 10°C. After completed addition the mixture was stirred 30 min. at room temperature, then heated to reflux for 1 h. The slurry was cooled to 0-5°C, and 100 g chipped ice was carefully added, followed by 200 ml icewater. The slurry was slowly stirred at room temperature overnight. The mixture was subjected to steam distillation until all the unreacted aniline had been removed (typically 5-6 liters of distillate volume). The solids in the distillation flask were collected by filtration and repeatedly leached out with boiling water. The crude green product was purified by flash chromatography (CH_2Cl_2, 0 → 2 % MeOH).

Yield: 24.7 g (67 %)

^{1}H NMR ($CDCl_3$, 300 MHz): δ 7.85 (d, $4H_{ar}$, J=9.3 Hz); 6.64 (d, $4H_{ar}$, J=9.3 Hz); 3.07 (s, 12H) ppm

^{13}C NMR ($CDCl_3$, 75 MHz): δ 194.1; 154.3; 132.4; 121.7; 111.0; 40.2 ppm

3a, 6a-bis(4-*N*,*N*-dimethylaminophenyl)-glycoluril, 4.03

A mixture of bis(4-*N*,*N*-dimethylamino)benzil (0.07 mol, 20.75 g), urea (0.15 mol, 9.0 g), trifluoroacetic acid (15 ml), and 250 ml benzene was heated to reflux 20 h using a Dean-Stark trap. Benzene and trifluoroacetic acid were removed by rotary evaporation and the residue was stirred in methanol overnight. The precipitate was collected by filtration, washed with methanol and acetone and dried.

Yield: 21.8 g (82 %)

^{1}H NMR (300 MHz, DMSO-d_6): δ 7.44 (s, $4H_{NH}$), 6.88 (d, $4H_{ar}$, J=8.7 Hz), 6.43 (d, $4H_{ar}$, J=8.7 Hz), 2.76 (s, 12H) ppm

(4-*N*,*N*-Dimethylamino)phenyl-"tennis ball" monomer, 4.04

To a suspension of 3a, 6a-bis(4-*N*,*N*-dimethylaminophenyl)-glycoluril (44.4 mmol, 16.89 g) in 200 ml DMSO at 100°C was added finely ground KOH (88.8 mmol, 4.98 g). After stirring for 15 minutes, tetrabromodurene (2.22 mmol, 1.0 g) was added. Stirring was continued for 60 minutes at 100°C. After cooling to rt the mixture was poured in 2500 ml water and the precipitate collected by filtration. The filtercake was thoroughly washed with water and after drying at 100°C was extracted with 300 ml boiling CH_2Cl_2. After evaporation of CH_2Cl_2 the residue was washed with boiling THF and acetone. The crude material was dissolved in CH_2Cl_2, stirred with charcoal, filtered, and evaporated. The residual material after evaporation of the filtrate was taken up in 25 ml methanol/CH_2Cl_2 (4:1), sonicated, filtered, washed with 1ml CH_2Cl_2, and dried under vacuum.
Yield: 180 mg (9 %)
^{1}H NMR (DMF-d_7, 500 MHz): δ 7.7-7.9 (br, $4H_{NH}$), 7.25 (s, $2H_{ar}$), 7.16 (br, $4H_{ar}$), 6.93 (d, $4H_{ar}$, J=8.5 Hz), 6.60 (d, $4H_{ar}$, J=9.0 Hz), 6.48 (br, $4H_{ar}$), 4.65-4.70 (br, 4H), 4.09 (d, 4H, J=15.5 Hz), 2.83 (s, 12H), 2.81 (s, 12H) ppm. (see also figure *4-4*)
HRMS calculated for $[M + H]^+$ $C_{50}H_{55}N_{12}O_4$ 887.4469, found 887.4476

4.5
References

(1) Branda, N. R. Ph.D. Thesis, Massachusetts Institute of Technology, 1994.

(2) Branda, N.; Grotzfeld, R. M.; Valdés, C.; Rebek, J., Jr. *J. Am. Chem. Soc.* **1995**, *117*, 85-88.

(3) Grotzfeld, R. M.; Branda, N. R.; Valdés, C.; Rebek, J. J. *NATO ASI Series, Series C: Mathematical and Physical Sciences* **1995**, *473, Supramolecular Stereochemistry;* Siegel, J.S. Ed., 195-198.

(4) Dunnavant, W. R.; James, F. L. *J. Am. Chem. Soc.* **1956**, *78*, 2740-2743.

(5) Tüzün, C.; Ogliaruso, M.; Becker, E. I. *Organic Syntheses*; Wiley: New York, 1973; Collect. Vol. V, pp 111-114.

Chapter 5

Towards a More Effective Synthesis of Self-Assembled Systems Based on the Glycoluril Moiety

5.1
Introduction

The traditional synthesis of "tennis ball"-type systems always involved alkylating a large excess of glycoluril with a polyhalogenated (aromatic) spacer in the final step. This approach had some negative consequences: **1)** The large excess of glycoluril needed (in order to prevent overalkylation) required facile access to the diketones from which the glycolurils were derived. Potentially interesting "tennis ball" derivatives based on diketones difficult to synthesize could not be made in this way. **2)** The desired isomer was isolated only in low yields from the polymeric byproducts. Scale-up of the synthesis was difficult due to the large amounts of solvent used in the workup.

An alternative route was sought in order to increase yields and facilitate product isolation. It has been described in the literature that if *N*-monosubstituted ureas are condensed with benzil in the same way the traditional glycoluril synthesis is carried out, disubstituted glycolurils are obtained[1-3].

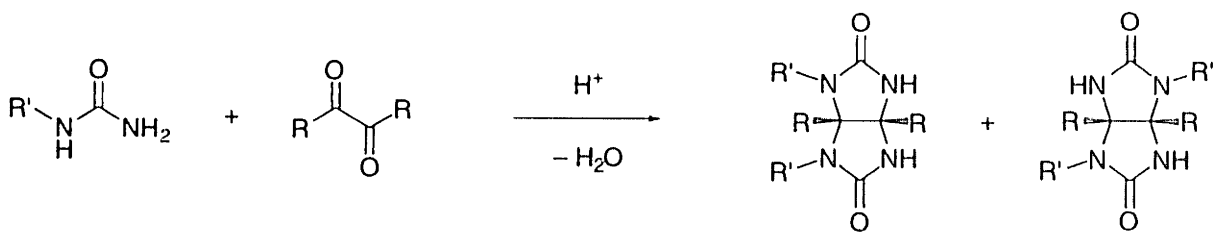

Figure *5-1*: Condensation of *N*-monosubstituted ureas with diketones[1-3].

5.2
Tethered Bisureas

The condensation of *N*-monosubstituted ureas with diketones gives predominantly the *cis*-isomer[3,4]. I therefore attempted to effect an intramolecular condensation on tethered ureas, i.e. to build up the glycoluril moiety directly on the spacer. Two test systems were devised to elucidate the viability of this approach: One (fig. *5-2*), in which a seven-

membered ring would be formed in the cyclization, a mimic of the "tennis balls" derived from phenyl spacers[5-11]. The other (fig. *5-3*), in which a six-membered ring would be formed, analogous to the "small tennis ball" based on an ethylene spacer[10,12].

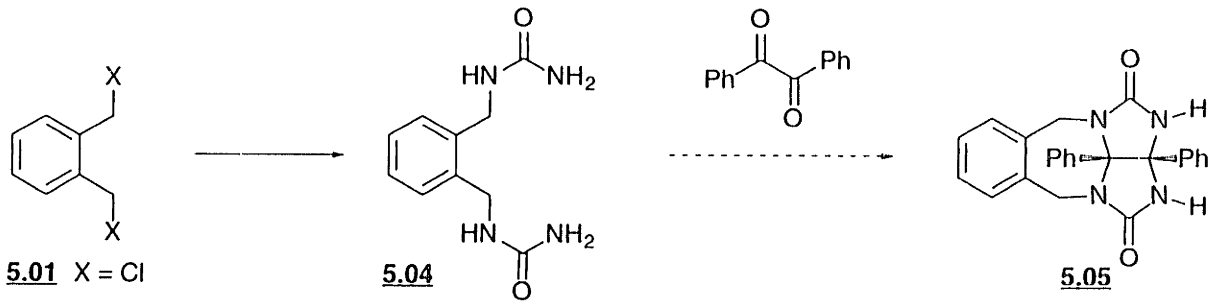

5.01 X = Cl

5.02 X = N_3

5.03 X = NH_3Cl

5.04

5.05

Figure *5-2*: Test system for intramolecular glycoluril condensation generating a seven-membered ring. The *cis*-2-butene- and butane-derived analogs of **5.04** were also prepared.

Attempts to reproduce the synthesis of the bisurea **5.04** by alkylation of urea with 1,2-bis(chloromethyl)benzene[13] showed that a more effective procedure was required. Therefore, the ureas were prepared by reacting the appropriate amines with alkaline cyanates[14]. The required diamines were conveniently prepared by either Gabriel synthesis or hydrogenation of azides[15].

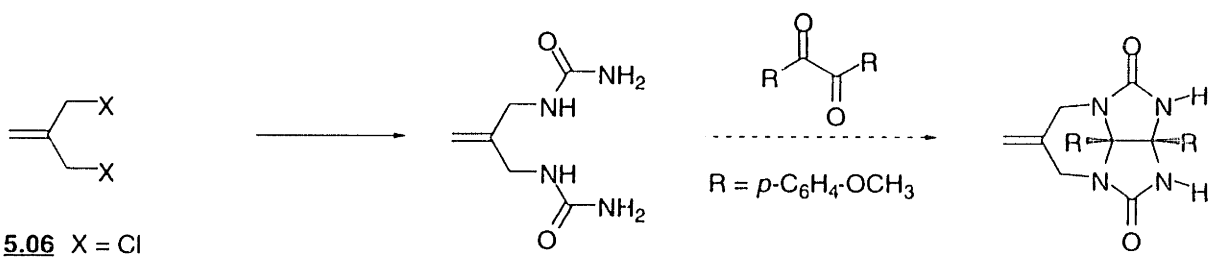

5.06 X = Cl

5.07 X = phthalimido

5.08 X = NH_3Cl

5.09

5.10

Figure *5-3*: Test system for intramolecular glycoluril condensation generating a six-membered ring.

While the bisureas could be easily prepared in both cases, all attempts failed to effect a condensation with diketones. The condensation reactions were followed by TLC and compared to authentic samples prepared the traditional way from glycoluril alkylation.

Under acidic conditions, mostly starting material was recovered in both cases. In the case of the six-membered ring (**5.10**), a faint TLC spot of the same R_f as the authentic material was observed after 24 h reaction time. Apparently the ring formation is accompanied by increase in strain, leading to dramatic rate reduction. Basic conditions were used only for 1,4-bisureido-butane **5.12** and gave a mixture of starting material and the bishydantoin **5.13** (fig. *5-4*).

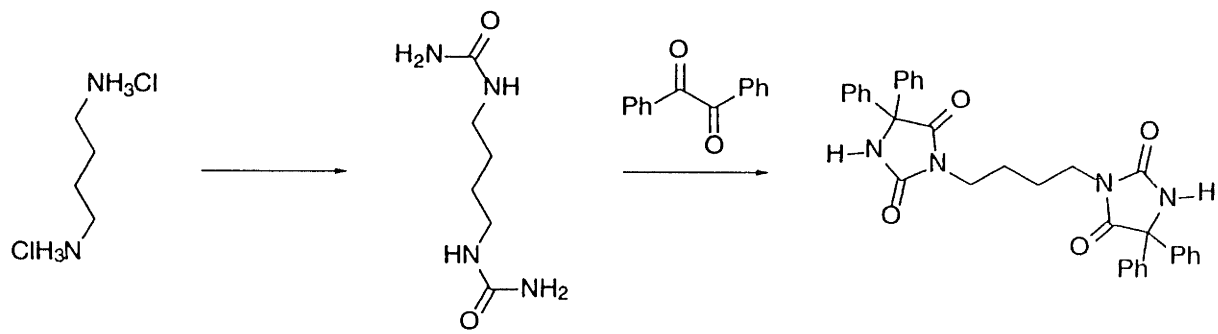

5.11 **5.12** **5.13**

Figure *5-4*: Attempt to effect intramolecular glycoluril condensation under basic conditions.

This finding came to no surprise since the reaction of monosubstituted ureas with diketones under basic conditions is known to lead to hydantoins via rearranged phenyl groups[16-18].

5.3
cis-Bisprotected Glycolurils

A different, promising approach for a more effective synthesis of "tennis ball" systems has been suggested by Dr. Tomas Szabó[19]. As already pointed out in the previous section, the condensation of *N*-alkylureas with benzils under acidic conditions yields predominantly *cis*-dialkyl-glycolurils. The proposed mechanism[3] is outlined in figure *5-5*.

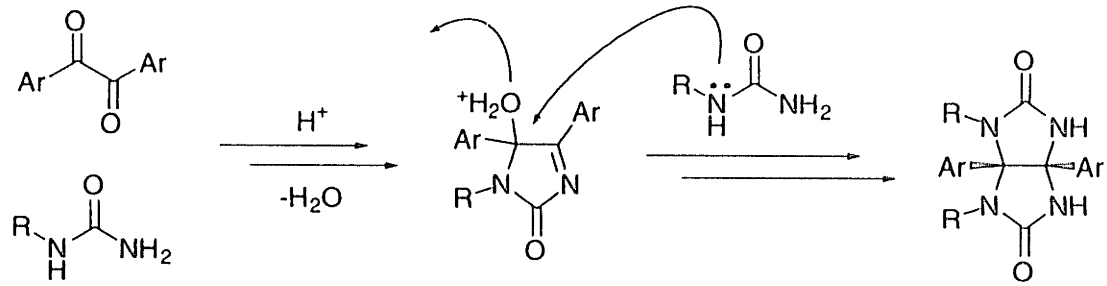

Figure *5-5*: Rationale for the formation of cis-dialkylated glycolurils.

The intermediate condensation product **5.16** in its protonated state features the good leaving group water. Attack by the more nucleophilic nitrogen in *N*-methylurea then defines the resulting cis-substitution product. Appropriately chosen monosubstituted ureas would therefore lead to *cis*-disubstituted glycolurils in which the *N*-substituents represent protecting groups. The goal was to synthesize *cis*-diprotected glycolurils which could be alkylated by stoichiometric amounts of spacer molecules. The glycoluril-*N*-substituents were chosen in such a way that they could be cleaved after the alkylation step. An electron rich benzil derivative, especially the 4-methoxybenzyl group was the obvious choice for the case at hand[20]. The synthesis is outlined in figure ***5-6***. Dr. Rudkevich found that the oxidative deprotection reaction with cerium ammonium nitrate (CAN)[21,22] is an appropriate method for cleavage of the 4-methoxybenzyl protecting group. However, the use of CAN in the deprotection step puts a constraint on the R groups that can be chosen for the glycoluril **5.20**. Since all electron-donating substituted aromatics are activated for the CAN oxidation, the glycolurils cannot contain any methoxy- or dimethylamino-phenyl groups, for example. The first successful synthesis of a "tennis ball" system using this new approach was performed by Dr. Rudkevich with **5.20a**, R = *p*-Me-C_6H_4[23].

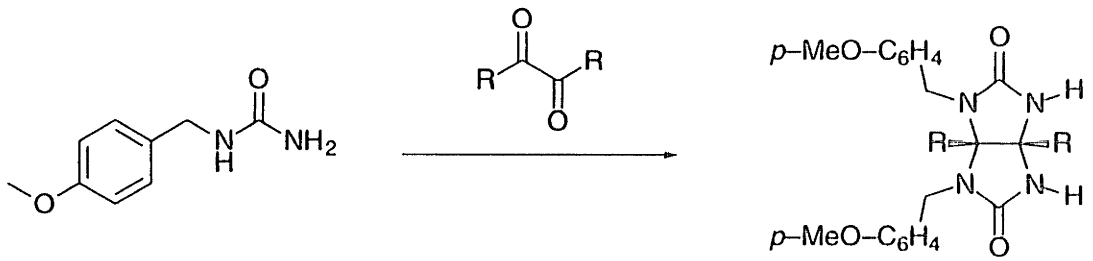

5.18 **5.19** **5.20**

Figure *5-6*: Synthesis of *cis*–disubstituted glycolurils with removable substituents.

To increase the versatility of this new method, I planned to enhance the solubility of the compounds. As mentioned in Chapter 3, 4,4'-dimethylbenzil derivatives of increased solubility (e.g. **5.24**) can readily be obtained from 4,4'-dimethylbenzoin **5.21** as shown in figure *5-7*.

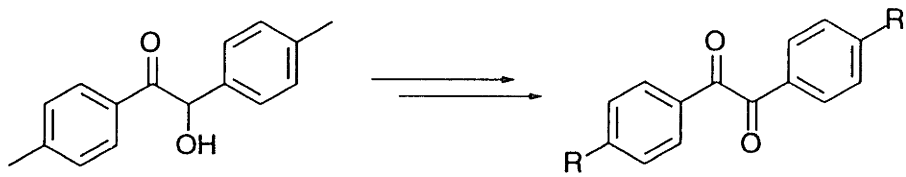

5.21

5.22 R = CH_3

5.23 R = CH_2Br

5.24 R = CH_2OCH_3

Figure *5-7*: Synthesis of diketones derived from 4,4'-dimethylbenzoin **5.21**.

I prepared the *cis*–protected glycoluril **5.20b** (R = *p*-$MeOCH_2$-C_6H_4) and reacted it with tetrakis(bromomethyl)benzene to test the stability of the functionalized derivatives under the deprotection conditions. While the alkylation with the spacer was easily accomplished, effective deprotection of **5.25** could not be achieved.

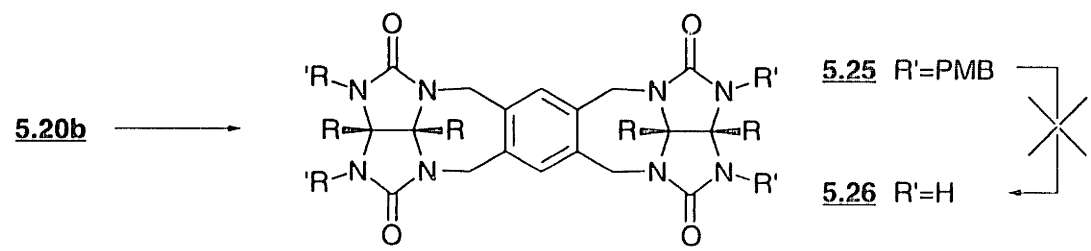

5.25 R'=PMB

5.26 R'=H

R = *p*-C_6H_4-CH_2OCH_3

Figure *5-8*: Planned "tennis ball" synthesis based on *cis*-diprotected glycolurils.

After 18 hours reaction time, a complex mixture was obtained which still contained some unreacted **5.25**. No tetra-deprotected compound **5.26** could be isolated. An attempt to deprotect the *cis*-glycoluril **5.20b** alone confirmed that CAN does not discriminate very well between the aromatics and therefore also oxidizes the glycoluril-methoxy-methylphenyl groups. Ongoing investigations by Dr. Szabó focus on the use of dimethoxybenzylureas which will allow the protecting groups to be cleaved off under milder conditions than CAN[19].

5.4
Experimental

For general apparatus, methods, and materials information, see Chapter 3, page 53.

1,2-Bis(azidomethyl)benzene, 5.02

was prepared analogous to a published procedure[24].

1,2-Bis(chloromethyl)benzene (20 mmol, 3.50 g) and methanol (45 ml) was added to a slurry of sodium azide (50 mmol, 3.25 g) in water (5ml) and the mixture was heated to reflux overnight. Methanol was evaporated, the residue taken up in water (80 ml) and extracted with ether (2 x 50 ml). The combined organic phases were dried over $MgSO_4$ and evaporated.

Yield: 3.7 g (quantitative)

^1H NMR ($CDCl_3$, 300 MHz): δ 7.39 (m, $4H_{ar}$); 4.43 (s, 4H) ppm

1,2-Bis(aminomethyl)benzene dihydrochloride 5.03

A slurry of 1,2-bis(azidomethyl)benzene (20 mmol, 3.7 g) and Pd/C (10%, 100 mg) in ethanol (50 ml) was placed in a Parr shaker and hydrogenated at 50 psi for 4 h. After filtration through Celite, HCl conc. (5 ml) was added and the mixture was evaporated to dryness. The residue was taken up in 10 ml THF/methanol (1:1), filtered, washed with 10 ml THF/methanol (1:1), and dried under vacuum.

Yield: 3.52 g (84%)

^1H NMR (DMSO-d_6, 300 MHz): δ 8.63 (b, $6H_{NH}$); 7.60–7.54 (m, $2H_{ar}$); 7.47–7.41 (m, $2H_{ar}$); 4.15 (d, 4H, J=4.8 Hz) ppm

^{13}C NMR (DMSO-d_6, 75 MHz): δ 133.3; 130.5; 128.7; 39.2 ppm

1,2-Bis(ureidomethyl)benzene, 5.04

A solution of potassium cyanate (40 mmol, 3.3 g) in 10 ml water was added to a solution of 1,2-bis(aminomethyl)benzene dihydrochloride (18 mmol, 3.8 g) in 10 ml water and the mixture was evaporated to dryness on a steam bath. The residue was taken up in 5 ml water sonicated, filtered, and washed with 5 ml water. The crude product was recrystallized from methanol.

Yield: 1.88 g (47%)

^{1}H NMR (DMSO-d_6, 300 MHz): δ 7.26–7.16 (m, 4H_{ar}); 6.35 (t, 2H_{NH}, J=5.9 Hz); 5.52 (s, 4H_{NH}); 4.20 (d, 4H, J=6.0 Hz) ppm

1,4-Diamino-*cis*-2-butene dihydrochloride

was prepared by acidic hydrolysis of 1,4-diphthalimido-*cis*-2-butene according to a published procedure[25].

^{1}H NMR (DMSO-d_6, 300 MHz): δ 8.25 (b, 6H_{NH}); 5.79 (t, 2H, J=4.7 Hz); 3.55 (d, 4H, J=4.8 Hz) ppm

1,4-Diureido-*cis*-2-butene

A solution of 1,4-diamino-*cis*-2-butene dihydrochloride (4 mmol, 645 mg) in 5 ml water was added to a solution of potassium cyanate (9 mmol, 730 mg) in 2 ml water and evaporated on a steam bath until crystallization began. After cooling to room temperature the crystals were filtered off, washed with 5 ml water and 5 ml methanol.

Yield: 304 mg (44%)

^{1}H NMR (DMSO-d_6, 300 MHz): δ 5.99 (t, 2H_{NH}, J=5.4 Hz); 5.44 (s, 4H_{NH}); 5.36 (t, 2H_{CH}, J=4.2 Hz); 3.62 (t, 4H_{CH}, J=5.3 Hz) ppm

1,4-Diureidobutane, 5.12

A concentrated aqueous solution of potassium cyanate (90 mmol, 7.3 g) was given to a concentrated aqueous solution of putrescin hydrochloride **5.11** (40 mmol, 6.44 g) and the mixture was concentrated on a steam bath until crystallization began. After sitting at room temperature overnight the product was filtered off, washed with 10 ml water, and dried under vacuum.

Yield: 5.96 g (86%)

^{1}H NMR (DMSO-d_6, 300 MHz): δ 5.90 (t, 2H_{NH}, J=5.6 Hz); 5.34 (s, 4H_{NH}); 2.93 (m, 4H_{CH}, J=5.7 Hz); 1.32 (m, 4H_{CH}) ppm

3-Phthalimido-2-phthalimidomethyl-1-propene, 5.07

was prepared according to a modified literature procedure[26].

3-Chloro-2-chloromethyl-1-propene **5.06** (10 mmol, 1.25 g) and potassium phthalimide (30 mmol, 5.6 g) was heated to 100°C in DMF (20 ml) for 3h, then heated to reflux overnight. After cooling to 100°C the mixture was poured in 150 ml water, and the precipitate was filtered off. The crude product was suspended in sat. aq. $NaHCO_3$ solution, stirred

vigorously for 30 minutes, and collected by filtration. The filter cake was washed with water, methanol, and ether, and dried under vacuum.
Yield: 2.62 g (76%, Lit[26]: 60%)
^{1}H NMR ($CDCl_3$, 300 MHz): δ 7.87-7.84 (m, $4H_{ar}$); 7.74-7.71 (m, $4H_{ar}$); 5.12 (s, 2H); 4,35 (s, 4H) ppm

3-Amino-2-aminomethyl-1-propene dihydrochloride, 5.08

was prepared according to a modified literature procedure[26].
Hydrazine hydrate (11 mmol, 0.6 ml) was added to a refluxing mixture of 3-phthalimido-2-phthalimidomethyl-1-propene **5.07** (5 mmol, 1.73 g) in ethanol (50 ml). After heating to reflux for 3 h, HCl conc. (15 ml) was carefully added through the condenser and the mixture was further heated to reflux for 3 h. After cooling to room temperature, the insoluble material was filtered off and the filtrate evaporated. The evaporation residue was taken up in 20 ml water, and after removal of the insoluble material used directly for the synthesis of the corresponding bisurea.

3-Ureido-2-ureidomethyl-1-propene, 5.09

A solution of potassium cyanate (11 mmol, 0.89 g) in 20 ml water was added to the crude solution of 3-amino-2-aminomethyl-1-propene dihydrochloride **5.08** (max. 5 mmol) and the mixture was evaporated on a steam bath in a crystallizing dish. The crude bisurea was washed with 5 ml water, and 5 ml methanol.
Yield: 0.45 g (52%, based on the bisphthalimido compound)
^{1}H NMR (DMSO-d_6, 300 MHz): δ 6.08 (t, $2H_{NH}$, J=4.7 Hz); 5.49 (s, $4H_{NH}$); 4.83(s, 2H); 3.54 (d, 4H, J=5.7 Hz) ppm

General attempt for acidic condensation of bisureas with benzil

An mixture of bisurea (1 mmol), benzil (1 mmol) [4,4'-dimethylbenzil in the case of 3-ureido-2-ureidomethyl-1-propene, **5.09**], 0.2 ml trifluoroacetic acid and 50–250 ml solvent (benzene, toluene, xylenes) was heated to reflux using a Dean-Stark trap. The reaction was monitored by TLC with authentic product material as reference.

Attempt for basic glycoluril condensation. 1,4-Bis(hydantoin) 5.13

A solution of 1,4-diureidobutane (1 mmol, 174 mg), benzil (1 mmol, 210 mg), and KOH (0.1 mmol, 5 mg) was heated to reflux in 250 ml ethanol overnight. The solvent was

evaporated, the residue taken up in 20 ml methanol, sonicated, filtered off, washed with methanol and dried under vacuum.

Yield: 105 mg (38%, based on 0.5 mol theoretical yield)

^{1}H NMR (DMSO-d_6, 300 MHz): δ 9.61 (s, $2H_{NH}$); 7.40–7.25 (m, $20H_{Ph}$); 3.45 (m, 4H); 1.47 (m, 4H) ppm

Reference Compounds:

dibromoxylene + phenyl-glycoluril, 5.05

This reference compound was obtained from Dr. René Wyler[27]

***cis*–dichlorobutene + phenyl-glycoluril**

This reference compound was obtained from Neil Branda[28]

dichloroisobutene + di(4-methoxyphenyl)glycoluril, 5.10

To a solution of di(4-methoxyphenyl)glycoluril (25 mmol, 8,9 g) in 200 ml DMSO heated to 50°C was added potassium *tert*-butoxide (50 mmol, 5.6 g) in 10 ml DMSO. A solution of 3-Chloro-2-chloromethyl-1-propene **5.06** (2.5 mmol, 313 mg) in 10 ml DMSO was added and the mixture was stirred at 50°C for 30 minutes. The slurry was poured in 1800 ml ice water and acidified with conc. HCl. The precipitate was filtered off, washed thoroughly with water, and dried. The material was boiled with 500 ml $CHCl_3$, filtered, and the filtrate evaporated. The residue after evaporation was triturated with Et_2O, taken up in $CHCl_3$ and filtered. The filtrate was purified by column chromatography (CH_2Cl_2, 0 → 2 % MeOH) to give a small amount of dialkylated product and a larger fraction of the monoalkylated product **5.10**.

Yield: 451 mg (45%)

^{1}H NMR ($CDCl_3$, 300 MHz): δ 7.14 (d, $2H_{ar}$, J=8.9Hz); 7.06 (d, $2H_{ar}$, J=8.8Hz); 6.67 (d, $2H_{ar}$, J=8.9Hz); 6.63 (d, $2H_{ar}$, J=8.9Hz); 5.52 (s, $2H_{NH}$); 5.02 (s, 2H); 4.48 (d, 2H, J=15.4Hz); 3.71 (s, 3H); 3.69 (s, 3H); 3.48 (d, 2H, J=15.1Hz) ppm

Dialkylated product:

^{1}H NMR ($CDCl_3$, 250 MHz): δ 7.06 (d, $4H_{ar}$, J=8.7Hz); 6.66 (d, $4H_{ar}$, J=8.7Hz); 4.98 (s, 4H); 4.48 (d, 4H, J=15.2Hz); 3.71 (s, 6H); 3.52 (d, 4H, J=15.0Hz) ppm

4-Methoxybenzylurea, 5.18

was prepared according to a modified procedure[20]

A solution of 4-methoxybenzylurea (0.1 mol, 13.7 g) in 30 ml water was neutralized with halfconc. aq. HCl and a solution of potassium cyanate (0.1 mol, 8.1 g) in 30 ml water was added. The mixture was heated on a steam bath until for 2 h. The crystalline mass was collected by filtration, washed with water, and dried under vacuum.

Yield: 15.3 g (85 %)

^{1}H NMR (DMSO-d_6, 300 MHz): δ 7.16 (d, $2H_{ar}$, J=9.0Hz); 6.87 (d, $2H_{ar}$, J=7.8Hz); 6.31 (t, H_{NH}, J=6 Hz); 5.44 (s, $2H_{NH}$); 4.09 (d, 2H, J=6.9Hz); 3.72 (s, 3H) ppm

1,6–Bis(4–methoxybenzyl)–3a,6a–bis(4–methoxymethylphenyl)glycoluril, 5.20b

A mixture of 4,4'–bis(methoxymethyl)benzil 5.18 (10 mmol, 2.98 g), 4-methoxybenzylurea (20 mmol, 3.60 g) and 0.5 ml TFA in 50 ml benzene was heated to reflux under a Dean-Stark trap overnight. The resulting solution was evaporated completely, dissolved in 40 ml benzene, cooled in an ice bath, and ether was added until the mixture became cloudy. The mixture was allowed to crystallize in a refrigerator, with occasional sonication. The solids were filtered off, washed with methanol and recrystallized from methanol. Evaporation of the mother liquor and renewed crystallization from ethanol gave a second product crop.

Yield: 2.80 g (45 %)

^{1}H NMR ($CDCl_3$, 300 MHz): δ 7.12 (pd, $6H_{ar}$, J=8.4Hz); 7.34 (d, $2H_{ar}$, J=8.4Hz); 6.92 (d, $2H_{ar}$, J=8.4Hz); 6.80 (d, $4H_{ar}$, J=9.0Hz); 6.71 (d, $2H_{ar}$, J=8.7Hz); 5.49 (s, $2H_{NH}$); 4.38 (d, 2H, J=16.2Hz); 4.27 (s, 2H); 4.26 (s, 2H); 3.90 (d, 2H, J=16.2Hz); 3.77 (s, 6H); 3.25 (s, 3H); 3.24 (s, 3H) ppm

Tetrakis(PMB-protected)-"tennis ball" monomer, 5.25

Potassium *tert*-butoxide (0.87 mmol, 391 mg) was added to a solution of 1,6–bis(4–methoxybenzyl)–3a,6a–bis(4–methoxymethylphenyl)glycoluril (1.74 mmol, 1.08 g) in 10 ml DMSO. The mixture was sonicated and stirred until a solution had formed, and a solution of tetrakis(bromomethyl)benzene in 10 ml DMSO was added. The mixture was stirred 30 min at room temperature, and consumption of starting material was checked by TLC (CH_2Cl_2, 5% MeOH). The reaction was quenched by pouring in 600 ml aq. HCl

(5:1), the precipitate filtered off, washed thoroughly with water, and drained well. The solids were boiled in 50 ml methanol, and filtered while hot.
Yield: 714 mg (60 %)
^{1}H NMR ($CDCl_3$, 300 MHz): δ 7.54 (s, $2H_{ar}$); 7.10 (d, $4H_{ar}$, J=8.7Hz); 7.02 (d, $4H_{ar}$, J=8.4Hz); 7.92 (d, $4H_{ar}$, J=8.4Hz); 6.88 (d, $8H_{ar}$, J=8.7Hz); 6.76 (d, $4H_{ar}$, J=8.4Hz); 6.67 (d, $8H_{ar}$, J=8.7Hz); 4.96 (d, $4H_{ar}$, J=15.9Hz); 4.30 (s, $4H_{ar}$); 4.26 (s, $4H_{ar}$); 4.25 (pd, $8H_{ar}$, J=15.9Hz); 3.80 (d, 4H, J=16.2Hz); 3.70 (s, 12H); 3.26 (s, 6H); 3.25 (s, 6H) ppm

Attempt for deprotection of 5.25, Methoxymethylphenyl–"tennis ball"

To a solution of **5.25** (0.5 mmol, 686 mg) in a mixture of 40 ml CH_3CN and 10 ml H_2O was added cerium ammonium nitrate (8.0 mmol, 4.39 g) and the mixture was stirred at room temperature overnight. The slurry was poured in 600 ml water and the precipitate filtered off. The filter cake was washed with MeOH, the residue boiled in CH_2Cl_2, sonicated, and filtered. The residue after filtration (65 mg) contained mainly unreacted starting material. The MeOH wash solution was evaporated, and the evaporation residue taken up in CH_2Cl_2. Separation of the more soluble product fractions by column chromatography did not yield any desired product.

5.5

References:

(1) Biltz, H. *Chem. Ber.* **1907**, *40*, 4806-4816.

(2) Nematollahi, J.; Ketcham, R. *J. Org. Chem.* **1963**, *28*, 2378-2380.

(3) Butler, A. B.; Leitch, E. *J. Chem. Soc., Perkin Trans. 2* **1980**, 103-105.

(4) Butler, A. R.; Hussain, I. *J. Chem. Soc. Perkin Trans. 2* **1981**, 310-316.

(5) Wyler, R.; de Mendoza, J.; Rebek, J., Jr. *Angew. Chem. Int. Ed. Engl.* **1993**, *32*, 1699-1701.

(6) Branda, N.; Wyler, R.; Rebek, J., Jr. *Science* **1994**, *263*, 1267-1268.

(7) Branda, N.; Grotzfeld, R. M.; Valdés, C.; Rebek, J., Jr. *J. Am. Chem. Soc.* **1995**, *117*, 85-88.

(8) Valdés, C.; Spitz, U. P.; Kubik, S. W.; Rebek, J., Jr. *Angew. Chem. Int. Ed.* **1995**, *34*, 1885-1887.

(9) Meissner, R. S.; Rebek, J., Jr.; de Mendoza, J. *Science* **1995**, *270*, 1485-1488.

(10) Valdés, C.; Spitz, U. P.; Toledo, L. M.; Kubik, S. W.; Rebek, J., Jr. *J. Am. Chem. Soc.* **1995**, *117*, 12733-12745.

(11) Grotzfeld, R. M.; Branda, N.; Rebek, J., Jr. *Science* **1996**, *271*, 487-489.

(12) Valdés, C.; Rebek, J., Jr. *Chem., Eur. J.* **1996**, in press.

(13) Dauth, C.; Becker, H. G. O. *J. Prakt. Chem.* **1971**, *313*, 686-698.

(14) Houben-Weyl *Methoden der Organischen Chemie*; Georg Thieme Verlag: Stuttgart, 1952; Vol. 8, pp 156-157.

(15) Moore, A. T.; Rydon, H. N. *Organic Syntheses*; Wiley: New York, 1973; Collect. Vol. V, pp 586-589.

(16) Dunnavant, W. R.; James, F. L. *J. Am. Chem. Soc.* **1956**, *78*, 2740-2743.

(17) Butler, A. R.; Leitch, E. *J. Chem. Soc., Perkin Trans. II* **1977**, 1972-1976.

(18) Mergen, F.; Poupaert, J. H.; de Keyser, J.-L.; Dumont, P. *Parmazie* **1989**, *44*, 110-112.

(19) Szabo, T., unpublished results.

(20) Moschel, R. C.; Hudgins, W. R.; Dipple, A. *J. Org. Chem.* **1986**, *51*, 4180-4185.

(21) Yoshimura, J.; Yamaura, M.; Suzuki, T.; Hashimoto, H. *Chem. Lett.* **1983**, 1001-1002.

(22) Yamaura, M.; Suzuki, T.; Hashimoto, H.; Yoshimura, J.; Okamoto, T.; Shin, C. *Bull. Chem. Soc. Jpn.* **1985**, *58*, 1413-1420.

(23) Rudkevich, D., unpublished results.

(24) Sommers, A. H.; Barnes, J. D. *J. Am. Chem. Soc.* **1957**, *79*, 3491-3492.

(25) Amundsen, L. H.; Mayer, R. H.; Pitts, L. S.; Malentacci, L. A. *J. Am. Chem. Soc.* **1951**, *73*, 2118-2121.

(26) Schulze, K.; Winkler, G.; Dietrich, W.; Mühlstädt, M. *J. Prakt. Chem.* **1977**, *319*, 463-474.

(27) Wyler, R., unpublished results.

(28) Branda, N. R., unpublished results.

Chapter 6

A Self-Complementary Monomer Forming a D_{3d}-Symmetric Dimeric Capsule

6.1
Introduction

In continuation of the work on molecules forming three–dimensional pseudo–spherical structures upon self–assembly (see previous chapter), our goal was to develop a self–assembling host system larger than the previous ones[1-3]. The new system was intended to be a dimeric assembly, strongly held together by many hydrogen bonds, which would encapsulate molecules of the size of benzene or cyclohexane.

6.2
Design Considerations

Based on the successful design of the "first generation tennis balls", our plan was to use the combination of an appropriate aromatic spacer and glycoluril moieties. The main design constraint is the width of the "gap" between the glycoluril moieties which is defined by the length of the spacer. Too large a distance prevents the formation of equal hydrogen bonds on both sides of the glycolurils. A too narrow "gap" prevents the glycoluril units from the two host monomers from interlocking, just like a small and a large hand can not execute a "matching" handshake.

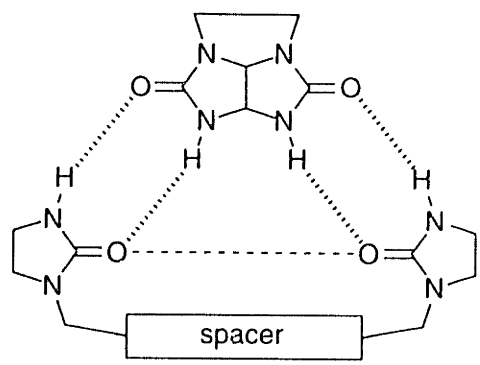

In order to keep the distance between the glycoluril carbonyl–oxygen atoms in the same range as in the older design, we made a switch from C_2 to C_3–symmetry. This is best

illustrated in figure ***6-1***, which shows a comparison of various geometries of assemblies based on C_2-symmetric tennis ball-monomers and the new C_3–symmetric monomer.

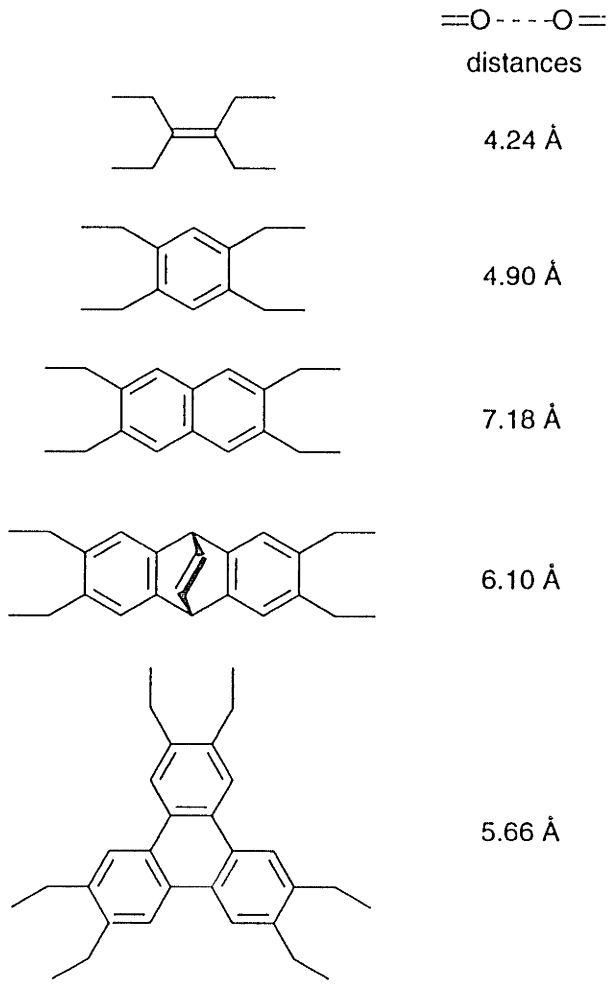

Figure *6-1*: Comparison of critical distances in the monomers depending on the underlying spacer. The atomic distances were obtained from molecular modeling[4] using the MM2 force field.

The close resemblance between the assemblies based on phenyl and triphenylene spacer, i.e. almost identical critical distances, can be seen in figure ***6-1***. The higher symmetry in the case of the triphenylene spacer also increases the number of hydrogen bonds within the assembly. Twelve instead of eight hydrogen bonds can now be formed between the two monomers upon dimerization.

The volume of the new design is substantially larger than the volume of the first-generation "tennis ball" assembly. The approximate dimensions of the inner cavity of the two host systems are shown in figure ***6-2***.

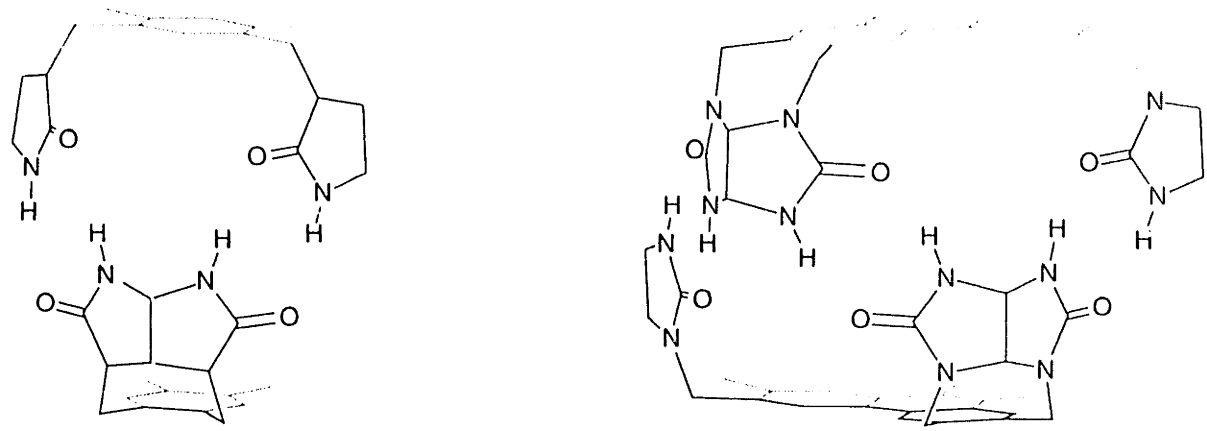

height 7.10 Å
approx. Ø 6.56 Å

height 7.30 Å
approx. Ø 9.76 Å

Figure *6-2*: Approximate dimensions of the cavity within the dimeric assemblies. The atomic distances were obtained from molecular modeling[4] using the MM2 force field. Heights and diameters represent the effective distance (atomic distance minus two van der Waal's radii) between the aromatic spacers and between glycoluril oxygen atoms on opposite sides of the cavity, respectively.

6.2.1
Appropriate Spacers

Similar to the previous host monomers, the synthesis of the new system would be based on a bromomethyl substituted aromatic system (figure ***6-3***), in this case hexakis(bromomethyl)triphenylene (X = CH) or corresponding heterocyclic systems, i.e. hexaazatriphenylene (X = N). Alkylation of an excess of glycoluril with a spacer gives a mixture of isomers. A higher symmetry of the spacer increases the complexity of the isomer mixture. However, in the case at hand only two isomers are formed with the desired all-*cis* isomer in 25% statistical yield. Previous experience gained from similar systems indicated that isomer separation can be achieved by column chromatography.

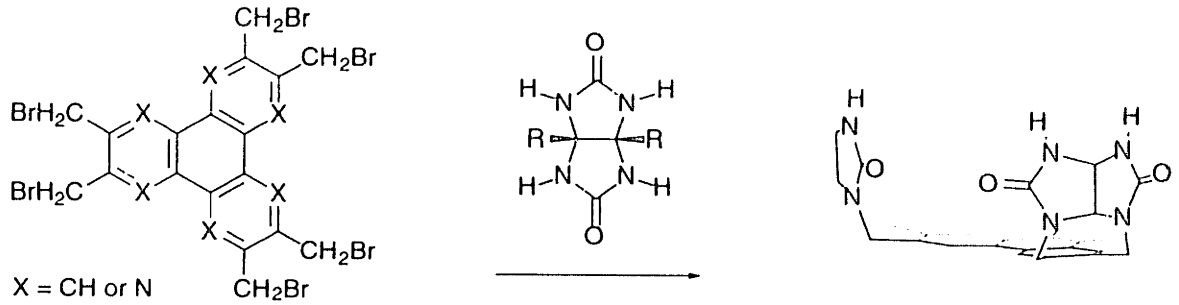

Figure *6-3*: Triple alkylation of a D_{3h}-symmetric spacer giving the desired C_{3v}-symmetric in 25% statistical yield.

None of the required hexahalo–derivatives had been described in the literature. Several carbon substituted hexaazatriphenylene derivatives of the appropriate symmetry were known, therefore the heterocyclic spacer at first seemed the most attractive candidate.

6.2.2
Hexaazatriphenylene-Spacer

The hexaazatriphenylene (HAT) core **6.01** is readily obtained from condensation of either **a)** hexaoxocyclohexane with diaminomaleonitrile or **b)** hexaaminobenzene with diketones as outlined in figure ***6-4***.

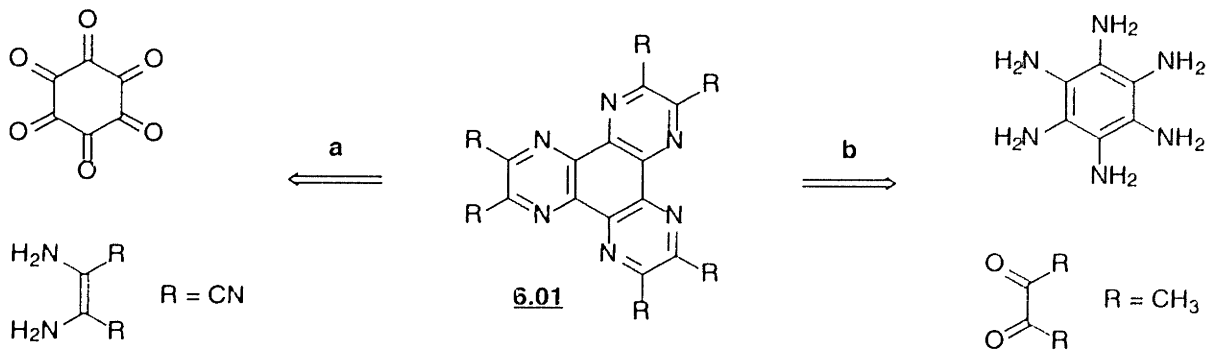

Figure *6-4*: General synthetic routes to hexaazatriphenylene and its derivatives.

Route **a)** leads to HAT derivatives with the substituents in the oxidation state of carboxylic acids. The synthesis and properties of these compounds have been studied in detail by Czarnik et al.[5-10]. A suitable substrate for alkylation of glycolurils would be the

corresponding reduced derivative with leaving groups, e.g. hexakis(bromomethyl)HAT (**6.01**, R=CH_2Br), which would be obtained from hexakis(hydroxymethyl)HAT (**6.01**, R=CH_2OH). However, since the pyrazine unit in quinoxaline is reduced with $NaBH_4$ or $LiAlH_4$[11], it was expected that neither HAT hexacarboxylic acid (**6.01**, R=CO_2H) nor its alkyl esters could be reduced to hexakis(hydroxymethyl)HAT (**6.01**, R=CH_2OH).

Route **b)**, which leads to either unsubstituted HAT or its alkyl derivatives (**6.01**, R=H, C_nH_{2n+1}), has been investigated by Czarnik et al.[10] , Praefcke et al.[12,13] and Rogers[14]. It was thought to be possible to obtain the desired hexabromoderivative (**6.01**, R=CH_2Br) by bromination of the hexamethylderivative (**6.01**, R=CH_3), but it was found that bromination is difficult to control, even with stoichiometric amounts of bromine. The only bromination product that can be obtained cleanly is hexakis(dibromomethyl)HAT (**6.01**, R=$CHBr_2$), for which a synthetic procedure has recently been published[10].

If a 1,2-diketone is condensed with 1,2-phenylenediamine, it readily reacts to form the corresponding quinoxaline derivative[15]. In particular, bis(bromomethyl)quinoxaline can be obtained in this way from 1,4-dibromo-butane-2,3-dione[16,17]. However, all attempts to effect a similar condensation reaction with hexaaminobenzene failed to give the desired hexabromoderivative (**6.01**, R=CH_2Br). I then attempted to condense 1,4–diacetoxy–butane–2,3–dione[18] with hexaaminobenzene as outlined in figure ***6-5***.

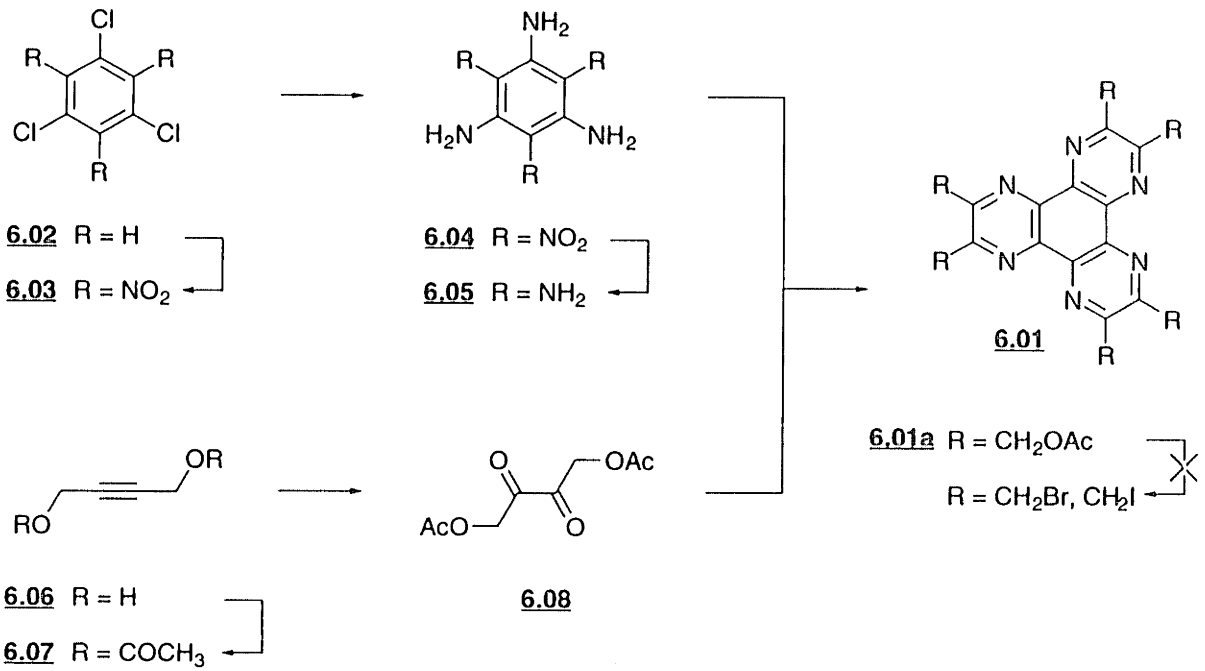

Figure *6-5*: Attempted synthesis of a spacer based on the hexaazatriphenylene core.

The hexaacetate (**6.01**, R=CH_2OAc) was obtained, but all subsequent attempts to convert it into the hexabromide or iodide (**6.01**, R=CH_2Br, CH_2I) failed. At this stage, the HAT derived spacer was abandoned and efforts were undertaken to obtain an all–carbon spacer based on triphenylene.

6.2.3
Triphenylene-Spacer

Several examples of 2,3,6,7,10,11–hexasubstituted triphenylenes have been described in the literature. While most of these compounds are alkoxysubstituted triphenylenes, a CAS search (registry file, search for triphenylene with carbon substituents in the 2,3,6,7,10,11–positions) reveals a few all–carbon substituted derivatives, namely alkyl carboxylates[19,20] and alkynyl derivatives[21,22]. (However, some of the mentioned carboxylates[19] were misreferenced, the original paper only lists oxycarbonyl derivatives of triphenylene). The alkynyl compounds were prepared from hexabromotriphenylene[23], the synthesis of which turned out to be difficult to reproduce. Triphenylene–2,3,6,7,10,11–

hexacarboxylic hexamethylester[20] has been prepared only on a small scale reaction scavenging a reactive intermediate.

Since neither of these potential routes to a spacer materialized as an obvious choice, it was attempted to synthesize hexamethyltriphenylene, for which a preliminary crystal structure but no preparation had been published[24].

The triphenylene parent structure can be obtained by three general routes: a) by aryne cyclization of bromoiodobenzene[25], bromofluorobenzene[26,27] or fluorobenzene[28], b) cyclocondensation of cyclohexanone and subsequent aromatization[29], and c) Friedel–Crafts type alkylation of benzene with 1,4–dichlorobutane[30] and subsequent aromatization[31-33].

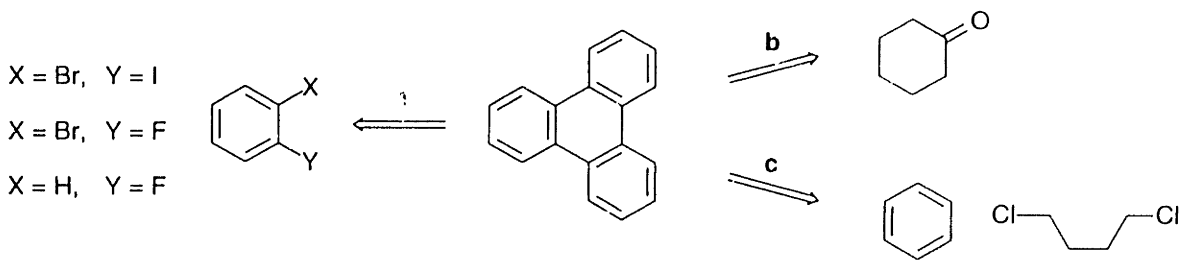

6.3
Synthesis

The most promising route for a facile large–scale synthesis of 2,3,6,7,10,11–hexamethyltriphenylene seemed to be route **a**), the benzyne–trimerization approach. Bromofluoroxylene was chosen as a starting material due to its higher stability compared to the bromoiodo derivative. The conventional synthesis began with 3,4–dimethylaniline **6.09**, which in several steps was converted to bromofluoroxylene **6.12**[27,34]. A shortcut was found which involved the preparation of 4-fluoro-*o*-xylene **6.11** followed by electrophilic bromination of the aromatic ring. The first cyclization reactions were carried out with magnesium in tetrahydrofuran in analogy to the corresponding preparation of triphenylene[27] and hexamethyltriphenylene **6.13** was obtained in the expected low yield. Brendan M. O'Leary later found that 4-fluoro-*o*-xylene **6.12** can be used directly and in higher yields for the cyclization reaction analogous to the preparation of triphenylene from fluorobenzene[28,35].

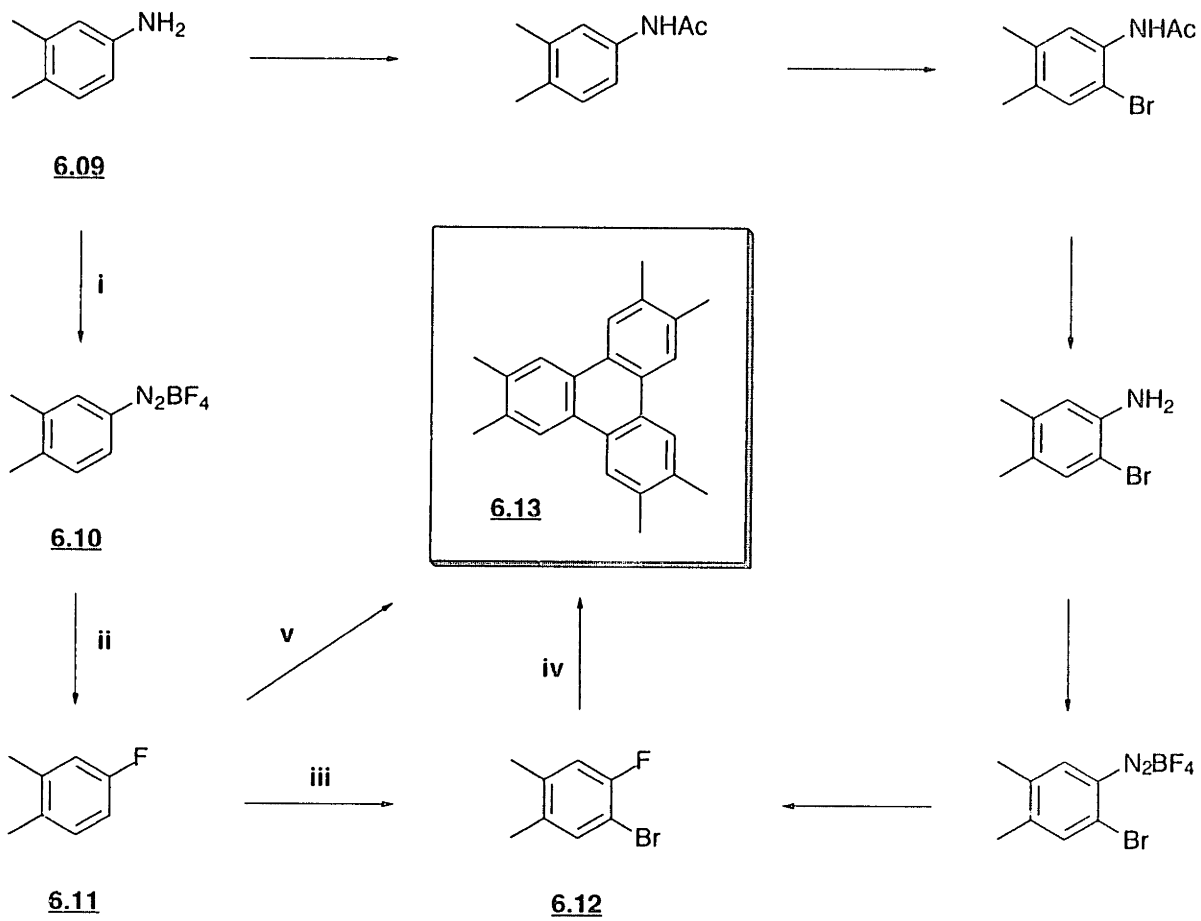

Figure *6-6*: Synthesis of hexamethyltriphenylene **6.13**. Reagents and conditions: **i** HCl, $NaNO_3$, $NaBF_4$; **ii** Δ; **iii** Br_2, $FeCl_3$, CH_2Cl_2; **iv** Mg, THF; **v** n–BuLi, *tert*–BuONa, THF, –100°C.

Selective monobromination of all methyl groups was not possible by using standard conditions with N–bromosuccinimide. As more bromine atoms are added, the compounds become increasingly insoluble so that at best an inseparable mixture of the penta– and hexabrominated material was isolated. It was possible to convert the mixture of brominated compounds into the corresponding acetoxy derivatives and separate these. However, reaction conditions which were successful for conversion of e.g. tetrakis(acetoxymethyl)anthracene to the corresponding bromoderivative (HBr, HOAc)[36] did not lead to the desired hexabromoderivative in this case. Attempts to obtain the hexaiodide under mild conditions[37] were not successful, either. It was therefore necessary to use reaction conditions for the bromination under which the product would remain

soluble. The reaction in refluxing 1,2–dibromoethane with bromine[38,39] was successfully employed for the synthesis of the desired hexabromoderivative **6.14**. Standard alkylation conditions were used for reaction with the glycoluril, and the host monomer could be isolated without major difficulties, albeit in very low yield (figure *6-7*).

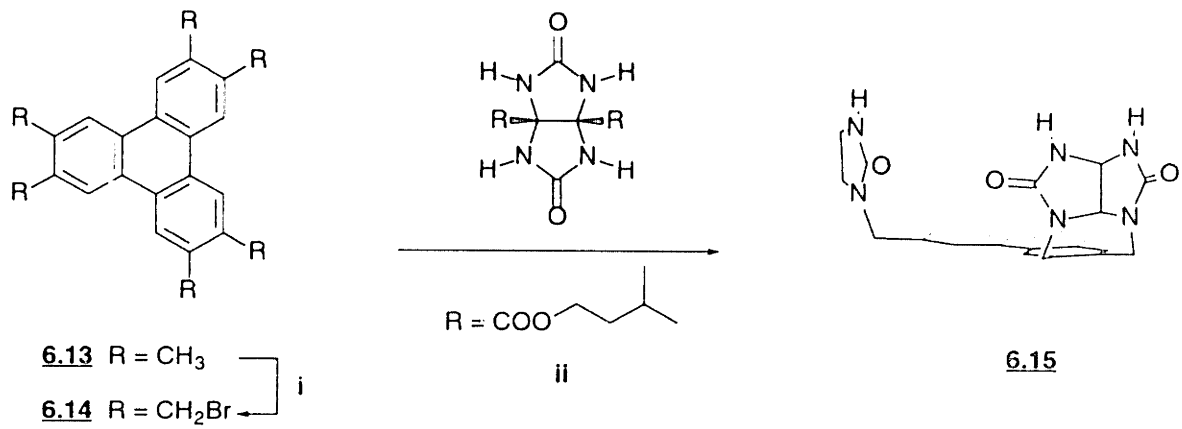

Figure *6-7*: Synthesis of hexaxis(bromomethyl)triphenylene **6.14** and subsequent alkylation to the host monomer **6.15**. Reagents: **i** Br_2, 1,2–dibromoethane, h·ν, reflux; **ii** 1) DMSO, *tert*–BuOK, 2) aq. HCl

In the ^{1}H NMR spectrum of **6.15** in solvents such as chloroform-*d* and benzene–d_6, the observed shift for the NH protons was in the 9 ppm range. This indicates that under these conditions all the NH groups are involved in hydrogen bonding, i.e. the observed species is an assembly of individual monomers $(\mathbf{6.15})_2$.

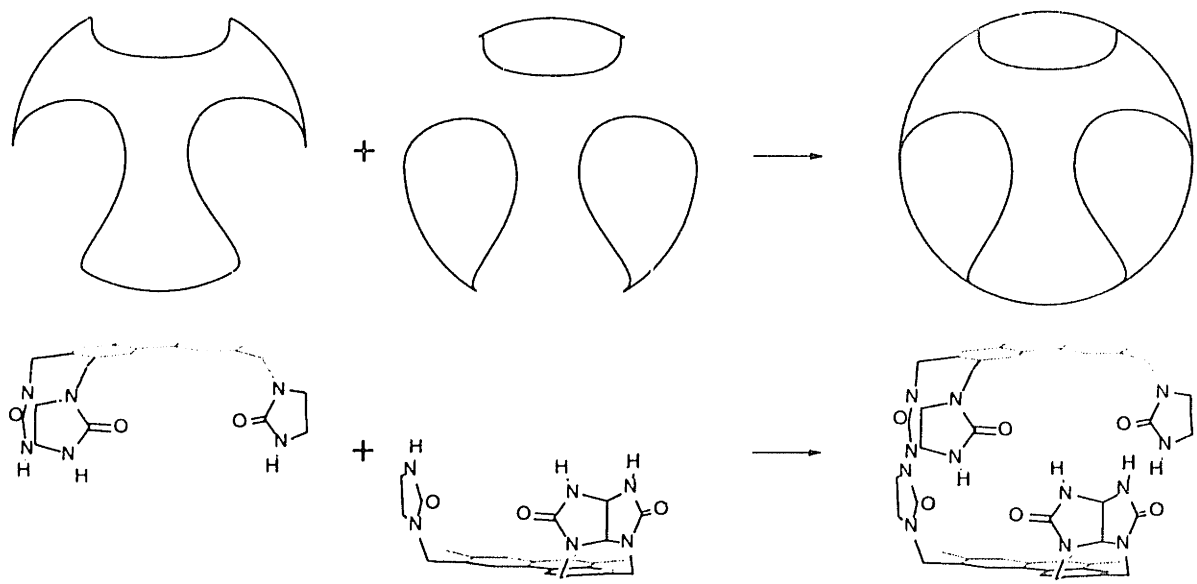

6.15 **6.15** **$(6.15)_2$**

Figure *6-8*: Self–Assembly of the two half–shells **6.15** to a dimer **$(6.15)_2$** held together by 12 hydrogen bonds.

The simplicity of the ^1H NMR spectrum and sharpness of the proton resonances points to a high symmetry of the assembly. Due to the curvature and the rigidity of compound **6.15** the only possibility is a dimeric assembly **$(6.15)_2$**. In other words, the system behaves in the way it was designed, in that two bowl–shaped monomers **6.15** would assemble to form a "tennis ball–like" structure **$(6.15)_2$** as depicted in figure ***6-8***. The ^1H NMR spectrum of **$(6.15)_2$** in chloroform-*d* is shown in figure ***6-9***.

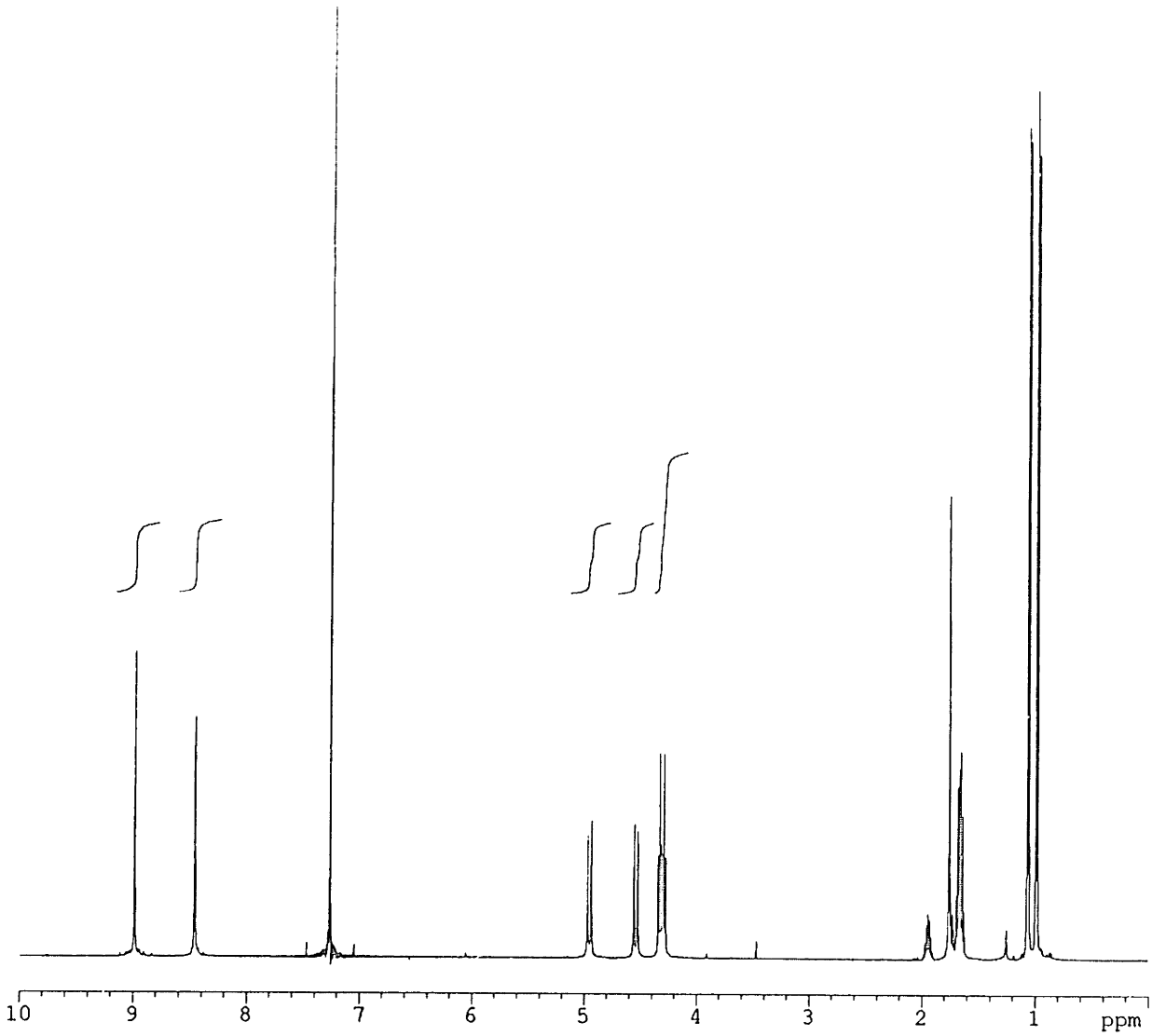

Figure *6-9*: ^{1}H NMR ($CDCl_3$, 500 MHz, 23°C) spectrum of the host dimer $(\underline{\mathbf{6.15}})_2$. Only the dimeric assembly is observed, as evidenced by the N-H resonance at 8.99 ppm indicating hydrogen bonding. The signal for the aromatic C-H of the spacer appears at 8.46 ppm. The benzylic protons are diastereotopic and appear as doublets at 4.95 ppm and 4.54 ppm, respectively. Remaining signals arise from the two sets of 3-methyl-butyl esters.

6.4
Studies on the Stability of the Assembly

In the concentration range investigated (5.7 - 1.0 mol·l^{-1}), ^{1}H NMR signals for the monomer in chloroform-*d* solution could never be observed. It is therefore not possible to quantify an association constant. The monomer-dimer equilibrium lies completely on the side of the dimeric assembly, the stability of the assembly arising from the 12 hydrogen bonds. Two methods can be used to probe the association of the dimer: Addition of competing hydrogen bond donors and acceptors, e.g. a polar solvent, and increase of thermal energy to the point where the weak hydrogen bonding interactions are overcompensated by the thermal energy of the molecules.

6.4.1
Competitive Solvents

The stability of the dimeric assembly has been tested by addition of polar solvents that can undergo hydrogen bonding interactions with the glycoluril moieties. Theoretically, it should be possible to break apart the dimeric assembly once a critical concentration has been reached.

Upon titration of a solution of **(6.15)$_2$** in chloroform-*d* with methyl-d_3 alcohol, Brendan M. O'Leary found that no change in the position of the NH signal was observed up to a concentration of 25% (v/v) methyl-d_3 alcohol at which point the assembly began to precipitate[35]. For this study, methyl-d_3 alcohol (CD_3OH) despite its cost is a better choice than methanol-d_4 (CD_3OD) because it allows the amide proton signal to be observed. The amount of assembly does not have to be estimated from the overall broadness of the signals in the proton spectrum[40]. Titration of a chloroform-*d* solution of **(6.15)$_2$** with dimethyl sulfoxide-d_6, on the other hand, showed that the dimeric assembly is broken up at around 30% (v/v) dimethyl sulfoxide-d_6[35].

6.4.2
Elevated Temperature Study

The highest boiling solvent in which the ^{1}H NMR resonances of the dimeric assembly (**6.15**)$_2$ can be unambiguously observed is toluene-d_8. Increasing the temperature of a toluene solution of (**6.15**)$_2$ from 22 to 100°C only induces a marginal shift of the NH resonances in the ^{1}H NMR spectrum. The temperature-dependent shift of the NH resonance is similar in magnitude to the shift of the aromatic CH of the spacer. No significant signal broadening is observed, indicating that the dimeric complex is stable at 100°C in toluene solution.

6.5
Encapsulation Studies

The "Jelly-Doughnut" was designed to accommodate guest molecules of the size of benzene and cyclohexane. The name is intended to illustrate the size and shape compared to the original "tennis ball". Molecular modeling[4] predicts a snug fit for these two shapes as shown in figure ***6-10***.

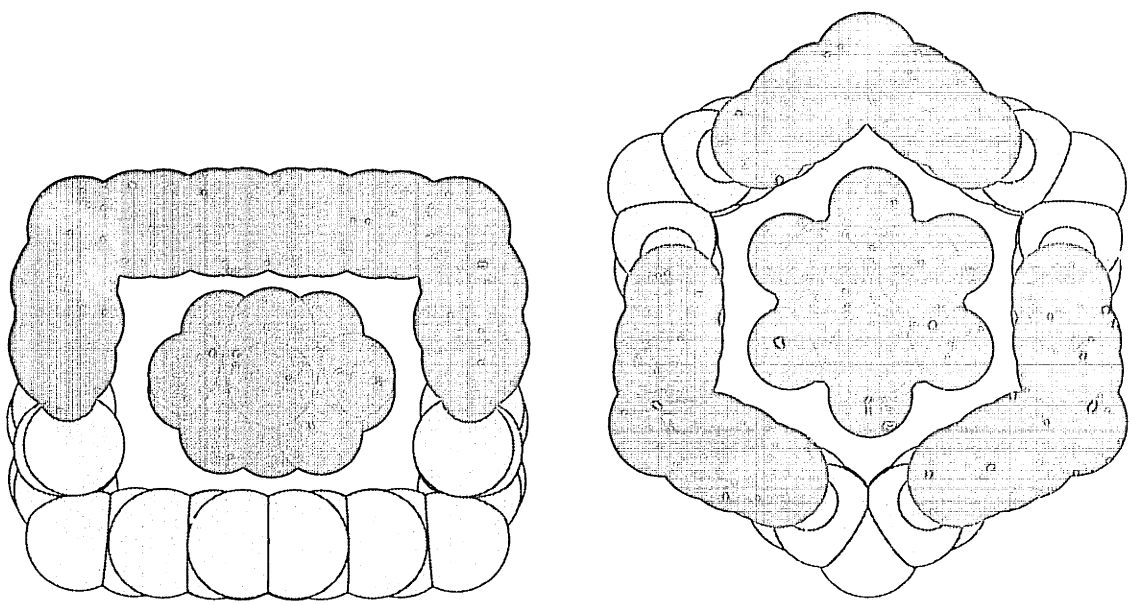

Figure *6-10*: Vertical (left) and horizontal (right) cross sections of the dimeric assembly (**6.15**)$_2$ with encapsulated cyclohexane.

6.5.1
Encapsulation of Benzene

A solution of **(6.15)$_2$** in chloroform-*d* consists of solvated dimers presumably encapsulating chloroform-*d*. Although a ^{1}H NMR resonance for the encapsulated chloroform ($CHCl_3$) has never been observed, it is fair to assume that chloroform is encapsulated and competes with other potential guests for encapsulation. The aromatic CH and especially the NH signals of the dimeric host **(6.15)$_2$** in the ^{1}H NMR spectrum appear at different positions depending on the encapsulated guest species. Upon addition of benzene–d_6 to a solution of **(6.15)$_2$** in chloroform-*d*, a new set of NH and CH_{ar} signals appears (figure ***6-11***). The presence of the two signal sets is an indication for the existence of two host dimers **(6.15)$_2$** in solution, containing chloroform-*d* and benzene-d_6 respectively.

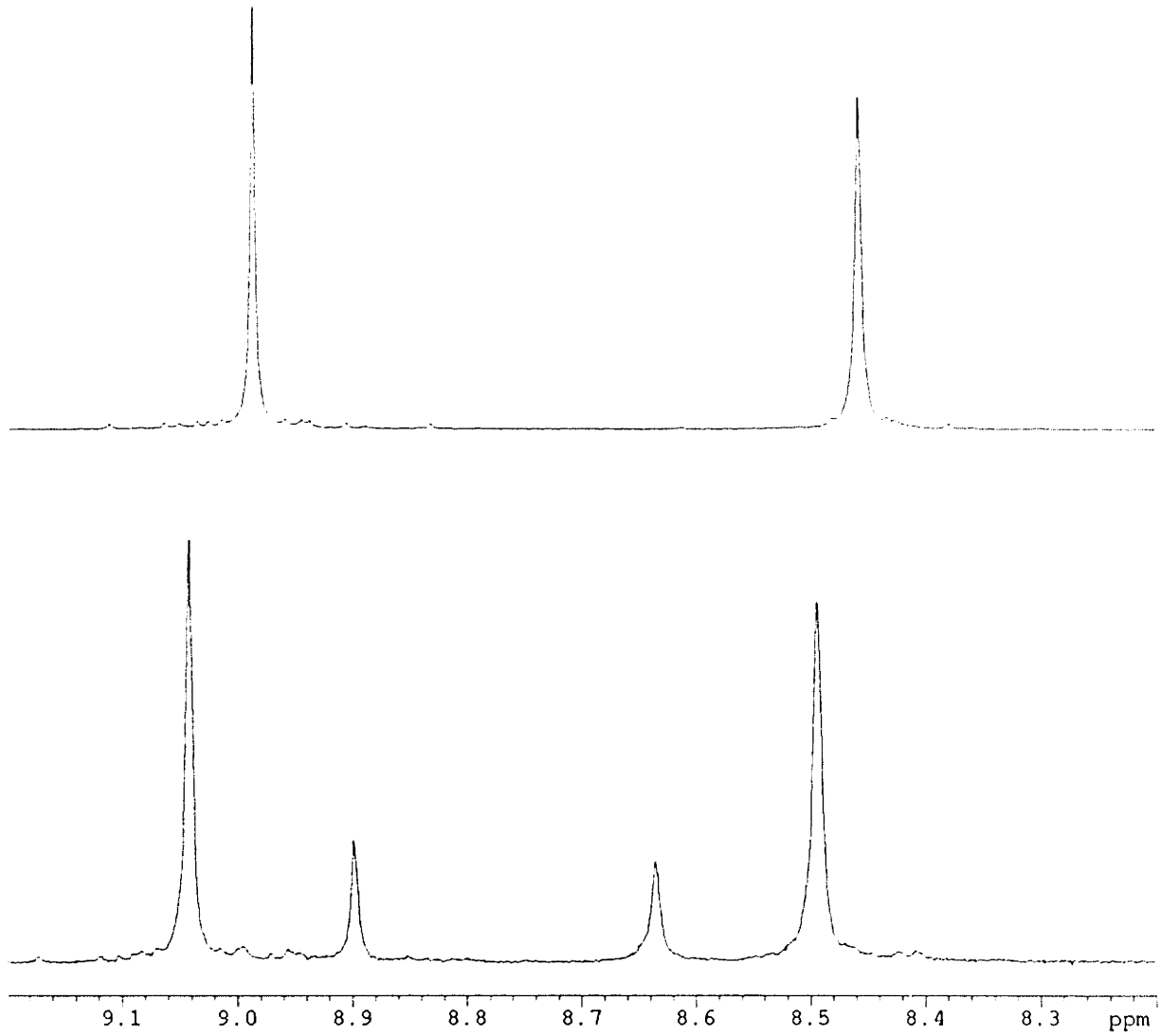

Figure *6-11*: Downfield region of the ^{1}H NMR (500 MHz, 23°C) spectrum of **6.15**. *Top*: In $CDCl_3$ only the chloroform containing host dimer **(6.15)$_2$** is observed as evidenced by the NH resonance at 8.99 and the CH_{ar} resonance at 8.46 ppm. *Bottom*: Upon titration of the same solution with C_6D_6, a new NH and CH_{ar} signal appears. Shown here is the ^{1}H NMR spectrum of **6.15** in a solution containing approximately 5% (v/v) C_6D_6 in $CDCl_3$. One can see the coexistence of host dimers **(6.15)$_2$** containing $CDCl_3$ and C_6D_6.

Titration of a solution of **6.15** in either methylene chloride-d_2, chloroform-d, or 1,1,2,2-tetrachloroethane-d_2 with benzene-d_6 shows that the presumably benzene

containing species increases with the benzene concentration at the expense of the original species (figure ***6-12***). The plausible explanation is that one guest is replaced by the other, both are competing for the capsule, at a slow rate compared to the NMR time scale.

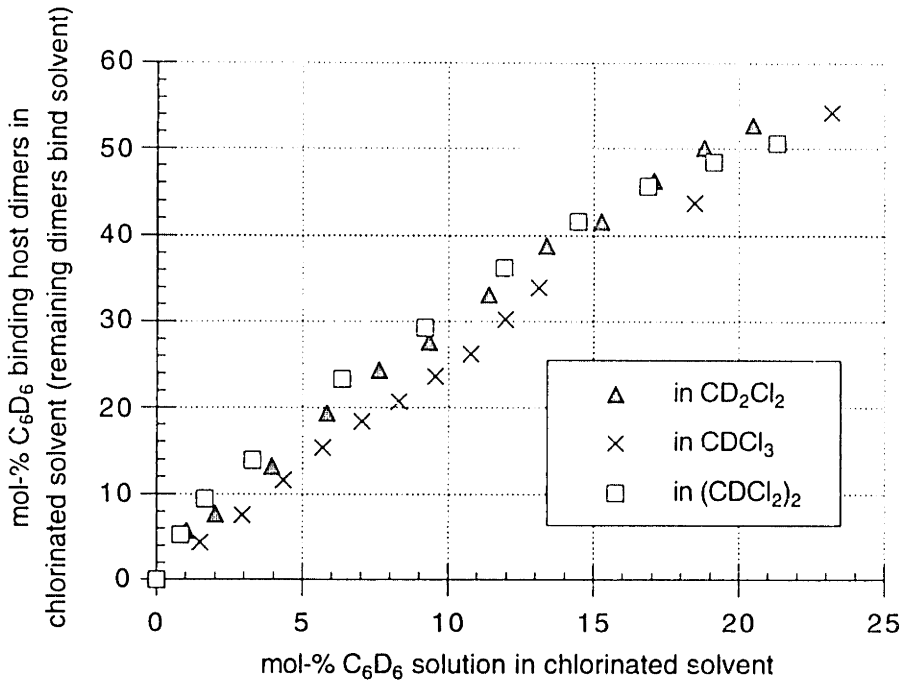

Figure *6-12*: A solution of **6.15** in a chlorinated solvent was titrated with benzene-d_6 and the relative amounts of solvent- and benzene-encapsulating guests determined from the integration of the corresponding NH and CH_{ar} ^1H NMR signals.

Direct evidence for encapsulated benzene could not be obtained from the ^1H NMR spectrum. An encapsulation study using labeled benzene ($^{13}C_6H_6$) however, gave conclusive evidence for two different benzene species. The ^{13}C NMR spectra of a blank solution of $^{13}C_6H_6$ in chloroform-*d* without host dimer and the same solution with host dimer are shown in figure ***6-13***. In the presence of the host a new signal for encapsulated benzene is observed—shifted upfield by 2 ppm from its original position.

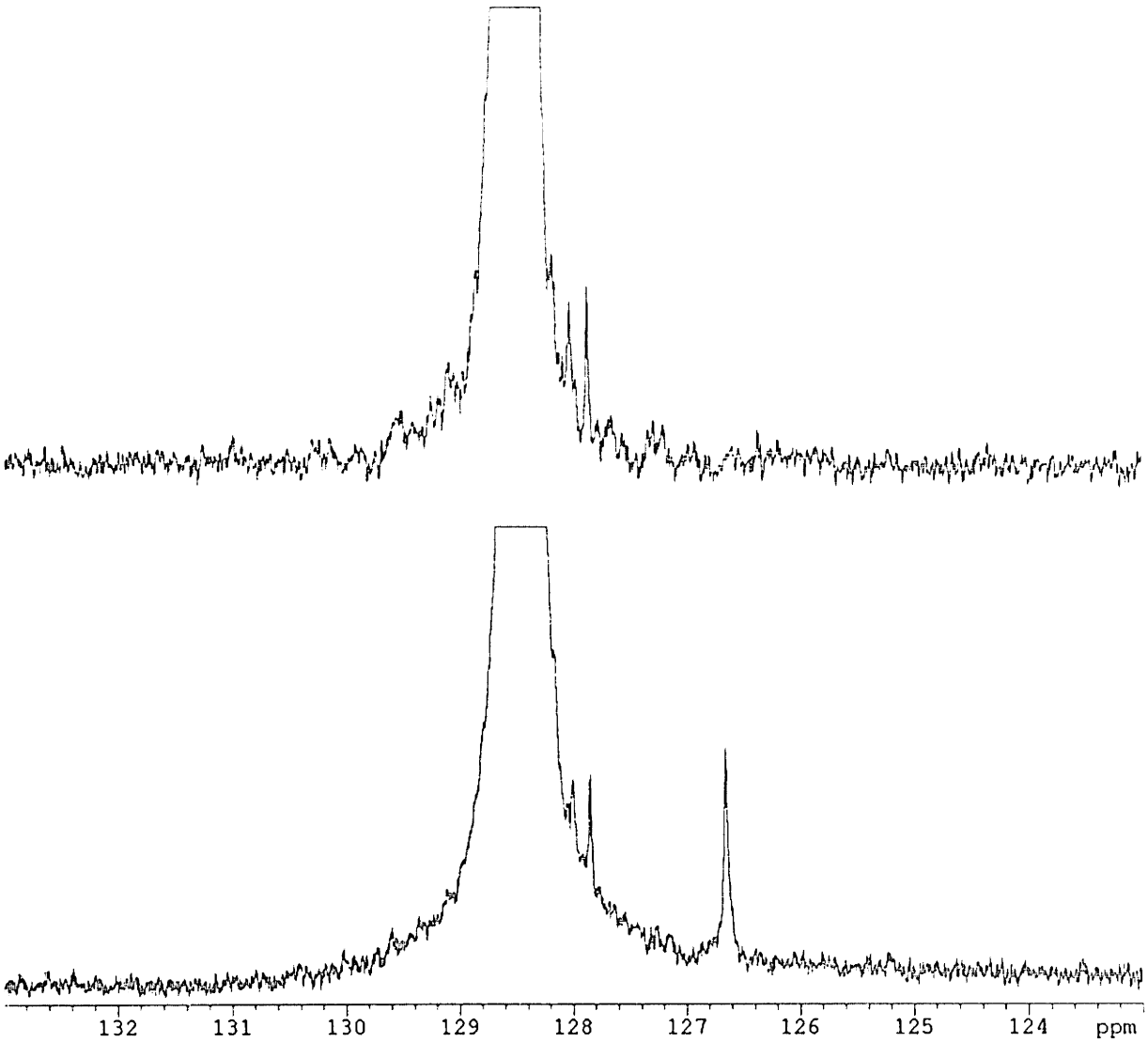

Figure ***6-13***: ^{13}C NMR ($CDCl_3$, 125 MHz, 22°C) *Top*: Reference spectrum of a solution of 5% $^{13}C_6H_6$ (v/v) in $CDCl_3$. *Bottom*: The same solution now in the presence of the host **6.15**. The signal for the encapsulated $^{13}C_6H_6$ can be seen shifted upfield by 2 ppm from the signal for the $CDCl_3$-solvated $^{13}C_6H_6$. A 20 µl NMR micro cell, immersed in $CDCl_3$, was used for this experiment.

The thermodynamic data for the encapsulation process were determined for the encapsulation of benzene-d_6 in chloroform-*d*.

$$\{Host{\cdot}CDCl_3\} + C_6D_6 \rightleftharpoons \{Host{\cdot}C_6D_6\} + CDCl_3$$

$$K_a = \frac{[\,Host \cdot C_6D_6\,] \circ [\,CDCl_3\,]}{[\,Host \cdot CDCl_3\,] \circ [\,C_6D_6\,]}$$

The ratios of chloroform-*d* and benzene-d_6 containing host dimers $(\underline{6.15})_2$ were again determined from the integration ratios of the NH and CH_{ar} signals in the ^1H NMR spectrum. The van't Hoff diagram (figure ***6-14***) gives slightly differing thermodynamic values from the NH- and the CH- derived data.

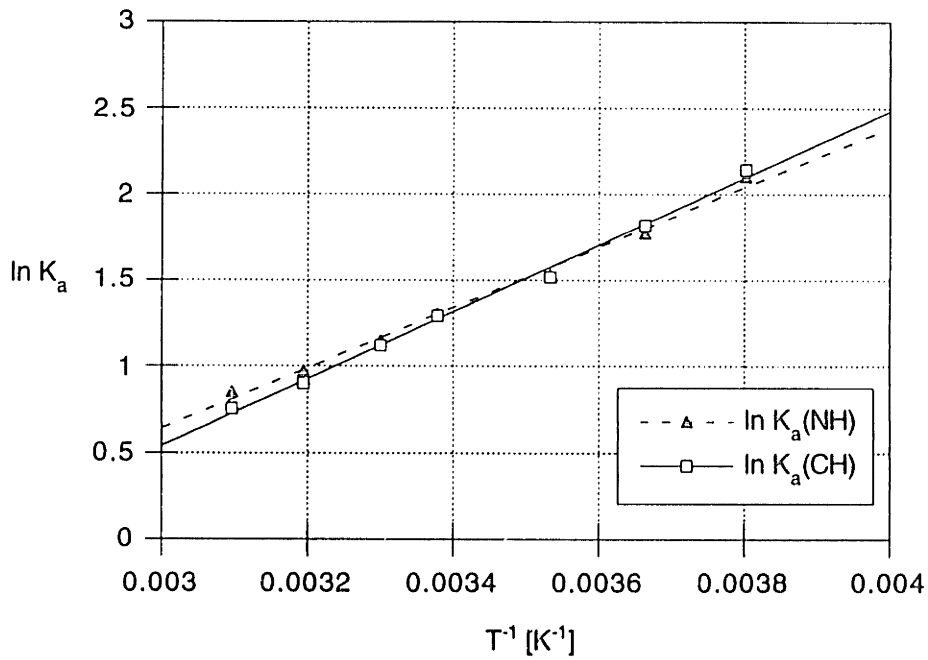

Figure *6-14*: Van't Hoff diagram for the encapsulation of 17% (v/v) benzene in chloroform solution. Two data sets were used to estimate the accuracy. Integration ratios of NH signals and CH signals (for chloroform and benzene containing host dimers) were treated separately. The thermodynamic parameters ΔG, ΔH, and ΔS obtained were averaged, giving the error margin indicated.

For the reaction

$$\{Host{\cdot}CDCl_3\} + C_6D_6 \rightleftharpoons \{Host{\cdot}C_6D_6\} + CDCl_3$$

one obtains the following values:

ΔG_{298}	=	-0.74	±	0.01	kcal·mol^{-1}
ΔH	=	-3.7	±	0.02	kcal·mol^{-1}
ΔS	=	-9.9	±	0.7	cal·K^{-1}·mol^{-1}

The encapsulation of benzene-d_6 in chloroform-*d* solution is enthalpy driven, further evidence for the encapsulation of only one chloroform-*d* molecule per dimer prior to benzene-d_6 encapsulation. The entropic cost of about 10 cal·K^{-1}·mol^{-1} for the encapsulation of benzene-d_6 is in agreement with one three-particle complex being converted to another three-particle complex.

6.5.2
Encapsulation of Cyclohexane

Another nonpolar guest on which encapsulation studies were performed was cyclohexane. Titration of a chloroform-*d* solution with cyclohexane-d_{12} did not lead to any observable cyclohexane-d_{12} binding by the host $(\underline{\mathbf{6.15}})_2$. Apparently the slightly polar chloroform-*d* interacts better with the interior walls of the cavity than does cyclohexane-d_{12}.

The picture changes if a solvent is used that is not as well encapsulated as chloroform-*d*. Sterically demanding solvents have been used previously to enforce encapsulation of various guests e.g. into carcerands[41,42]. *p*-Xylene-d_{10} is the solvent of choice, it is too large to be comfortably encapsulated and sterically more demanding than ethylbenzene-d_{10} which can adopt different conformations. The affinity for cyclohexane in *p*-xylene-d_{10} was so high that cyclohexane-h_{12} (C_6H_{12}) could be used for the encapsulation studies and the signal for encapsulated cyclohexane-h_{12} could be seen and integrated. Upon addition of cyclohexane-h_{12} to a solution of $(\underline{\mathbf{6.15}})_2$ in *p*-xylene-d_{10} no major change

in the ^{1}H NMR spectrum is observed at first, but after two days an equilibrium has been attained and all of the host dimers **(6.15)$_2$** contain cyclohexane-h_{12} (figure ***6-15***).

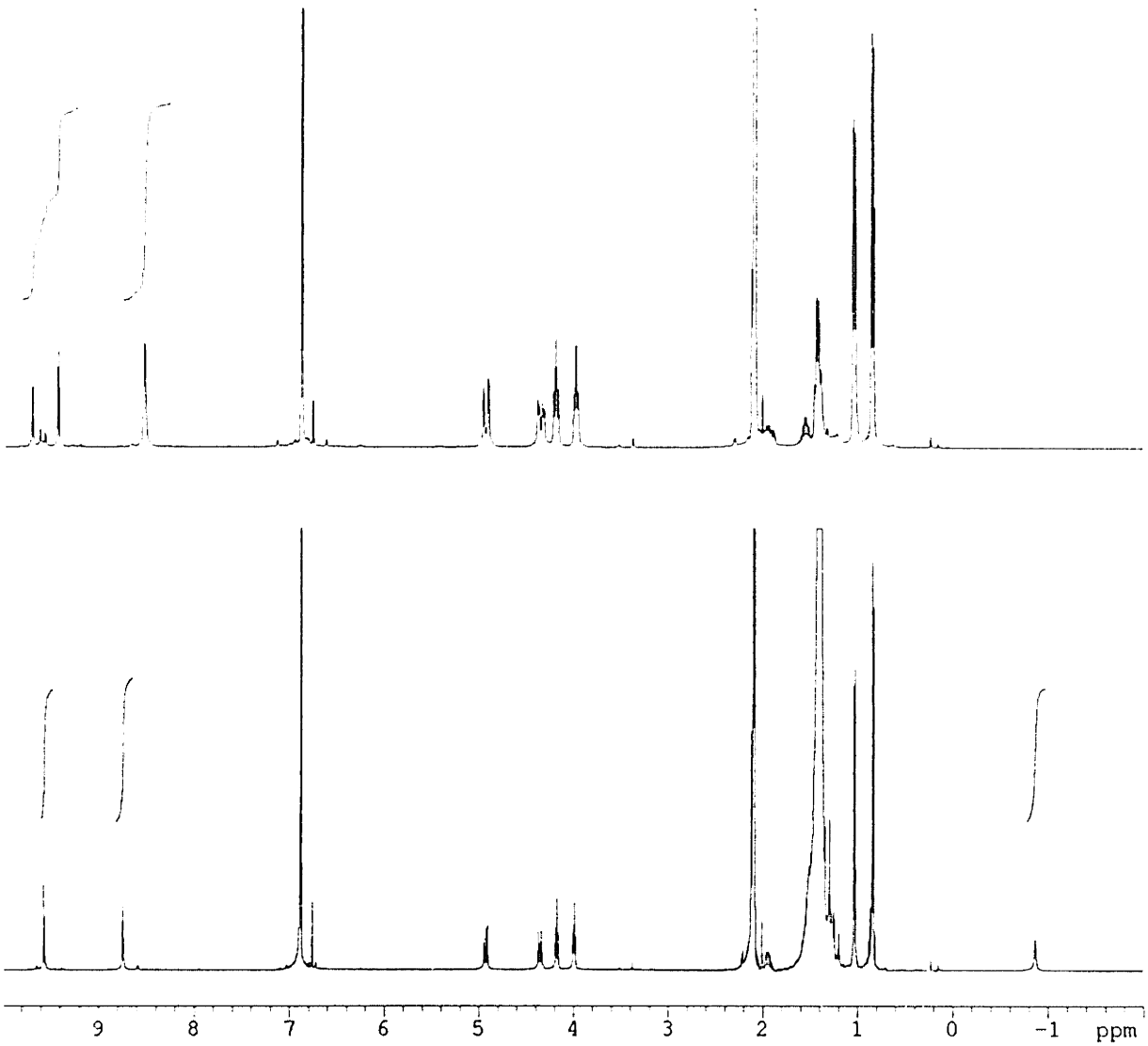

Figure *6-15*: ^{1}H NMR (*p*-xylene-d_{10}, 500 MHz, 23°C). *Top*: Reference spectrum of **6.15**. The desymmetrization presumably arises from impurities in the solvent, which are also encapsulated. *Bottom*: the same sample after addition of cyclohexane-h_{12} and a 2 day equilibration period. All host dimers **(6.15)$_2$** contain one molecule cyclohexane-h_{12} each as evidenced by the integration of the 12 NH and CH_{ar} of the host and the CH of the encapsulated cyclohexane-h_{12} at -0.87 ppm.

The signal for encapsulated cyclohexane-h_{12} (figure ***6-15***) is broadened, indicating restricted mobility. Preliminary studies on encapsulated cyclohexane-h_{12} in toluene-d_8 show that the signal broadens further upon cooling and virtually disappears at -10°C. Due to the low concentration of encapsulated cyclohexane-h_{12} the data could not be quantified.

6.5.3.
Guest–Guest–Exchange

The facile observation of the encapsulated cyclohexane-h_{12} in *p*-xylene-d_{10} allowed observation of guest-guest exchange processes. An equilibrated solution of **(6.15)$_2$** with excess cyclohexane in *p*-xylene-d_{10} (all capsules contain cyclohexane-h_{12}) was diluted with equal amounts of cyclohexane-d_{12}. The decrease of encapsulated cyclohexane-h_{12} was monitored over time (figure ***6-16***).

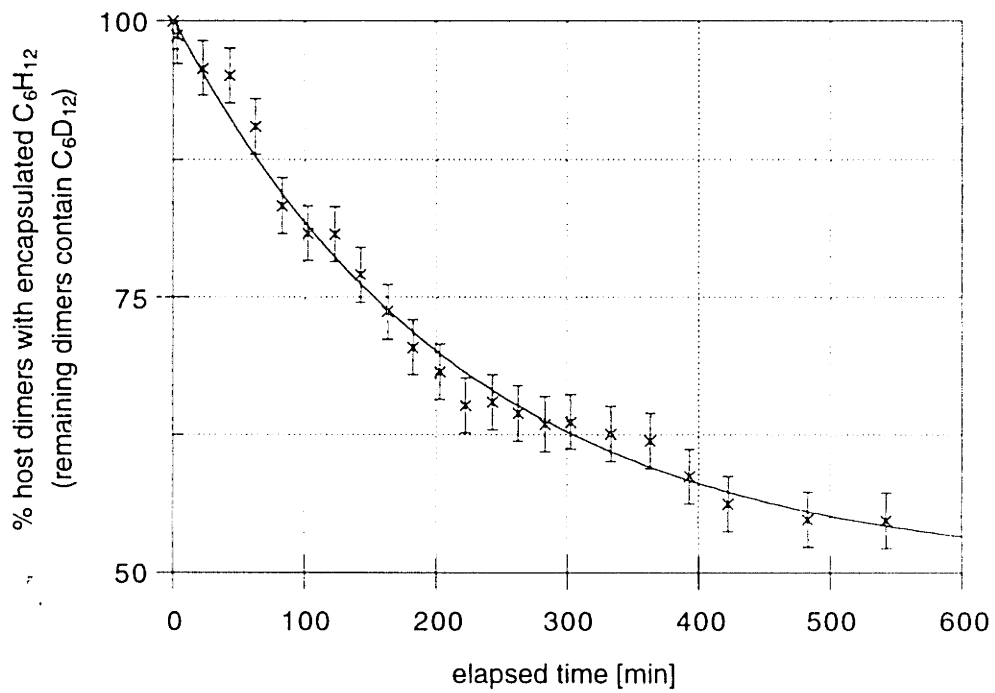

Figure *6-16*: Exchange of encapsulated cyclohexane-h_{12} by cyclohexane-d_{12}.

The half-life for this exchange process lies in the range of 2.5 hours, indicating that a considerable number of the twelve hydrogen bonds in **(6.15)$_2$** must be broken in order to permit exit and entry of the guests.

6.6
Experimental

For general apparatus, methods, and materials information, see Chapter 3, page 53.

1,4–Diacetoxy–2–butyne, 6.07

was pepared as described in the literature[43].

^{1}H NMR ($CDCl_3$, 300 MHz) δ 4.72 (s 4H); 2.10 (s, 6H) ppm

1,4–Diacetoxy–2,3–butynedione, 6.08

was prepared with slight modification of a literature procedure[18].

Nitrogen dioxide (12 ml) was condensed in a 100 ml flask, a solution of 1,4–diacetoxy–2–butyne **6.07** (0.04 mol, 6.81 g) in 1,2–dichloroethane (60 ml) was added, and the mixture was stirred at 40°C over night. Nitrogen dioxide was driven off by passing a stream of air through the solution, and the solvent was removed by rotary evaporation. Ether (15 ml) was added, and the crystalline product was obtained after refrigeration. The yellow crystals were collected by filtration, washed with 15 ml cold ether, and dried under vacuum.

Yield: 1.45–1.60 g (18–20%); mp: 97–98°C

^{1}H NMR ($CDCl_3$, 300 MHz): δ 5.11 (s 4H); 2.19 (s, 6H) ppm

1,3,5–Triamino–2,4,6–trinitrobenzene, 6.04

was prepared from 1,3,5–trichlorobenzene **6.02** via 1,3,5–trichloro–2,4,6–trinitrobenzene **6.03**[44] according to the literature[12].

Hexaaminobenzene, 6.05

was prepared according to the literature[14] from 1,3,5–Triamino–2,4,6–trinitrobenzene **6.04**.

2,3,6,7,10,11–Hexakis(acetoxymethyl)–1,4,5,8,9,12–hexaazatriphenylene, 6.01a

was prepared in analogy to the condensation of diketones with hexaaminobenzene[12].

Freshly prepared hexaaminobenzene **6.05** (4 mmol, 0.67 g) was given to a solution of 1,4–Diacetoxy–2,3–butynedione **6.08** (15 mmol, 3 g) in 30 ml ethanol/HOAc/water (20/8/2). After stirring the dark solution for 30 min. at room temperature, a voluminous precipitate

had formed. The mixture was heated to reflux for 2 h. The solvents were evaporated, the resulting dark semisolid was taken up in methanol, sonicated, and the solids were collected by filtration and washed with methanol. Flash chromatography (CH_2Cl_2, 0→5% MeOH) over silica gel gave virtually pure material.

Yield: 0.88 g (33%)

^1H NMR ($CDCl_3$, 250 MHz): δ 5.70 (s, 12H); 2.25(s, 18H) ppm

^{13}C NMR ($CDCl_3$, 75 MHz): δ 170.2; 152.0; 140.3; 64.8; 20.6 ppm

4–Fluoro–*o*–xylene, 6.11

was prepared analogous to fluorobenzene[45].

To a stirred suspension of finely ground 4–amino–*o*–xylene **6.09** (0.8 mol, 97 g) in 200 ml water was added 250 ml conc. HCl and 50 g crushed ice. A solution of $NaNO_2$ (0.85 mol, 59 g) in 100 ml water was added slowly, the temperature being kept below 10 °C using an ice bath. The resulting diazonium solution was filtered directly into a freshly prepared, filtered, and chilled solution of $NaBF_4$ (1.12 mol, 125 g) in 220 ml water. The precipitated **6.10** in the mother liquor was kept in an ice bath for 30 min, collected by filtration, drained well, washed first with MeOH/Et_2O, then Et_2O, and dried.

Yield: 131–137 g (75–78%)

The diazonium fluoroborate **6.10** was thermally decomposed in two batches in a 500 ml flask using the setup described in the literature[45] (Distillation bridge on the decomposition flask, followed by two 100 ml ice cooled recipient flasks and two wash bottles with NaOH solution to trap the BF_3). 4–Fluoro–*o*–xylene **6.11** was distilled, taken up in Et_2O, and washed with 1N NaOH to remove phenolic byproducts. After drying over $MgSO_4$ and stirring with charcoal, the solution was filtered, and Et_2O was removed by distillation.

Yield: 59–63 g (59–63%, based on 4–amino–*o*–xylene **6.09**)

^1H NMR ($CDCl_3$, 300 MHz): δ 7.05 (t, H_{ar}, J=7.1 Hz); 6.87–6.74 (m, $2H_{ar}$); 2.24 (s, 3H); 2.21 (s, 3H) ppm

^{13}C NMR ($CDCl_3$, 75 MHz): δ 161.2 (d, J=240 Hz); 138.4 (d, J=7 Hz); 131.9 (d, J=3 Hz); 131.6 (d, J=8 Hz); 116.2 (d, J=23 Hz); 112.1 (d, J=21 Hz); 19.7; 18.8 ppm

1–Bromo–2–fluoro–4,5–dimethylbenzene, 6.12

A mixture of 4–fluoro–*o*–xylene **6.11** (0.475 mol, 59 g), 50 ml CH_2Cl_2, 200 mg ferrum reducium, and 500 mg $FeCl_3$ was cooled in an ice bath. Bromine (0.48 mol, 76.8 g, 24.4 ml) was added dropwise and the mixture was stirred for 3h after completed addition. After complete consumption of starting material the mixture was poured in aq. Na_2SO_3 solution, and the organic phase washed with 20% aq. HCl. After back extraction of the aqueous phases with hexanes, the combined organic layers were dried over $MgSO_4$, stirred with charcoal, filtered, and evaporated. The resulting oil was placed in a refrigerator for crystallization, the crystals taken up in 10 ml cold MeOH, collected by filtration, and dried 5h under vacuum (volatile solids!).

Yield: 57 g (59%)

^1H NMR ($CDCl_3$, 300 MHz): δ 7.27 (d, H_{ar}, J=7.2 Hz); 6.89 (d, H_{ar}, J=9.3 Hz); 2.20 (s, 6H) ppm

^1H NMR (DMSO-d_6, 250 MHz): δ 7.45 (d, H_{ar}, J=7.4 Hz); 7.17 (d, H_{ar}, J=9.9 Hz); 2.18 (s, 6H) ppm

^{13}C NMR ($CDCl_3$, 75 MHz): δ 157.3 (d, J=240 Hz); 138.1 (d, J=7.5 Hz); 134.0 (d, J=7.5 Hz); 117.6 (d, J=22.5 Hz); 105.1 (d, J=22.5 Hz);19.7; 19.0 ppm

2,3,6,7,10,11–Hexamethyl–triphenylene, 6.13

was prepared in analogy to the Mg–induced cyclization of *o*–bromofluorobenzene[27]. An improved synthesis analogous to the cyclization of fluorobenzene[28] has been worked out by Brendan M. O'Leary[35].

A flame–dried 500 ml 3–neck flask was flushed with Ar, charged with Mg turnings (0.268 mol, 1.15 eq., 6.5 g), a trace I_2, and 50 ml dry THF. 10 ml of a solution of 1–bromo–2–fluoro–4,5–dimethylbenzene **6.12** (0.233 mol, 1.0 eq., 47.4 g) in 100 ml dry THF was added, and the reaction started by addition of a small amount of 1,2–dibromoethane. The remainder of the bromofluoroxylene solution was added at such a rate that reflux was maintained. After completed addition the mixture was heated to reflux 3h and cooled to roomtemperature. The supernatant was decanted from the remaining Mg, the solids rinsed with EtOAc, and the solutions carefully poured in 2N aq. HCl while stirring. After sitting over night, a fine crystalline solid had formed which was collected by filtration (first product crop).

The aqueous phase of the filtrate was extracted with EtOAc, and the combined organic layers were evaporated without prior drying. The resulting gummy material was subjected to steam distillation, about 6g of starting material were recovered from the distillate. The residue after the steam distillation was taken up in toluene, washed with brine, dried over $MgSO_4$, and evaporated. The evaporation residue was taken up in PE 30/50 and after addition of a little CH_2Cl_2 was placed in a refrigerator for crystallization (second product crop).

Yield of combined product crops: 1.68 g (8%, based on reacted starting material).

^{1}H NMR ($CDCl_3$, 300 MHz): δ 8.34 (s, $6H_{ar}$); 2.51 (s, 18H) ppm

^{13}C NMR ($CDCl_3$, 75 MHz): δ 135.6; 127.8; 123.8; 20.5 ppm

MS (EI) *m/z* 312 (100%); 313 (26.3%); 314 (3.9%) [calculated intensities: 100 / 27.3 / 3.6]

HRMS calcd for M^+ $C_{24}H_{24}$ 312.18780, found 312.18782

Crystals of X-ray quality were obtained by recrystallization from toluene (see appendix)

2,3,6,7,10,11–Hexakis(bromomethyl)triphenylene (crude), 6.14

To a refluxing mixture of 2,3,6,7,10,11–hexamethyl–triphenylene **6.13** (0.5 mmol, 156 mg), in 10 ml 1,2–dibromoethane was slowly added a solution of bromine (3.5 mmol, 560 mg, 180 µl) in 3 ml 1,2–dibromoethane while irradiating with a 300 W tungsten lamp. [In order to minimize loss of bromine, the dropping funnel was extended with a piece of Teflon tubing that reached into the boiling liquid[38].] After completed addition (10–15 min) the mixture was heated to reflux for 10 min and allowed to cool to room temperature. The precipitate was collected by filtration, washed with 1,2–dibromoethane and CH_2Cl_2, and dried under vacuum.

Yield: 184–211 mg (49–54%) crude 2,3,6,7,10,11–hexamethyl–triphenylene which was used without further purification.

^{1}H NMR (DMSO–d_6, 300 MHz): δ 8.99 (s, $6H_{ar}$); 5.11 (s, 12H) ppm

2,3,6,7,10,11–Hexakis(acetoxymethyl)triphenylene

To check the composition of the mixture of brominated compounds, a sample was converted to the corresponding acetoxy derivatives:

A sample of crude 2,3,6,7,10,11–hexakis(bromomethyl)triphenylene in DMF was heated with excess NaOAc and a trace of tetrabutylammonium bromide in a 110°C oil bath over night. The mixture was then poured in water and heated gently until the precipitate

agglomerated. The solids were filtered off and dried. TLC (C_6H_6/EtOAc) revealed that the hexasubstituted derivative is the main component.
^{1}H NMR ($CDCl_3$, 300 MHz): δ 8.65 (s, 6H_{ar}); 5.46 (s, 12H); 2.17 (s, 18H) ppm

D_{3d}–"Jelly Doughnut" monomer, 6.15

To a solution of bis(3-methyl-butyl ester)glycoluril **3.18e** (7.0 mmol, 2.6 g) in 30 ml anhydrous DMSO under argon was added *tert*-buOK (14.0 mmol, 1.6 g) and the mixture was heated to 50°C. Crude hexakis(bromomethyl)triphenylene **6.14** (0.23 mmol, 184 mg) was suspended in 20 ml anhydrous DMSO, sonicated, heated until a solution had formed and added dropwise to the glycoluril solution. The resulting cherry red suspension was stirred 30 min at room temperature and poured in 800 ml 1N aq. HCl. The precipitate was collected by filtration, washed thoroughly with water, drained well, and dried. The filter cake was suspended in 150 ml MeOH, filtered, and evaporated. The residue after evaporation was triturated with $CHCl_3$ and THF. The insoluble material was filtered off and washed with THF. (1.7 g unreacted excess glycoluril was recovered.) The combined filtrates were evaporated, and the residue after evaporation rinsed with ether. After washing with ether, the material was triturated with CH_2Cl_2 and filtered. The CH_2Cl_2 filtrate was evaporated and purified by chromatography over silica gel (CH_2Cl_2, 0 → 2 % MeOH)
Yield: 8 mg (10%)
^{1}H NMR of dimer **(6.15)$_2$**:
^{1}H NMR ($CDCl_3$, 500 MHz): δ 8.99 (s, 12H_{NH}); 8.46 (s, 12H_{CHar}); 4.95 (d, 12H_{benz}, J=15.6 Hz); 4.54 (d, 12H_{benz}, J=15.6 Hz); 4.33 (t, 12H_{OCH}, J=7.1Hz); 4.29 (t, 12H_{OCH}, J=6.6Hz); 1.97–1.91 (m, 6H); 1.78–1.71 (m, 6H); 1.70–1.63 (m, 24H); 1.06 (d, 36H, J=8.6Hz); 0.99 (d, 36H, J=5.0Hz) ppm (see also figure ***6-9***)
IR (CH_2Cl_2): 3214.2, 3094.9 (amide NH, hydrogen-bonded); 1754.2 (CO, ester); 1715.7 (CO, cyclic urea)
Electrospray Mass Spectrometry:
calcd. for [M + H]$^+$ 1411.6 found 1411.7
calcd. for [M + Na]$^+$ 1433.6 found 1433.5
calcd. for [M_2 + CH_2Cl_2 + Na]$^+$ 2928.2 found 2927.7
The electrospray mass spectra were recorded by Brendan M. O'Leary[35] on an Applied Biosystems Biopolymer Mass Analyzer BioIon 20 plasma desorption mass spectrometer.

6.7
References

(1) Wyler, R.; de Mendoza, J.; Rebek, J., Jr. *Angew. Chem. Int. Ed. Engl.* **1993**, *32*, 1699-1701.

(2) Branda, N.; Wyler, R.; Rebek, J., Jr. *Science* **1994**, *263*, 1267-1268.

(3) Branda, N.; Grotzfeld, R. M.; Valdés, C.; Rebek, J., Jr. *J. Am. Chem. Soc.* **1995**, *117*, 85-88.

(4) Mohamadi, F.; Richards, N. G.; Guida, W. C.; Liskamp, R.; Lipton, M.; Caufield, C.; Chang, G.; Hendrickson, T.; Still, W. C. *J. Comput. Chem.* **1990**, *11*, 440-467.

(5) Kanakarajan, K.; Czarnik, A. W. *J. Org. Chem.* **1986**, *51*, 5241-5243.

(6) Kanakarajan, K.; Czarnik, A. W. *J. Heterocyclic Chem.* **1988**, *25*, 1869-1872.

(7) Sarma, M. S. P.; Czarnik, A. W. *Synthesis* **1988**, 72-73.

(8) Kanakarajan, K.; Czarnik, A. W. *Polym. Commun.* **1989**, *30*, 171-173.

(9) Rademacher, J. T.; Kanakarajan, K.; Czarnik, A. W. *Synthesis* **1994**, 378-3980.

(10) Aumiller, W. D.; Dalton, C. R.; Czarnik, A. W. *J. Org. Chem.* **1995**, *60*, 728-729.

(11) Cheeseman, G. W. H.; Cookson, R. F. *Condensed Pyrazines*; John Wiley & Sons: New York, 1979; Vol. 35.

(12) Kohne, B.; Praefcke, K. *Liebigs Ann. Chem.* **1985**, 522-528.

(13) Praefcke, K.; Kohne, B.; Kohlschreiber, T.; Korinth, F. *Liebigs Ann. Chem.* **1988**, 609-610.

(14) Rogers, D. Z. *J. Org. Chem.* **1986**, *51*, 3904-3905.

(15) Simpson, J. C. E. *Condensed Pyridazine and Pyrazine Rings. (Cinnolines, Phthalazines, and Quinoxalines)*; Interscience Publishers, Inc.: New York, 1953; Vol. 5.

(16) Wegmann, J.; Dahn, H. *Helv. Chim. Acta* **1946**, *29*, 101-113.

(17) Westphal, O.; Jann, K. *Liebigs Ann. Chem.* **1957**, *605*, 8-15.

(18) Nikolaeva, A. D.; Mikhailovskii, D. I.; Kirsanov, A. P. *J. Org. Chem. U.S.S.R.* **1975**, *11*, 689-692.

(19) Cotrait, M.; Marsan, P.; Destrade, C.; Malthete, J. *J. Phys., Lett.* **1979**, *40*, 519-522.

(20) Schiess, P.; Heitzmann, M. *Helv. Chim. Acta* **1978**, *61*, 844-847.

(21) Praefcke, K.; Kohne, B.; Singer, D. *Angew. Chem. Int. Ed. Engl.* **1990**, *29*, 177-179.

(22) Praefcke, K.; Singer, D.; Kohne, B. *Liq. Cryst.* **1993**, *13*, 445-454.

(23) Breslow, R.; Jaun, B.; Klutiz, R. Q.; Xia, C.-Z. *Tetrahedron* **1982**, *36*, 863-867.

(24) Yerkess, J.; Jones, D. W.; Denne, W. A. *Acta Cryst. B* **1969**, *52*, 2649-2650.

(25) Heaney, H.; Millar, I. T. *Organic Syntheses*; Wiley: New York, 1973; Collect. Vol. V, pp 1120-1123.

(26) Wittig, G.; Knauss, E. *Chem. Ber.* **1958**, *91*, 895-1132.

(27) Bartle, K. D.; Heaney, H.; Jones, D. W.; Lees, P. *Tetrahedron* **1965**, *21*, 3289-3296.

(28) Fossatelli, M.; Brandsma, L. *Synthesis* **1992**, 756.

(29) Shirai, H.; Amano, N.; Hashimoto, Y.; Fukui, E.; Y., I.; Ogawa, M. *J. Org. Chem.* **1991**, *56*, 2253-2256.

(30) Reppe, W. *Justus Liebigs Ann. Chem.* **1955**, *596*, 133-134.

(31) Adkins, H.; Richards, L. M.; Davis, J. W. *J. Am. Chem. Soc.* **1941**, *63*, 1320-1325.

(32) Hausigk *Chem. Ber.* **1968**, *101*, 473-476.

(33) Houben-Weyl *Methoden der Organischen Chemie;* 4 ed.; Georg Thieme Verlag: Stuttgart, 1981; Vol. 5,2b, pp 107-118.

(34) Wittig, G.; Matzura, H. *Liebigs Ann. Chem.* **1970**, *732*, 97-106.

(35) O'Leary, B. M., unpublished results.

(36) Kubik, S., unpublished results.

(37) Ho, T.-L.; Olah, G. A. *Synthesis* **1977**, 417-418.

(38) Stephenson, E. F. M. *Organic Syntheses*; Wiley: New York, NY; Collect. Vol. IV, pp 984-986.

(39) Tashiro, M.; Mataka, S.; Takezaki, Y.; Takeshita, M.; Arimura, T.; Tsuge, A.; Yamato, T. *J. Org. Chem.* **1989**, *54*, 451-458.

(40) Seto, C. T.; MAthias, J. P.; Whitesides, G. M. *J. Am. Chem. Soc.* **1993**, *115*, 1321-1329.

(41) Chapman, K. T.; Still, W. C. *J. Am. Chem. Soc.* **1989**, *111*, 3075-3077.

(42) Quan, M. L. C.; Cram, D. J. *J. Am. Chem. Soc.* **1994**, *113*, 2754-2755.

(43) Hennion, G. F.; Kupiecki, F. P. *J. Org. Chem.* **1953**, *18*, 1601-1608.

(44) Jackson, C. L.; Smith, P. S. *Am. Chem. J.* **1904**, *32*, 168-181.

(45) Vogel, A. I. In *Vogel's Textbook of Practical Organic Chemistry*; 5 ed.; B. S. Furniss, A. J. Hannaford, P. W. G. Smith and A. R. Tatchell, Ed.; Longman Scientific & Technical: Essex, 1989; pp 939-941.

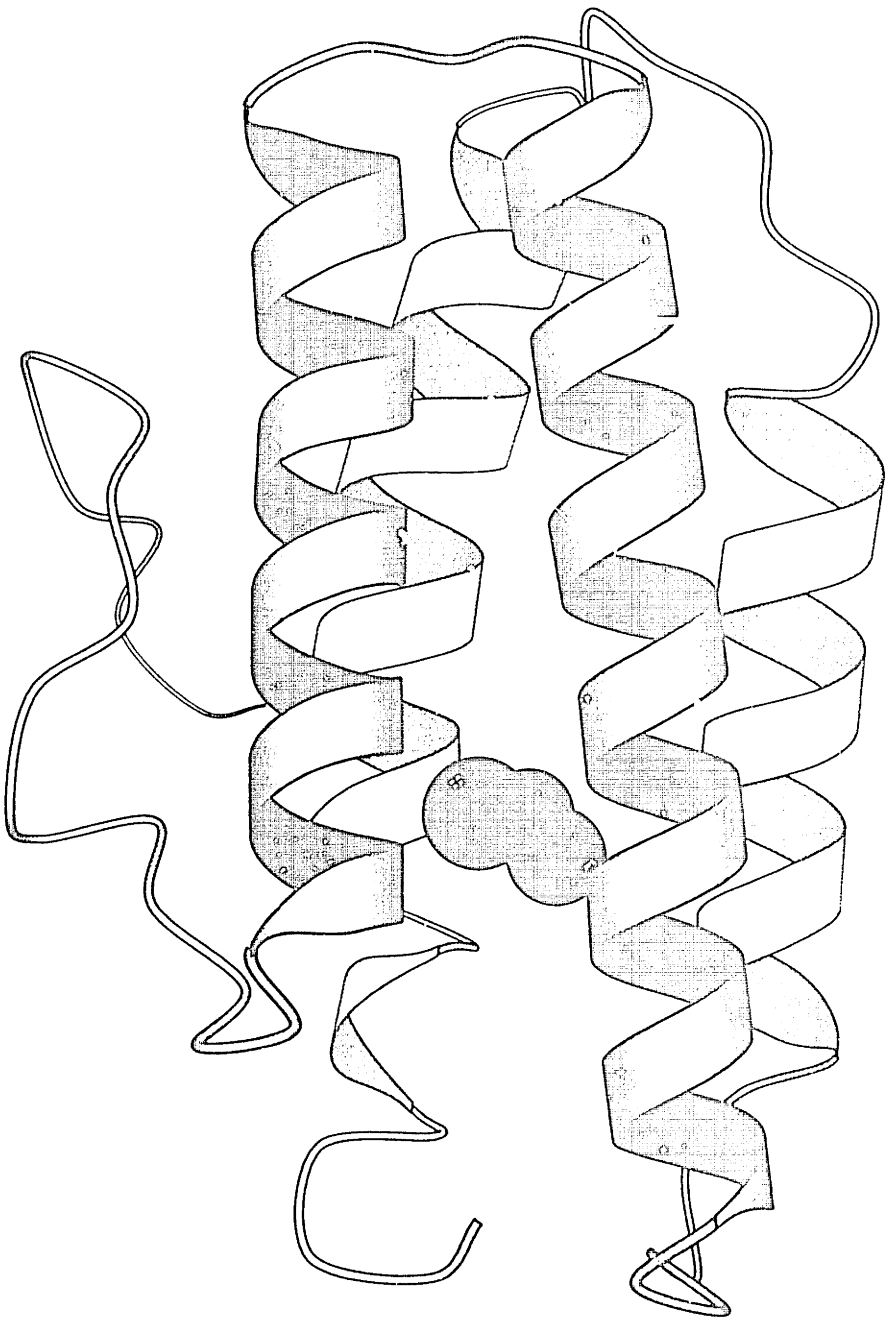

Schematic representation[1] of myohemerythrin[2]. The μ-oxo-diiron active site is located between four protein α–helices. The two iron ions (black) are bridged by an oxide ion (grey) and are octahedrally coordinated by amino acid residues (not shown) from the four α–helices. One iron center has a vacant coordination site where dioxygen is bound reversibly.

---

(1) Kraulis, P. J. *J. Appl. Cryst.* **1991**, *24*, 946-950.
(2) Sheriff, S.; Hendrickson, W. A.; Smith, J. L. *J. Mol. Biol.* **1987**, *197*, 273-296.

Part II

Modeling the Active Site of Metalloproteins

Chapter 7

Oxygen Transport and Metalloproteins

7.1
Introduction

Some two billion years ago photosynthetic processes began to change earth's initially reducing atmosphere to an oxidizing environment. Increasing amounts of atmospheric oxygen provided a new energy source for organisms[1]. Under anaerobic conditions glucose for example can only be broken down to lactic acid or ethanol. In the presence of oxygen (aerobic environment) however glucose can be metabolized completely to carbon dioxide and water. The amounts of energy provided by the different metabolic pathways are illustrated in the following net equations.

reducing (anaerobic) environment:

$C_6H_{12}O_6$	$\rightarrow 2\ C_2H_5OH + 2\ CO_2$	+70 kJ mol^{-1}
$C_6H_{12}O_6$	$\rightarrow CH_3CH(OH)CO_2H + C_2H_5OH + CO_2$	+ 90 kJ·mol^{-1}
$C_6H_{12}O_6$	$\rightarrow 2\ CH_3CH(OH)CO_2H$	+ 115 kJ·mol^{-1}

oxidizing (aerobic) environment:

$C_6H_{12}O_6 + 6\ O_2$	$\rightarrow 6\ CO_2 + 6\ H_2O$	+ 2800 kJ·mol^{-1}

In order to utilize oxygen for metabolic processes, i.e. respiration, systems for oxygen uptake, transport, and storage had to evolve, as well as metabolic enzymes making use of the oxygen delivered by the transport system. Oxygen has to be bound reversibly to

carrier proteins for transport and has to undergo stepwise reduction in respiratory and other enzymes. The active site of oxygen transport proteins and enzymes therefore contain various metal ions, depending on the function of the respective proteins.

7.2
Metalloproteins Featuring Iron Centers

Iron composes about 4.7 % of the earth's crust (upper 10 mile layer), is the 4th most abundant element and is *the* most abundant transition metal in the earth's crust[2]. Its natural abundance, the Lewis acidity and redox activity make it an ideal candidate for widespread use by Nature. In order to attach a metal ion to the protein, appropriate metal-ligating environments had to be created. One way for creating a metal center in proteins is the incorporation of a prosthetic group, a non-peptide moiety which contains the metal ion. A prominent example is the porphyrin core which binds iron in oxygen transporting proteins and oxidation enzymes[3].

An alternative method to incorporate a metal into a protein structure would be to let appropriate amino acid side chains coordinate directly to the metal ion. Many biological examples are known to ligate different transition metals to perform a multitude of biological tasks[4]. Polymetallic iron centers, in which two or more iron ions are bridged by oxygen for example, are ubiquitous in nature[5-9].

Figure 7-1: Common biological ligand environments for iron. **a)** Porphyrin core e.g. in hemoglobin, myoglobin, and cytochromes; **b)** μ-Oxo-diiron core e.g. in hemerythrin, ribonucleotide reductase, methane monooxygenase.

While most organisms in the animal kingdom rely on porphyrin-based hemoglobin for oxygen transport, certain invertebrates employ simpler systems without a prosthetic group. One example is hemocyanin, a binuclear copper complex which in its deoxy state

features an empty cavity between the copper ions. Dioxygen can be bound reversibly between the two copper ions. Another oxygen carrier without a prosthetic group is hemerythrin which will be discussed in more detail below. The distribution of the various oxygen carriers among different species is illustrated in figure *7-2*.

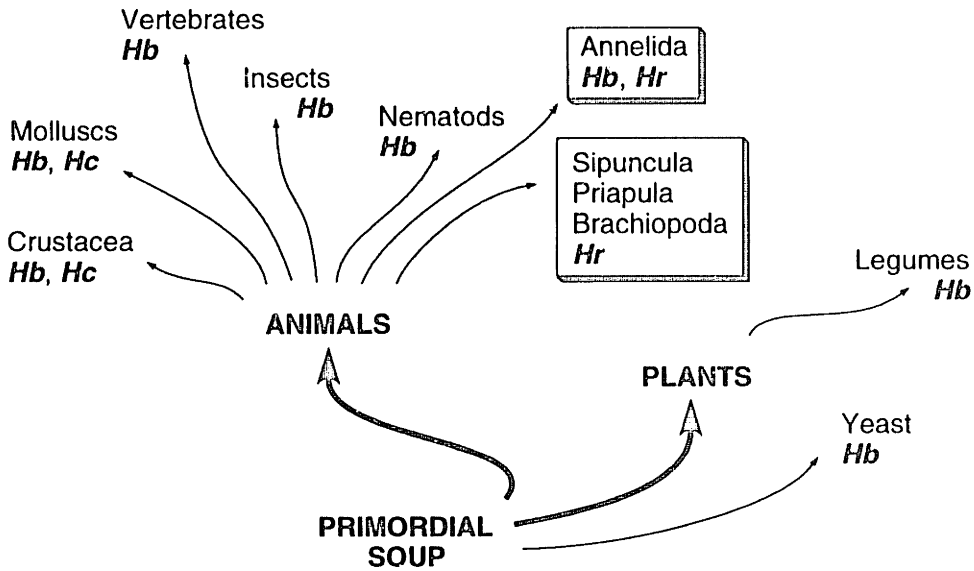

Figure *7-2*: Occurrence of oxygen transport proteins in Nature. ***Hb***, hemoglobin; ***Hc***, hemocyanin; ***Hr***, hemerythrin. Scheme adapted from ref[10].

The following table compares some key features in the three oxygen binding pigments.

	Hemoglobin	*Hemerythrin*	*Hemocyanin*
Metal	Fe	Fe	Cu
Oxidation state in deoxy form	+2	+2	+1
Stoichiometry (metal : O_2)	Fe : O_2	2 Fe : O_2	2 Cu : O_2
Metal Coordination	porphyrin, 1 His	5 His, 1 Asp, 1 Glu, 1 μ-O	6 His

7.2.1 Hemerythrin

Various marine worms and brachiopods use the non-heme ferroproteins hemerythrin[10-13] and myohemerythrin[14] for oxygen transport and storage. Hemerythrin is

found in various oligomeric forms: Monomeric myohemerythrin, and dimeric, trimeric, tetrameric, as well as octameric hemerythrin. The underlying subunit is a 13.5 kD, 113 amino acid protein featuring a four α-helix bundle. Two μ-oxo-bridged iron ions are bound inside the four-helix bundle by histidine side chain residues from the four α-helices. The cover figure for Part II on page 113 illustrates how the diiron active site is embedded in the protein. Two bridging carboxylates from side chain aspartates and glutamates complete the octahedral coordination sphere for one of the iron ions. The other iron has one coordination site vacant where dioxygen can be bound reversibly:

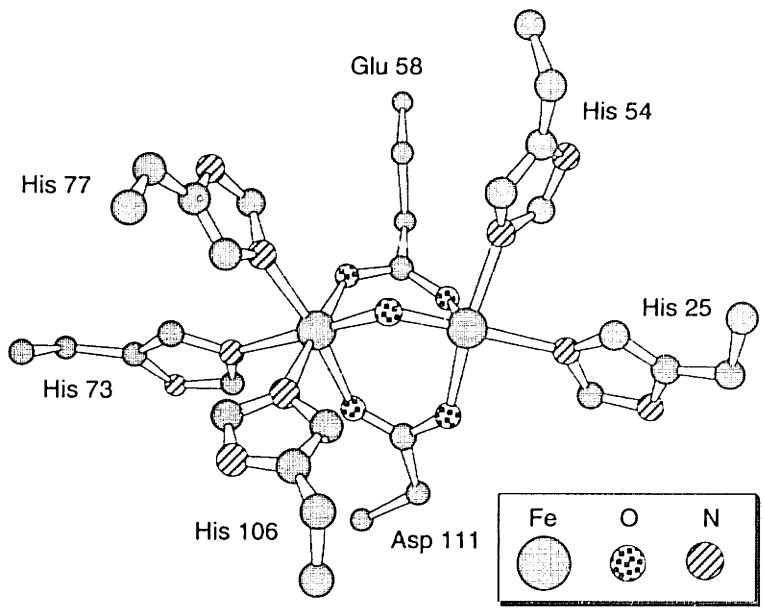

Figure *7-3*: The active center of myohemerythrin. The crystal structure[14] has been obtained in the azidomet state, i.e. both iron ions are in the +3 oxidation state and the vacant coordination site (at the lower right) of the second (right) iron atom is occupied by an azide ion.

In the active (deoxy) form of hemerythrin prior to oxygen binding both iron ions are in the +2 oxidation state and the μ-oxo-bridge is protonated. Oxygen is bound as hydroperoxide with a hydrogen bond to the central μ-oxo atom as shown in figure *7-4*.

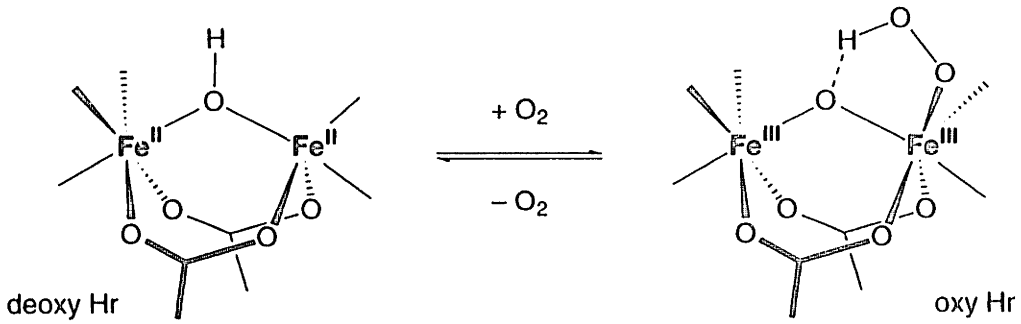

Figure 7-4: Reversible oxygen binding to hemerythrin.

The redox behavior of hemerythrin has been explored in detail and several distinguishable forms have been characterized. Artificially oxidized met hemerythrin with both iron ions in the +3 oxidation states is the most stable form and several crystal structures with various anions occupying the oxygen-binding site have been obtained. Two different semi-met forms (+2/+3 mixed-valence states) are known. One-electron oxidation of deoxy Hr leads to $(\text{semi-met})_O$ whereas single electron reduction of met Hr gives $(\text{semi-met})_R$. The correlations between the different oxidation states are shown in figure *7-5*.

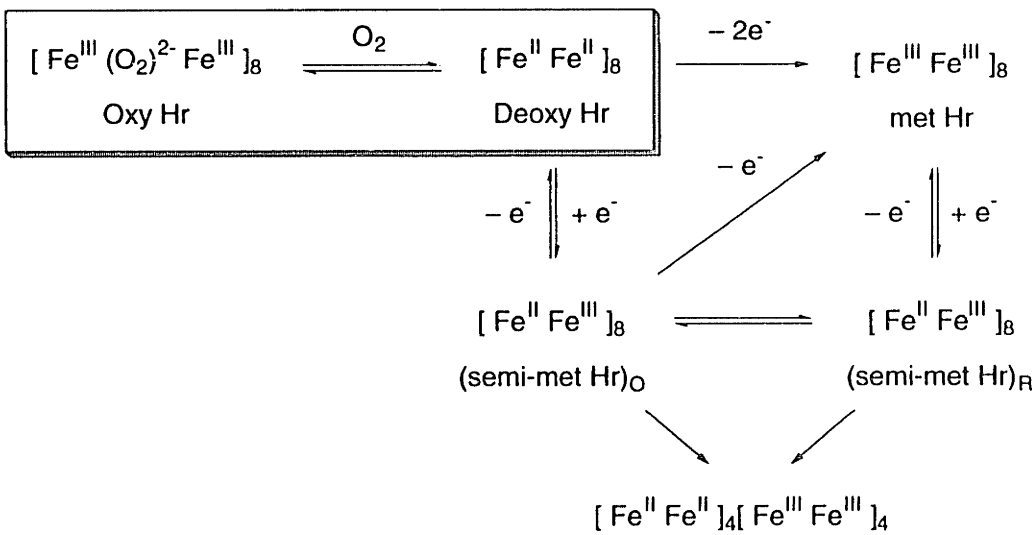

Figure 7-5: Redox states of hemerythrin[12]. *In vivo* redox states are boxed, redox states observed *in vitro* are outside the box.

7.2.2
Other occurrences of Fe–O–Fe centers

As already indicated above, the μ-oxo-diiron center is rather common in Nature. Several occurrences are known, some of which are fairly well understood.

A biological example for a C–H activation catalyst is *methane mono-oxygenase (MMO)* which is found in methanotrophic bacteria. It catalyzes the oxidation of methane to methanol and allows the bacteria to use methane as the only source for carbon and energy:

$$CH_4 + O_2 + NADH + H^+ \rightarrow CH_3OH + H_2O + NAD^+$$

The protein consists of several subunits, the actual substrate oxidation occurring at a μ-oxo-diiron site in the hydroxylase component of the protein. The other subunits serve to transfer electrons from NADH to the hydroxylase[4]. The active site is located within a hydrophobic pocket of the hydroxylase and coordinated by glutamate carboxylates and histidines[15,16].

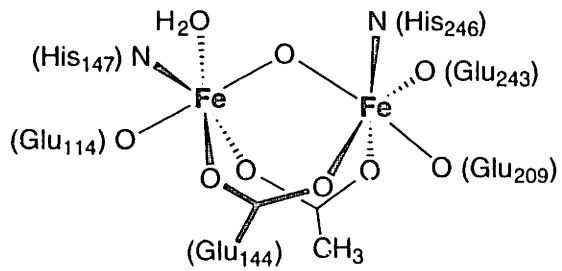

Figure 7-6: Schematic representation of the μ-oxo-diiron active site in oxidized form of the hydroxylase protein in methane mono-oxygenase of *Methylococcus capsulatus* (Bath)[15]

The mechanism is believed to begin with activation of dioxygen by the $Fe(II)_2$ diiron center which subsequently abstracts a hydrogen atom from methane. The resulting methyl radical then reacts with an iron-bound hydroxy group to form methanol[9].

Ribonucleotide reductase enzymes catalyze an important step in DNA biosynthesis: The reduction of ribonucleotides to deoxyribonucleotides.

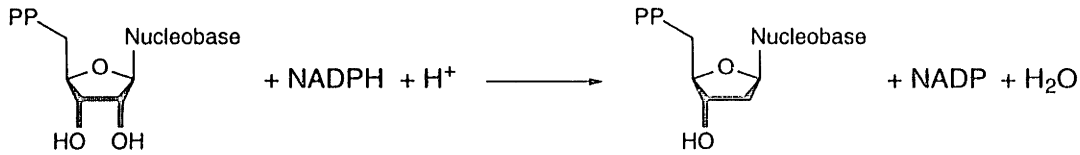

Enzymes of this class are widely encountered, from bacteria and viruses to mammals. The protein consists of two subunits, one which binds the substrate and the other featuring the μ-oxo-diiron center embedded within four α–helices, just as in hemerythrin or methane mono-oxygenase. Only one residue (glutamate) bridges the two irons besides the μ-oxo bridge. A tyrosyl radical located 5.3 Å away from one of the irons is essential for the active enzyme, replacement of tyrosine 122 with phenylalanine in a site directed mutagenesis study gives an inactive enzyme[4].

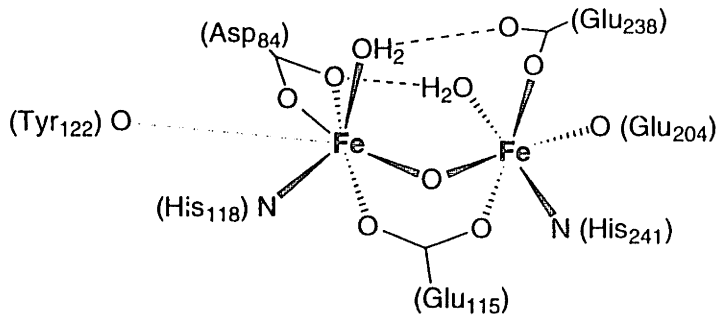

Figure 7-7: Schematic representation of the μ-oxo-diiron active site in ribonucleotide reductase[17].

The examples described above illustrate the importance of the Fe-O-Fe unit in biology. It is not surprising that reproducing these oxygen binding and oxidation capabilities with synthetic model compounds has been attempted by several research groups.

7.3
References

(1) Alberts, B.; Bray, D.; Lewis, J.; Raff, M.; Roberts, K.; Watson, J. D. *Molecular Biology of the Cell;* 3rd ed.; Garland Publishers: New York, NY, 1994.

(2) Hollemann, A. F. *Lehrbuch der anorganischen Chemie;* 91-100 ed.; de Gruyter: Berlin, New York, 1985.

(3) Stryer, L. *Biochemistry;* 3rd. ed.; Freeman: New York, NY, 1988.

(4) Lippard, S.; Berg, J. *Principles of Bioinorganic Chemistry*; University Science Books: Mill Valley, CA, 1994.

(5) Lippard, S. J. *Chem. Br.* **1986**, *22*, 222-229.

(6) Lippard, S. J. *Angew. Chem. Int. Ed. Engl.* **1988**, *27*, 344-361.

(7) Kurtz, D. M., Jr. *Chem. Rev.* **1990**, *90*, 585-606.

(8) Vincent, J. B.; Olivier-Lilley, G. L.; Averill, B. A. *Chem. Rev.* **1990**, *90*, 1447-1467.

(9) Wilkins, P. C.; Dalton, H. *Biochem. Soc. Trans.* **1994**, *22*, 700-704.

(10) Klotz, I. M.; Kurtz, D. M., Jr. *Acc. Chem. Res.* **1984**, *17*, 16-22.

(11) Stenkamp, R. E.; Sieker, L. C.; Jensen, L. H.; McCallum, J. D.; Sanders-Loehr, J. *Proc. Natl. Acad. Sci. USA* **1985**, *82*, 713-716.

(12) Wilkins, P. C.; Wilkins, R. G. *Coord. Chem. Rev.* **1987**, *97*, 195-214.

(13) Holmes, M. A.; Le Trong, I.; Turley, S.; Sieker, L. C.; Stenkamp, R. E. *J. Mol. Biol.* **1991**, *218*, 583-593.

(14) Sheriff, S.; Hendrickson, W. A.; Smith, J. L. *J. Mol. Biol.* **1987**, *197*, 273-296.

(15) Rosenzweig, A. C.; Frederick, C. A.; Lippard, S. J.; Nordlund, P. *Nature* **1993**, *366*, 537-543.

(16) Rosenzweig, A. C.; Lippard, S. J. *Acc. Chem. Res.* **1994**, *27*, 229-236.

(17) Nordlund, P.; Sjöberg, B.-M.; Eklund, H. *Nature* **1990**, *345*, 593-598.

Chapter 8

Hemerythrin Model Compounds

8.1
Introduction

Hemerythrin can be considered a prototype for enzymes containing a μ-oxo-diiron active site. Therefore, considerable effort has been spent to synthesize model coordination compounds[1] mimicking structure and function of hemerythrin.

The first realistic structural model compounds for the hemerythrin core were published independently by Wieghardt et al.[2,3] and Lippard et al[4,5]. The syntheses relied on the chelating properties of the tridentate capping triazacyclononane[6] derivatives **8.01**, **8.02** and trispyrazolylborate[7] **8.03** which were used together with acetates. In both cases, a (μ-oxo)bis(μ-acetato)diiron(III) complex formed spontaneously.

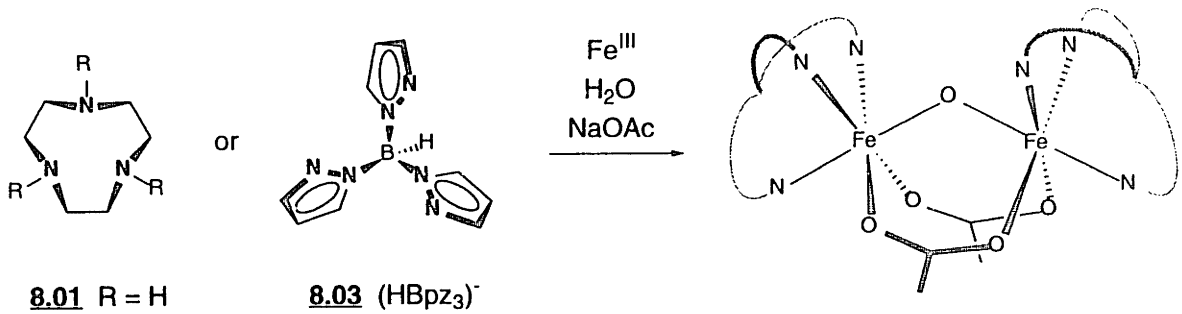

8.01 R = H
8.02 R = Me

8.03 $(HBpz_3)^-$

Even though these model compounds proved to be good structural analogs of the hemerythrin active site, they failed to reproduce the redox behavior of the enzyme. Upon reduction of the diferric complexes only the bis(chelate)iron(II) complexes were obtained. However, the diferrous oxidation state in deoxy hemerythrin could be modeled if ligand **8.02** was used[8]. The μ-hydroxo bridge between the two irons in the diferrous form was converted to a μ-oxo-bridge upon two-electron oxidation to the diferric compound. Furthermore, a mixed-valence (semimet Hr analog) compound could be observed after electrochemical reduction of the diferric complex based on **8.02**[9]. Only very recently has a μ-hydroxo mixed valence complex been characterized which shows the expected redox activity similar to semimet Hr[10].

A multitude of oxo- and hydroxo-bridged diiron complexes has been investigated[11]. Some model systems are known to bind dioxygen to diferrous complexes[12,13] or a "half-Hr" model[14] and C–H activation in alkanes has been demonstrated[15]. However, model compounds for hemerythrin that mimic the geometry and reversibly bind dioxygen in the same way as hemerythrin are yet unknown.

8.2
Towards Functional Hemerythrin Model Compounds

A functional hemerythrin model which is able to reversibly bind dioxygen requires either a vacant coordination site on one of the iron ions, or a ligand that is readily replaced by oxygen. The (μ-oxo)bis(μ-carboxylato)diiron complexes capped by tridentate ligands can not serve this purpose since all the ligands coordinate too strongly to the metal ions. A first study towards replacing the tridentate ligands with bidentate and monodentate ligands focused on the spacer between linked bridging carboxylates[16,17]. It was found that *m*-phenylene-dipropionic acid provided the appropriate distance of 6 Å between the β-methylene carbon atoms for effective formation of two μ-carboxylato bridges between the metal ions. Another study showed that even a non ideal dicarboxylate geometry is able to form (μ-oxo)bis(μ-carboxylato)diiron complexes[18,19].

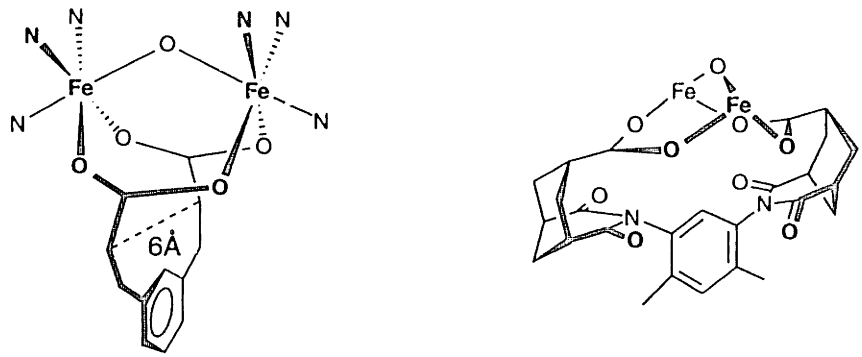

Figure *8-1*: Left: Ideal dicarboxylate geometry[16,17] provided by *m*-phenylenedipropionic acid. Right: Coplanar dicarboxylate[20,21] as the basis for a (μ-oxo)bis(μ-carboxylato)diiron complex[18,19].

8.3
A Cleft-Shaped Chelating Ligand

The projected ligand represented a fist step towards the ideal coordination environment for the diiron center. A cleft-shaped ligand was supposed to provide bridging carboxy functions as well as terminal nitrogen donors. A U-shaped geometry would serve to hold the different ligand parts in place within the same molecule. A certain amount of flexibility within the U-shaped structure would allow the complex to find its own best geometry and accommodate discrepancies between the molecular model and the actual geometry of the complex.

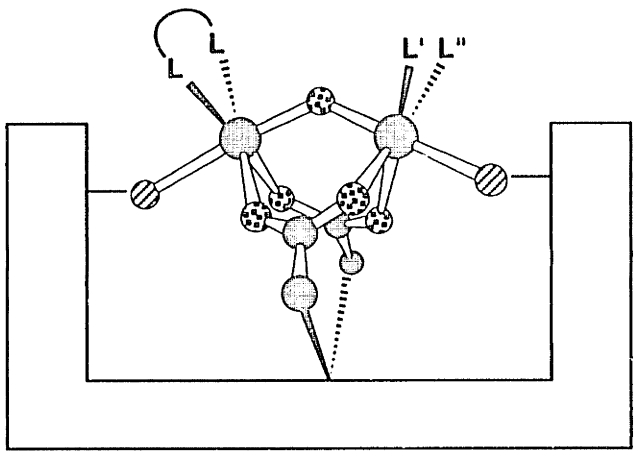

The cleft-shaped ligand would—in a first-generation system—only provide one nitrogen donor per iron ion. Additional ligands would be needed to provide a complete coordination sphere. The plan was to use for example a chelating bipyridyl system for one of the iron atoms, and two different monodentate ligands L' and L" for the other iron atom. If a labile ligand is chosen for either L' or L", it could be replaced for example by dioxygen, thereby representing a functional model for hemerythrin. If the first-generation design gives promising results, more nitrogen donors could be incorporated in future ligand designs.

Based on the experience gained form molecular clefts with convergent functional groups[22-24], a scaffold of two xanthene units separated by a biphenyl spacer was chosen.

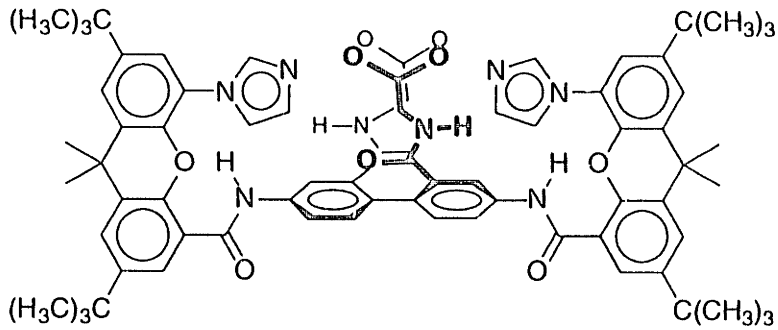

The biscarboxy-functionalized biphenyl spacer links together the two rigid xanthenes which provide the terminal nitrogen ligands. This basic scaffold contains several parameters that can be adjusted to optimize the chelating properties of the ligand as a whole:

- carboxylate-spacer linkage
- spacer-xanthene linkage
- nitrogen-xanthene linkage

The carboxylate–spacer linkage: A spacer based on diphenic acid can be combined with ω-amino acids of different chain lengths. The reach and flexibility of the carboxylates can be influenced in this way.

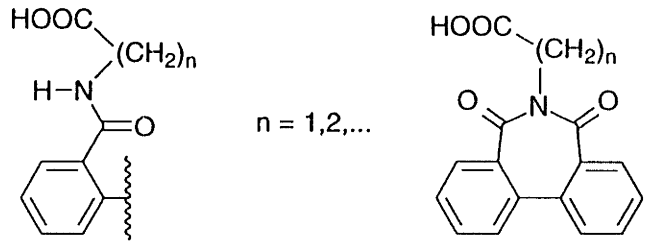

Another advantage of using a diphenic acid derived spacer is that access to a monocarboxylate ligand is given through an imide link as shown.

The spacer-xanthene linkage: For synthetic simplicity, the attachment of the xanthenes to the spacer is accomplished by an amide link. Depending on whether the amine originates from the spacer and the carboxylic acid from the xanthenes (or vice versa) the result will be either a shallow or a deep cleft.

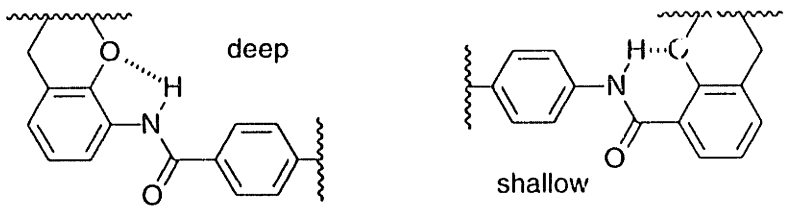

The intramolecular hydrogen bond between the amide proton and the xanthene oxygen is known to increase the energy barrier for rotation of the amide group. Conformations resulting in a deep or shallow clefts are stabilized accordingly[24].

The nitrogen-xanthene linkage: The converging nitrogen donors can be introduced within an aliphatic or heterocyclic (saturated or aromatic) building block. The closest analogy to biological systems would of course be a histidine residue. For synthetic ease, however, a *N*-functionalized imidazole derivative was chosen.

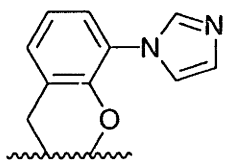

Taking into account solubilizing substituents on the xanthenes, we chose the target molecule for a first-generation chelating ligand as the dicarboxylate shown in figure *8-2*.

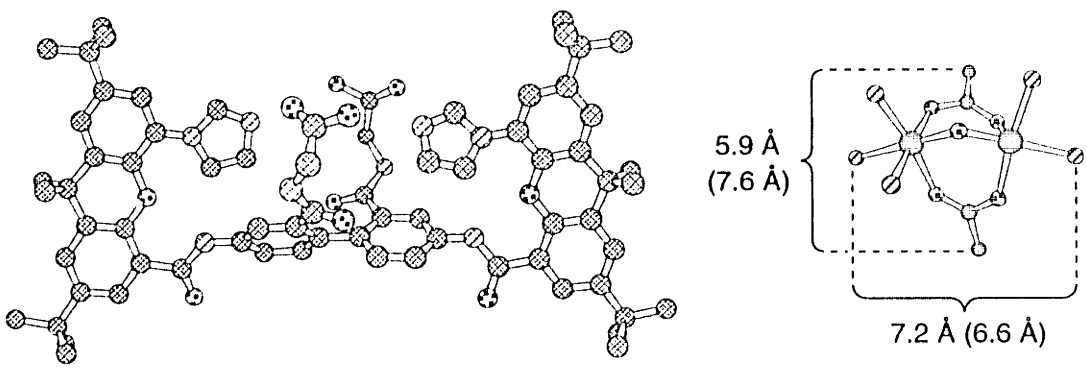

Figure *8-2*: Proposed ligand for the preparation of a functional model of hemerythrin. The distances between the carboxylate a-carbon atoms and the axial nitrogen atoms in myohemerythrin[25] are compared to the corresponding distances in the ligand (in brackets) as predicted by molecular modeling[26].

A convergent synthesis was planned with the biphenyl spacer and the xanthene moieties as separate entities which would be assembled into a cleft-shaped molecule.

8.3.1
The Biphenyl Spacer (Bottom Unit)

Based on the work of Thomas F. Jenny[27], the synthesis of the chiral spacer dl-4,4'-diamino-6,6'-dimethyl-biphenyl-2,2'-dicarboxylic acid **8.07** was approached.

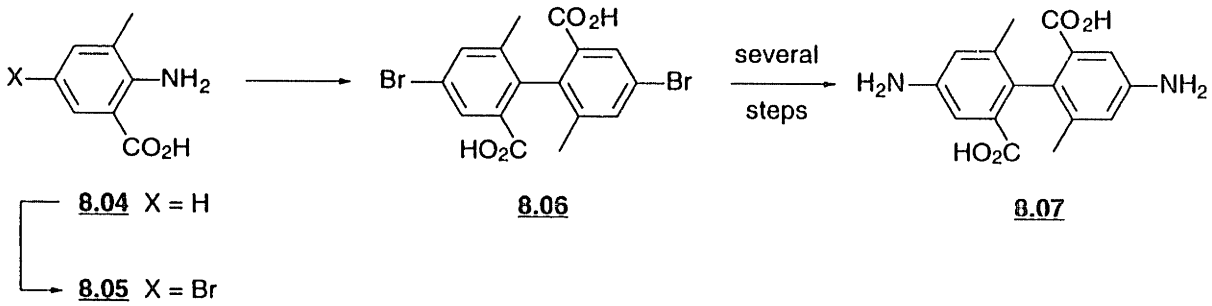

However, due to the disappointingly low yields in the copper mediated reductive aryl diazonium coupling[28-31] step, this approach was discontinued. Because chirality of the spacer is not a required feature, other approaches were tried with 4,4'-difunctionalized diphenic acid as the new target.

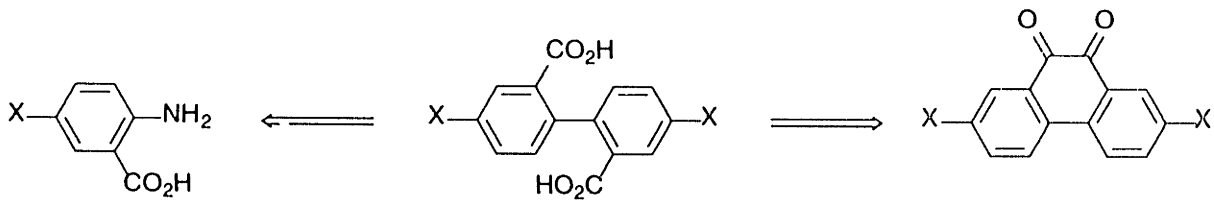

Substituted 9,10-phenanthrenediones can be oxidized easily and cleanly to the corresponding substituted diphenic acids[32,33]. However, neither bromination nor nitration of 9,10-phenanthrenedione gave the corresponding 2,7-disubstituted compounds in satisfying yields. Reductive coupling[28-31] of bromoanthranilic acid proved to be uneconomical. Ullmann coupling reactions[34,35] did not establish themselves as viable routes, either.

It was therefore attempted to effect 4,4'-difunctionalization of a biphenyl system. Direct bromination of diphenic acid gave a mixture of different isomers in poor yield, direct nitration of diphenic acid **8.08** led to a mixture of 4,4'-dinitro-diphenic acid **8.09** and 4,6'-dinitro-diphenic acid. Separation of the two isomers as the diacids was difficult, but the corresponding dimethyl esters were easily separated and the desired 4,4'-isomer could be prepared in large quantities. The diester was saponified, and the diacid **8.10** converted to the diacid chloride **8.11** with PCl_5 to avoid formation of the intramolecular anhydride. Reaction with ethylglycinate gave the spacer precursor compound **8.12**.

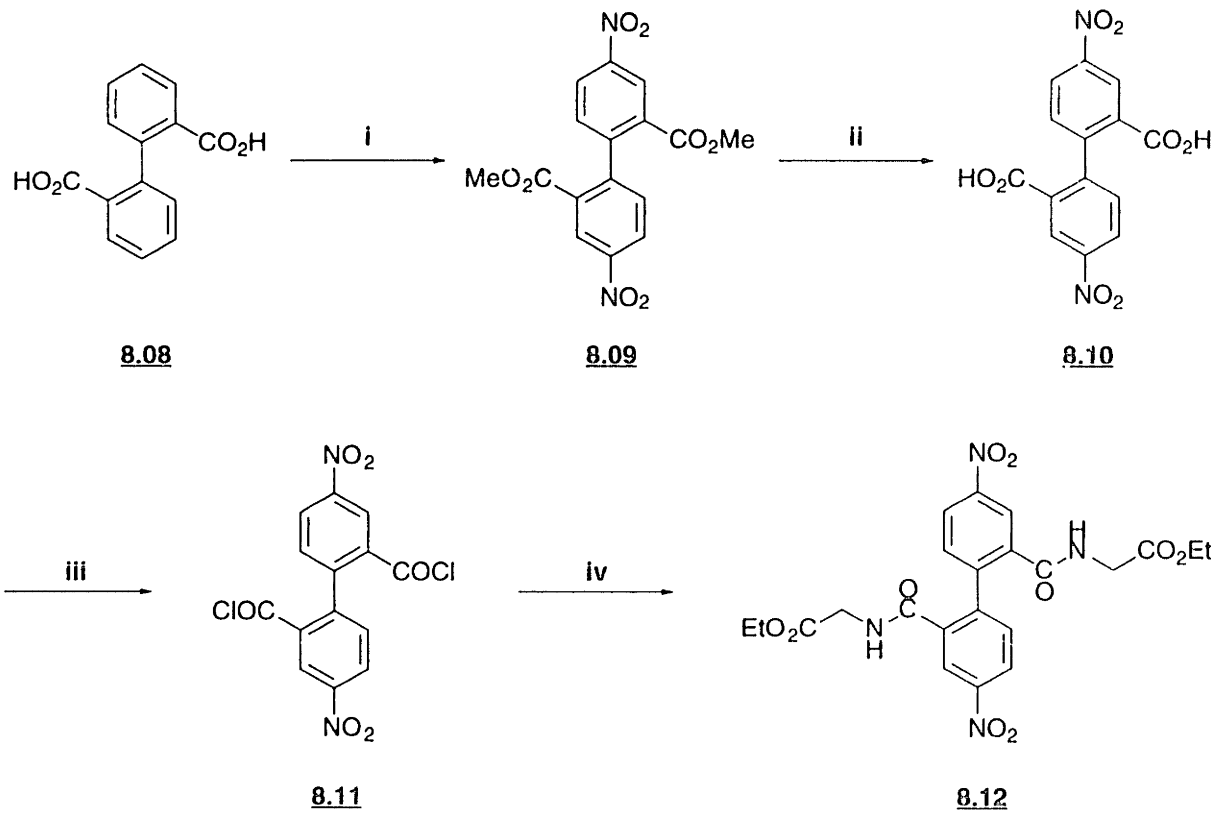

Figure *8-3*: Synthesis of the biphenylene derived spacer. Reagents: **i** a) HNO_3, H_2SO_4, b) MeOH, H_2SO_4 ; **ii** NaOH, THF, MeOH, H_2O; **iii** PCl_5, Et_2O; **iv** ethyl glycinate, Et_3N, CH_2Cl_2.

Catalytic hydrogenation of the dinitro compound **8.12** gives the corresponding diamine in good yields. In general, this procedure represents the first example of an effective synthesis of dicarboxysubstituted 4,4'-diaminodiphenic acids.

8.3.2
The Xanthene Units (Wall Units)

Some of the precursors for the required xanthene derivatives were known compounds[24]. Minor improvements to the published procedure for dimethyl-di-*tert*-butylxanthene **8.15** were found.

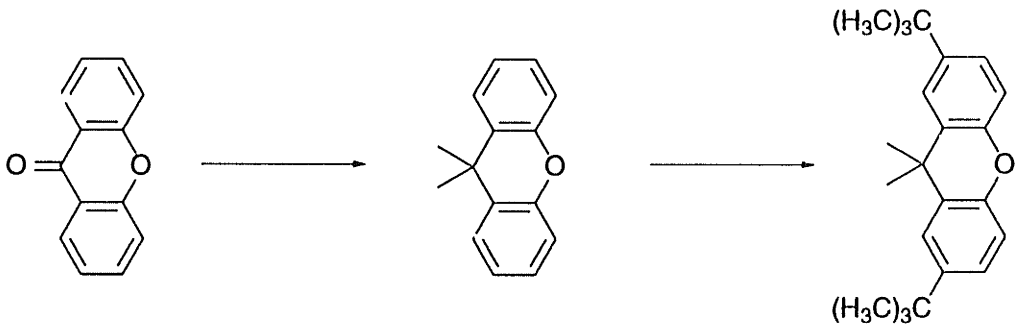

8.13 **8.14** **8.15**

Desymmetrization of the xanthenes had previously only been accomplished either at the diacid stage by monoesterification[24] or at the dimethyl ester stage by monohydrolysis[36].

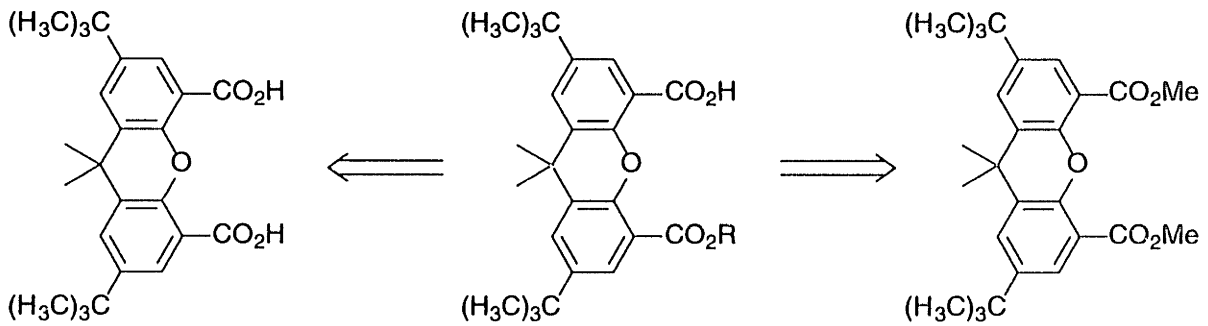

In order to obtain the desired imidazole-xanthene link, a different desymmetrization of the xanthene building block had to be found. Reinvestigation of the dibromination of dimethyl-di-*tert*-butylxanthene **8.15** showed that the rates for the first and the second electrophilic bromine substitution were rather different. By choosing appropriate reaction conditions it was now possible to obtain the monobrominated xanthene **8.16**. A two-step procedure, cyanation[37] of the aryl bromide and subsequent hydrolysis[38] of the nitrile **8.17**, proved to be a superior route to the carboxylic acid, compared with a procedure based on lithiation of the aryl bromide followed by a carbon dioxide quench[24]. Bromination of the

carboxylic acid **8.19** followed by aryl coupling in molten imidazole gave the carboxy-imidazolo xanthene **8.20**.

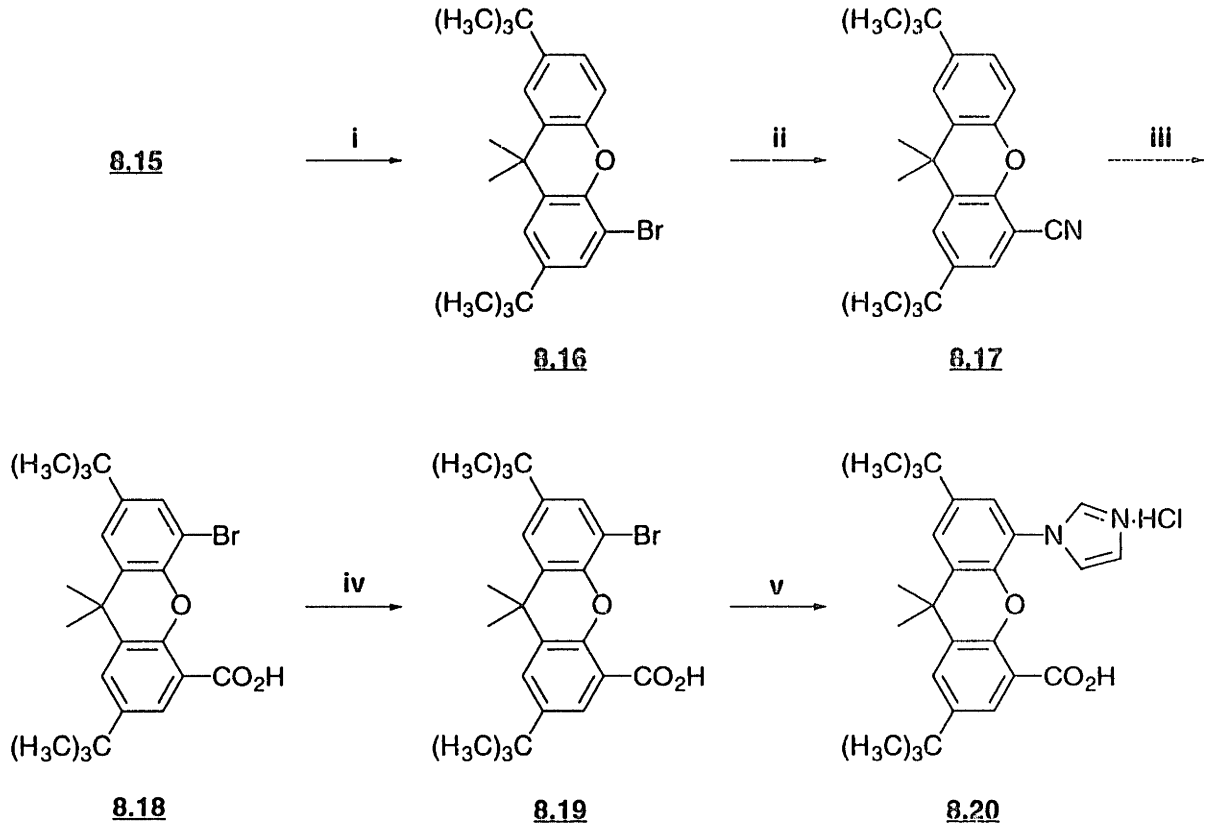

Figure *8-4*: Synthesis of the new carboxy-imidazolo-xanthene. Reagents: **i** Br_2, CH_2Cl_2; **ii** CuCN, 1-methylpyrrolidone; **iii** KOH, ethylene glycol; **iv** Br_2, HOAc; **v** imidazole, Cu_2O.

The synthetic accessibility of the xanthene derivative complementary to a 4,4'-dicarboxy substituted spacer was also investigated. The xanthene derivative complementary to a dicarboxy spacer has to carry an amino function instead of the carboxy group in **8.20**. Beginning with monobromoxanthene **8.16**, Gabriel synthesis of the xanthene-amine with parallel bromination followed by hydrazinolysis of the phthalimide **8.21** proved to be an effective synthesis of the bromoamine **8.23**. The bromoamine **8.23** could then be reacted with imidazole in analogy to the synthesis of the corresponding carboxy compound **8.24**.

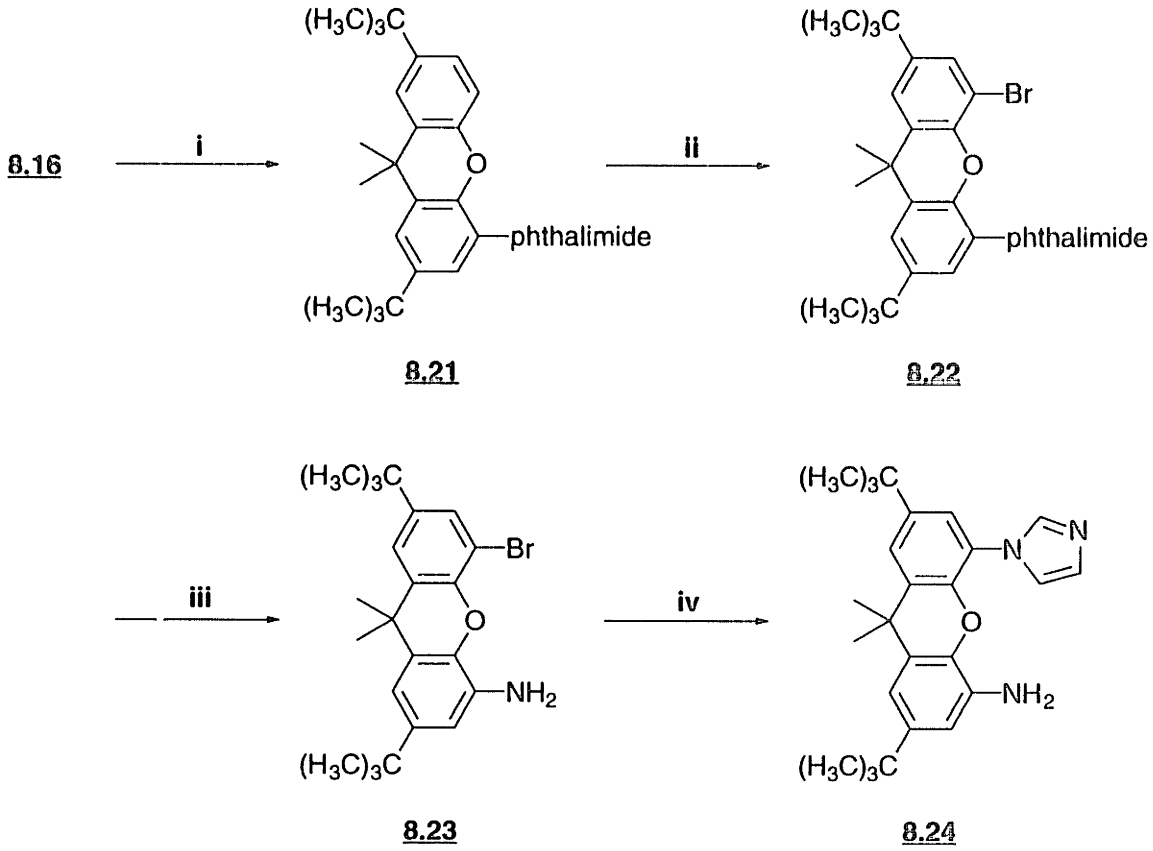

Figure *8-5*: Synthesis of the new amino-imidazolo-xanthene. Reagents: **i** phthalimide, DMF; **ii** Br_2, CH_2Cl_2; **iii** H_2NNH_2, MeOH, CH_2Cl_2; **iv** imidazole, Cu_2O.

Prior to the assembly of the cleft-shaped ligand, the 4,4'-dinitrosubstituted spacer 8.12 had to be reduced to the corresponding diamine 8.25. The reduction was conveniently carried out catalytically with Pd/C and hydrogen. The imidazolo-carboxylic acid 8.20 was converted to the acid chloride 8.26 with oxalyl chloride and added to a pyridine solution of the diamine 8.25. After column chromatography the cleft diester 8.27 was isolated in 55% yield.

8.3.3
Attempted Fe Binding Studies

The ethyl ... functions could be hydrolyzed under basic conditions. The resulting diacid however, was not found to be a chelating ligand. Trials with ferric perchlorate or ferric

nitrate all produced a fine brown precipitate, and at times the ligand crystallized separately. Even when the oxo-bridged complex $[Et_4N]_2[Fe_2OCl_6]$ (obtained from Dr. Stephen P. Watton) was used, no crystalline material could be obtained from the complexation experiments. Accordingly, the project was abandoned.

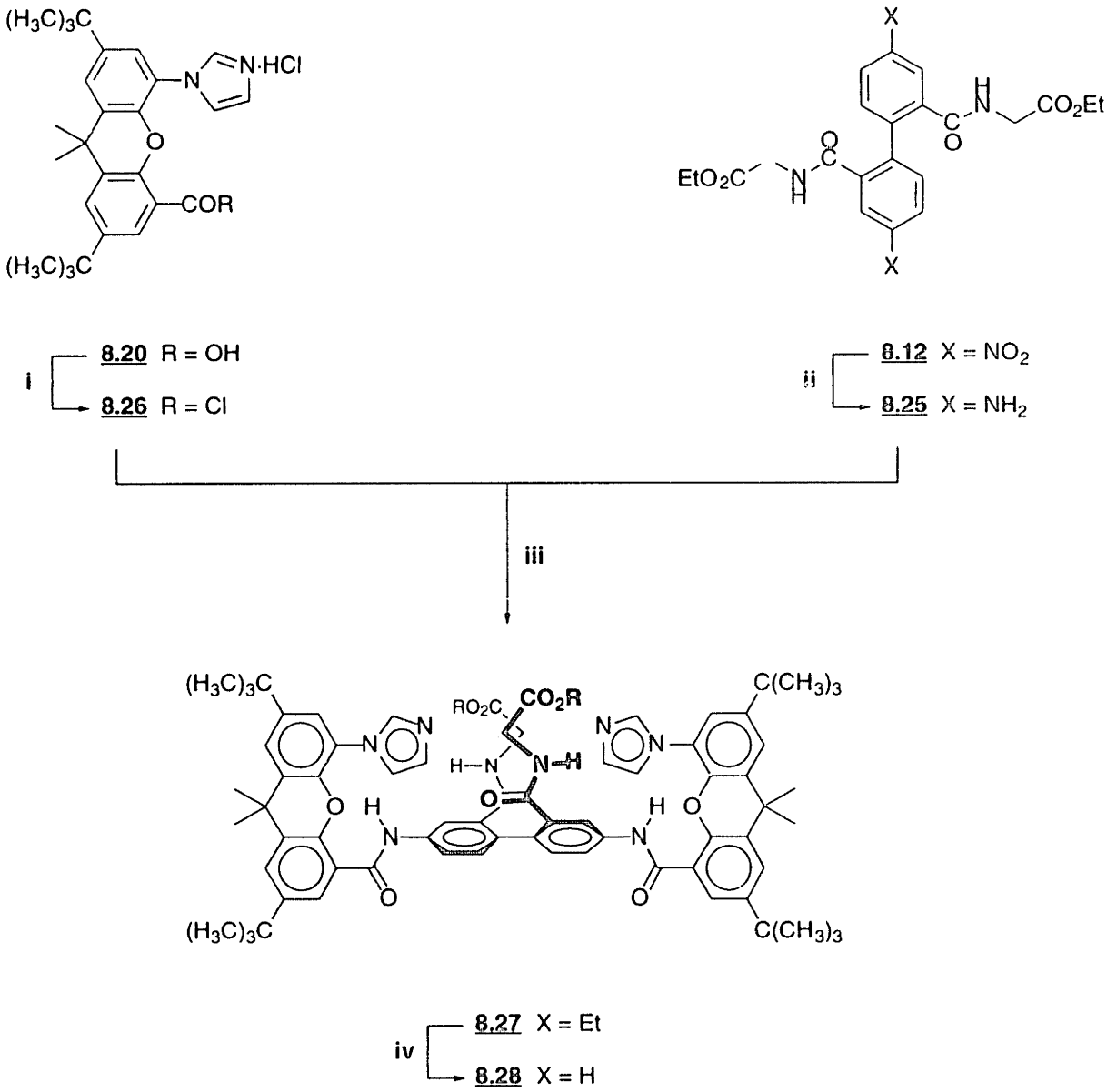

Figure *8-6*: Synthesis of the cleft-shaped ligand. Reagents: **i** oxalyl chloride, CH_2Cl_2; **ii** H_2, Pd/C, EtOH, benzene; **iii** pyridine; **iv** NaOH, THF, MeOH, H_2O.

8.4
Experimental

For general apparatus, methods, and materials information, see Chapter 3, page 50.

Carbon count in xanthenes:

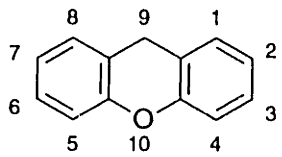

9,9-Dimethylxanthene, 8.14

was prepared as described in the literature[24].

2,7-Di-*tert*-butyl-9,9-dimethylxanthene, 8.15

was prepared according to a modified published procedure[24].

2-Chloro-2-methylpropane **8.14** (0.60 mol, 65 ml) was added to a solution of crude 9,9-dimethylxanthene (≤ 0.247 mol, 51.9 g)[24] in CH_2Cl_2 (250 ml) at 0°C. Anhydrous $FeCl_3$ (0.02 mol, 3.0 g) was added in small batches in 15 min intervals. (If the portions were too large, the mixture had the tendency to boil over.) The mixture was allowed to warm to room temperature while stirring over night. It was then washed thoroughly with water (3 x 350 ml), the combined aqueous phases were back extracted with CH_2Cl_2 (2 x 50 ml). The combined organic layers were dried over $MgSO_4$, concentrated by rotary evaporation, and crystalline material collected periodically by filtration to afford (after washing with little CH_2Cl_2) colorless crystals. The residual yellow oil was refrigerated over night and a second crop was obtained.

Yield: 55.6 g (69 % relative to xanthone)

^1H NMR (300 MHz, $CDCl_3$): δ 7.40 (d, $2H_{ar}$, J=2.4 Hz); 7.21 (dd, $2H_{ar}$, J_1=8.3 Hz, J_2=2.3 Hz); 6.96 (d, $2H_{ar}$, J=8.4 Hz); 1.65 (s, $6H_{Me}$); 1.33 (s, $18H_{t\text{-}bu}$) ppm

4-Bromo-2,7-di*tert*-butyl-9,9-dimethylxanthene, 8.16

To a solution of 2,7-di-*tert*-butyl-9,9-dimethylxanthene **8.15** (0.05 mol, 16.13 g) in CH_2Cl_2 at 0°C was added bromine (0.05 mol, 2.6 ml) and the mixture was allowed to warm to room temperature while stirring over night. Complete consumption of starting material was checked by NMR. (If necessary a very small amount of bromine was added, and the mixture was stirred further.) The reaction was quenched with 300 ml aq. Na_2CO_3

solution. The organic phase was dried over $MgSO_4$, stirred with charcoal, filtered through Celite, and evaporated. The evaporation residue was triturated with PE (30/50) to remove dibromoxanthene (which is only sparingly soluble in PE), and the PE solution was evaporated to afford slightly greenish needles.

Yield: 19.07-19.67 g (95-98 %)

^1H NMR (300 MHz, $CDCl_3$): δ 7.44 (d, H_{ar}, J=2.4 Hz); 7.39 (d, H_{ar}, J=2.4 Hz); 7.34 (d, H_{ar}, J=2.4 Hz); 7.24 (dd, H_{ar}, J_1=8.4 Hz, J_2=2.4 Hz); 7.08 (d, H_{ar}, J=8.4 Hz); 1.63 (s, $6H_{Me}$); 1.33 (s, $9H_{t\text{-}bu}$); 1.32 (s, $9H_{t\text{-}bu}$) ppm

4-Cyano-2,7-di-*tert*-butyl-9,9-dimethylxanthene, 8.17

A suspension of 4-bromo-2,7-di-*tert*-butyl-9,9-dimethylxanthene 8.16 (0.03 mol, 12.04 g) and CuCN (0.03 mol, 2.7 g) in 25 ml 1-methyl-2-pyrrolidone was heated in a 190°C oil bath for 6 h. After slight cooling the slurry was poured in 200 ml water while stirring. The precipitate was filtered off, washed with water, and boiled in 200 ml HNO_3/H_2O (1:3 vol.) for 15 min until the evolution of NO_2 had ceased. The product was collected by filtration, washed with water, and dried on a steam bath.

Yield: 9.87 g (95 %)

^1H NMR (300 MHz, $CDCl_3$): δ 7.62 (d, H_{ar}, J=2.4 Hz); 7.48 (d, H_{ar}, J=2.4 Hz); 7.39 (d, H_{ar}, J=2.4 Hz); 7.27 (dd, H_{ar}, J_1=8.4 Hz, J_2=2.4 Hz); 7.11 (d, H_{ar}, J=8.4 Hz); 1.65 (s, $6H_{Me}$); 1.34 (s, $9H_{t\text{-}bu}$); 1.33 (s, $9H_{t\text{-}bu}$) ppm

MS *m/z* 347 (M, 7%); 333 (26%); 332 (M – CH_3 100%); 317 (8%); 316 (M, 11%), 302 (13%); 300 (7%)

HRMS calcd for M^+ $C_{24}H_{29}NO$ 347.2249, found 347.2250

4-Carboxy-2,7-di-*tert*-butyl-9,9-dimethylxanthene, 8.18

A suspension of 4-cyano-2,7-di-*tert*-butyl-9,9-dimethylxanthene 8.17 (0.01 mol, 3.47 g) and KOH (0.02 mol, 1.2 g) in 25 ml ethylene glycol was heated to mild reflux over night. The dark slurry was allowed to cool, poured in 200 ml water, and acidified with conc. HCl. The precipitate was filtered off, dissolved in ether, and washed with brine. The organic phase was dried over $MgSO_4$ and evaporated. The evaporation residue was rinsed with little PE (30/50) and dried under vacuum.

Yield: 3.18 g (87 %)

^{1}H NMR ($CDCl_3$, 300 MHz): δ 10.7-9.8 (b, $1H_{COOH}$); 8.11 (d, H_{ar}, J=3.0 Hz); 7.68 (d, H_{ar}, J=2.4 Hz); 7.46 (d, H_{ar}, J=2.7 Hz); 7.29 (dd, H_{ar}, J_1=9.8 Hz, J_2=2.9 Hz); 7.07 (d, H_{ar}, J=8.7 Hz); 1.68 (s, $6H_{Me}$); 1.36 (s, $9H_{t\text{-}bu}$); 1.35 (s, $9H_{t\text{-}bu}$) ppm
^{13}C NMR ($CDCl_3$, 75 MHz): δ 167.0; 148.4; 147.7; 147.1; 146.4; 131.5; 129.4; 128.6; 128.5; 125.0; 122.7; 116.5; 115.9; 34.91; 34.86; 34.83; 32.0; 31.7; 31.6 ppm
MS (EI) *m/z* 366 (M, 32%); 352 (M+H – CH_3, 32%); 351 (M – CH_3, 100%)
HRMS calcd for M^+ $C_{24}H_{30}O_3$ 366.2195, found 366.2195

4-Bromo-5-carboxy-2,7-di*tert*-butyl-9,9-dimethylxanthene, 8.19

A suspension of 4-carboxy-2,7-di-*tert*-butyl-9,9-dimethylxanthene 8.18 (0.005 mol, 1.83 g), 30 ml glacial acetic acid, and excess bromine (1.5 ml) was heated so that the bromine was kept mildly refluxing for 6 h. The slurry was poured in aqueous $Na_2S_2O_3$ solution, the precipitate was filtered off, washed with water, and dried.
Yield: 2.14 g (96 %)
^{1}H NMR ($CDCl_3$, 300 MHz): δ 11.0-10.6 (b, $1H_{COOH}$); 8.19 (d, H_{ar}, J=2.4 Hz); 7.67 (d, H_{ar}, J=2.7 Hz); 7.51 (d, H_{ar}, J=2.1 Hz); 7.41 (d, H_{ar}, J=2.1 Hz); 1.67 (s, $6H_{Me}$); 1.36 (s, $9H_{t\text{-}bu}$); 1.34 (s, $9H_{t\text{-}bu}$) ppm
^{13}C NMR ($CDCl_3$, 75 MHz): δ 165.3; 148.9; 147.5; 147.3; 143.8; 131.3; 130.7; 129.4; 128.7; 128.6; 122.7; 116.4; 109.8; 35.4; 35.0; 34.9; 32.2; 31.5; 31.4 ppm
MS (EI) *m/z* 444/446 (M, 7%); 430/432 (M+H – CH_3, 24%); 429/431 (M – CH_3, 100%); 351 (M+H – Br – CH_3, 17%); 350 (M – Br – CH_3, 7%)
HRMS calcd for M^+ $C_{24}H_{29}BrO_3$ 444.1300, found 444.1305

4-Carboxy-5-(N-imidazolo)-2,7-di*tert*-butyl-9,9-dimethylxanthene hydrochloride, 8.20

A 25 ml flask with a stirbar was charged with a mixture of finely ground imidazole (5g), Cu_2O (1g), and 4-bromo-5-carboxy-2,7-di*tert*-butyl-9,9-dimethylxanthene 8.19 (0.002 mol, 0.891 g). [Cu_2O was thoroughly mixed with the ground imidazole in a mortar, then the carboxyxanthene was added and mixed in with a spatula, not by grinding with a pestle.] The flask was flushed with argon and placed in a preheated oil bath at 140-160°C and the mixture was stirred over night. [The flask should be placed in the oil bath while evacuated. This will ensure rapid formation of a liquid film on the walls of the flask. After flushing with argon, a homogenous mixture forms easily.] While still warm, the flask is rinsed out with methanol. 20% aq. HCl was added and the mixture was extracted with

CH_2Cl_2 (3 x 50 ml) Addition of brine facilitated phase separation. The combined organic layers were washed with 20% aq. HCl (3 x 100 ml), dried over $MgSO_4$, and evaporated. The evaporation residue was taken up in PE with a little acetone, stirred briefly, and the supernatant decanted. The PE/acetone wash was repeated once. The remaining colorless or off-white powder was dried under vacuum.

^1H NMR (DMSO-d_6, 300 MHz) δ 9.56 (H_{Im}); 8.09 (t, H_{Im}, J=2.3 Hz); 7.86 (t, H_{Im}, J=2.2 Hz); 7.77-7.75 (m, $2H_{ar}$); 6.61 (d, H_{ar}, J=2.5 Hz); 6.58 (d, H_{ar}, J=1.8 Hz); 1.71 (s, 6H); 1.35 (s, 9H); 1.30 (s, 9H) ppm

^{13}C NMR (DMSO-d_6, 75 MHz) δ 166.4; 146.4; 145.6; 145.4; 140.8; 136.7; 130.9; 130.0; 127.2; 125.8; 125.0; 123.6; 122.2; 122.0; 119.6; 119.4; 34.6; 34.5; 34.2; 32.3; 31.0 ppm

MS (EI) *m/z* 432 (M, 0.6%); 418 (8%); 417 (M – CH_3, 29%); 389 (33%); 388 (M – CO_2, 100%), 374 (13%); 373 (M – CH_3, – CO_2, 48%)

HRMS calcd for M^+ $C_{27}H_{32}N_2O_3$ 432.2413, found 432.2409

4-Phthalimido-2,7-di*tert*-butyl-9,9-dimethylxanthene, 8.21

A mixture of 4-bromo-2,7-di*tert*-butyl-9,9-dimethylxanthene **8.16** (0.01 mol, 4.014 g), phthalimide (0.015 mol, 2.21 g), and Cu_2O (0.03 mol 4.3 g) in 20 ml NMP was heated under argon in a 180°C oil bath over night. After cooling to 100°C the mixture was poured in water, sonicated, and the solids collected by filtration. The crude product was boiled 30 minutes in aq. HNO_3 (4 : 1), filtered off, and dried.

Yield: 4.26 g (91 %)

^1H NMR (300 MHz, $CDCl_3$): δ 7.99 (m, 4H); 7.81 (m, 4H); 7.52 (d, H_{ar}, J=2.1 Hz); 7.38 (d, H_{ar}, J=2.1 Hz); 7.16 (d, H_{ar}, J=2.4 Hz); 7.12 (dd, H_{ar}, J_1=8.7 Hz, J_2=2.4 Hz); 6.75 (d, H_{ar}, J=8.4 Hz); 1.68 (s, $6H_{Me}$); 1.35 (s, $9H_{t\text{-}bu}$); 1.30 (s, $9H_{t\text{-}bu}$) ppm

4-Bromo-5-phthalimido-2,7-di*tert*-butyl-9,9-dimethylxanthene, 8.22

Excess bromine (0.02 mol, 1 ml) was added to a solution of 4-phthalimido-2,7-di*tert*-butyl-9,9-dimethylxanthene **8.21** (0.01 mol, 4.67 g) in 75 ml CH_2Cl_2. After stirring over night, the mixture was poured in aq. $NaHSO_3$ solution and extracted with CH_2Cl_2. The combined organic extracts were dried over $MgSO_4$, evaporated, and purified by flash chromatography (hexanes, 0 → 20% EtOAc). The product war triturated with 30 ml PE 30/50 and dried under vacuum.

Yield: 4.26 g (78 %)

^{1}H NMR ($CDCl_3$, 300 MHz): δ 7.98 (m, 4H); 7.79 (m, 4H); 7.50 (d, H_{ar}, J=2.4 Hz); 7.32 (d, H_{ar}, J=2.4 Hz); 7.31 (d, H_{ar}, J=2.4 Hz); 7.23 (d, H_{ar}, J=2.4 Hz); 1.67 (s, $6H_{Me}$); 1.36 (s, $9H_{t\text{-}bu}$); 1.28 (s, $9H_{t\text{-}bu}$) ppm
^{13}C NMR ($CDCl_3$, 75 MHz): δ 167.6; 147.3; 146.4; 144.7; 144.1; 134.3; 132.7; 131.2; 130.8; 128.4; 125.2; 123.9; 123.8; 122.0; 119.2; 110.4; 35.6; 34.9; 34.8; 32.3; 31.7; 31.6 ppm

4-Amino-5-bromo-2,7-di*tert*-butyl-9,9-dimethylxanthene, 8.23

Excess hydrazine hydrate (10 mmol, 0.5 ml) was added to a solution of 4-bromo-5-phthalimido-2,7-di*tert*-butyl-9,9-dimethylxanthene **8.22** (5 mmol, 2.73 g) in a mixture of 20 ml methanol and 30 ml CH_2Cl_2. After stirring over night the slurry was evaporated to dryness. The residue was suspended with CH_2Cl_2, sonicated, and extracted thoroughly with CH_2Cl_2. The combined extracts were evaporated, the residue rinsed with 10 ml PE 30/50, and dried.
Yield: 2.05 g (99 %)
^{1}H NMR ($CDCl_3$, 300 MHz): δ 7.43 (d, H_{ar}, J=2.4 Hz); 7.34 (d, H_{ar}, J=2.4 Hz); 6.78 (d, H_{ar}, J=2.1 Hz); 6.71(d, H_{ar}, J=2.1 Hz); 4.0 (br, $2H_{NH}$); 1.61 (s, $6H_{Me}$); 1.32 (s, $9H_{t\text{-}bu}$); 1.30 (s, $9H_{t\text{-}bu}$) ppm
^{13}C NMR ($CDCl_3$, 300 MHz): δ 146.8; 146.6; 145.4; 135.7; 134.3; 132.0; 129.7; 128.0; 122.1; 111.7; 111.2; 110.4; 35.6; 34.8; 34.7; 31.9; 31.8; 31.7 ppm
MS (EI) *m/z* 416/418 (M+H, 9%); 415/417 (M, 31%); 401/403 (M+H – CH_3, 30%); 400/402 (M – CH_3, 100%); 321 (M– Br – CH_3, 9%)
HRMS calcd for M^+ $C_{23}H_{30}BrNO$ 415.1511, found 415.1513

4-Amino-5-imidazolo-2,7-di*tert*-butyl-9,9-dimethylxanthene, 8.24

A 10 ml flask with a stirbar was charged with a mixture of finely ground imidazole (3g), Cu_2O (1.0 g, 3 mmol), and 4-amino-5-bromo-2,7-di*tert*-butyl-9,9-dimethylxanthene **8.23** (1 mmol, 0.416 g). The flask was flushed with argon and placed in a preheated oil bath at 140-160°C and the mixture was stirred over night. [The flask should be placed in the oil bath while evacuated. This will ensure rapid formation of a liquid film on the walls of the flask. After flushing with argon, a homogenous mixture forms easily.] While still warm, the flask was rinsed out with methanol. The slurry was sonicated, filtered, and the filter cake was washed first with methanol, then with CH_2Cl_2. The combined filtrate and

wash solutions were evaporated, the residue after evaporation taken up in 20% aq. HCl and sonicated. The slurry was made alkaline by addition of NaOH, and extracted with CH_2Cl_2. The organic extract was dried over $MgSO_4$, filtered through Celite, and evaporated. Purification by flash chromatography (CH_2Cl_2, 0 → 10% MeOH) gave an oil which was solidified by addition of PE 30/50.

Yield: 210 mg (52 %)

^{1}H NMR ($CDCl_3$, 250 MHz): δ 7.84 (s, H_{Im}); 7.47 (d, H_{ar}, J=2.1 Hz); 7.34 (s, H_{Im}); 7.25 (s, H_{Im}); 7.21 (d, H_{ar}, J=2.1 Hz); 6.80 (d, H_{ar}, J=2.0 Hz); 6.66 (d, H_{ar}, J=1.9 Hz); 3.65 (s, $2H_{NH}$); 1.67 (s, $6H_{Me}$); 1.36 (s, $9H_{t\text{-}bu}$); 1.29 (s, $9H_{t\text{-}bu}$) ppm

^{1}H NMR (DMSO-d_6, 300 MHz): δ 8.05 (s, H_{Im}); 7.61 (s, H_{Im}); 7.56 (d, H_{ar}, J=1.8 Hz); 7.32 (d, H_{ar}, J=2.1 Hz); 7.15 (s, H_{Im}); 6.73 (d, H_{ar}, J=2.1 Hz); 6.64 (d, H_{ar}, J=2.1 Hz); 4.45 (s, $2H_{NH}$); 1.63 (s, $6H_{Me}$); 1.34 (s, $9H_{t\text{-}bu}$); 1.24 (s, $9H_{t\text{-}bu}$) ppm

^{13}C NMR ($CDCl_3$, 75 MHz): δ 146.9; 146.3; 142.1; 138.1; 138.0; 135.9; 134.2; 132.2; 129.4; 129.3; 124.9; 122.9; 120.9; 111.7; 111.2; 35.3; 34.9; 34.7; 32.1; 31.72; 31.66 ppm

MS (EI) *m/z* 404 (M + H, 12%); 403 (M, 41%); 389 (30%); 388 (M – CH_3, 100%); 373 (7%); 372 (M – CH_3, – NH_2, 13%)

4,4'-Dinitrodiphenic acid dimethyl ester, 8.09

Diphenic acid **8.08** (0.10 mol, 24.2 g) was carefully added in small portions to a nitration mixture of 70 ml conc. HNO_3 and 70 ml conc. H_2SO_4. After stirring over night. the slurry was poured on 500 ml crushed ice. The precipitate was filtered off, washed with water, and dried on a steam bath. The resulting material was heated to reflux over night in 200 ml methanol with 10 ml conc. H_2SO_4. (Heavy bumping occurred towards the end.) The precipitate was filtered off, washed with methanol, and dried on a steam bath. [Crystals from the filtrate are the 4,6'-dinitro compound.]

Yield: 16.7-17.7 g (46-49 %)

^{1}H NMR ($CDCl_3$, 300 MHz) δ 8.95 (d, $2H_{ar}$, J=1.8 Hz); 8.45 (dd, $2H_{ar}$, J_1=8.8 Hz, J_2=2.5 Hz); 7.38 (d, H_{ar}, J=8.7 Hz); 3.76 (s, $6H_{OMe}$) ppm

^{13}C NMR ($CDCl_3$, 75 MHz) δ 164.8; 148.1; 147.6; 130.9; 130.3; 126.6; 125.6; 52.9 ppm

4,4'-Dinitrodiphenic acid, 8.10

4,4'-Dinitrodiphenic acid dimethyl ester **8.09** (0.01 mol, 3.60 g) and NaOH (1g) in 100 ml THF, 10 ml MeOH, and 10 ml water was heated to reflux over night. The mixture

was acidified with conc. HCl, and concentrated by rotary evaporation. The precipitate was filtered off, washed with water, dissolved in sat. aq. $NaHCO_3$ solution, stirred with charcoal, and filtered through Celite. The filtrate was acidified with 2N aq. HCl, the product collected by filtration, and dried on a steam bath.

Yield: 3.32 g (quantitative)

^{1}H NMR (DMSO-d_6, 300 MHz) δ 13.55-13.30 (b, $2H_{COOH}$); 8.69 (d, $2H_{ar}$, J=3.0 Hz); 8.46 (dd, $2H_{ar}$, J_1=8.3 Hz, J_2=2.6 Hz); 7.55 (d, H_{ar}, J=8.1 Hz) ppm

^{13}C NMR (DMSO-d_6, 75 MHz) δ 165.6; 148.1; 147.0; 131.7; 131.3; 126.1; 124.5 ppm

4,4'-Dinitro diphenic acid diacidchloride, 8.11

A suspension of 4,4'-dinitrodiphenic acid **8.10** (0.01 mol, 3.32 g) and PCl_5 (0.02 mol, 4.2 g) in 50 ml ether was heated to reflux over night. The precipitate was filtered off, washed with PE (30/50), and dried under vacuum.

Yield: 3.17g (86 %)

[CH_2Cl_2 was added to the filtrate and the resulting solution was evaporated. The residue was rinsed with PE several times. The obtained 4,4'-dinitro diphenic anhydride could be converted to the diacidchloride by melting together with two equivalents of PCl_5.]

4,4'-Dinitrobiphenyl-2,2'-bis(ethyl glycinato)dicarboxamide, 8.12

To a vigorously stirred suspension of finely ground ethyl glycinate (6 g) in CH_2Cl_2 (150 ml) was added Et_3N (20 ml) and immediately afterwards a solution of 4,4'-Dinitro-diphenic acid chloride **8.11** (3.10 g, 8.4 mmol) in CH_2Cl_2 (50 ml). The slurry was stirred 1 h, filtered through Celite, extracted with 20% HCl, dried over $MgSO_4$ and evaporated. After column chromatography (silica gel, Hexanes/EtOAc 1:1) the product was obtained in fine, colorless crystals.

Yield: 3.77 g (86 %)

^{1}H-NMR ($CDCl_3$, 300 MHz) δ 8.42 (d, $2H_{ar}$, J=2.7 Hz); 8.31 (dd, $2H_{ar}$, J_1=8.3 Hz, J_2=2.3 Hz); 8.00 (t, $2H_{NH}$, J=5.7 Hz); 7.51 (d, $2H_{ar}$, J=7.8 Hz); 4.26 (dd, 2H, J_1=18.2 Hz, J_2=7.4 Hz); 4.10 (q, $4H_{Et}$, J=7.3 Hz); 3.76 (dd, 2H, J_1=18.0 Hz, J_2=4.2 Hz); 1.21 (t, $6H_{Et}$, J=7.2 Hz) ppm

^{13}C NMR ($CDCl_3$, 75 MHz) δ 170.2; 167.6; 147.6; 143.4; 137.2; 131.3; 124.6; 122.5; 62.0; 41.6; 14.1 ppm

MS *m/z* 502 (M, 2%); 457 (M – OEt, 6%); 400 (M – $NHCH_2CO_2Et$, 17%); 373 (32%); 372 (M – $CONHCH_2CO_2Et$, 100%), 354 (29%); 326 (43%); 298 (37%)
HRMS calcd for M^+ $C_{22}H_{22}N_4O_{10}$ 502.1336, found 502.1337

4,4'-Diaminobiphenyl-2,2'-bis(ethyl glycinato)dicarboxamide dihydrochloride, 8.25

A suspension of 4,4'-dinitrobiphenyl-2,2'-bis(ethyl glycinato)dicarboxamide **8.12** (2.51 g, 0.005 mol) and Pd/C (10 % Pd, 250 mg) in ethanol/benzene (30 ml, 5 ml) was stirred 4 h under H_2 atmosphere (1 atm.). The slurry was filtered through Celite, the filter cake washed with methanol, and the filtrate was evaporated. The residue was dissolved in CH_2Cl_2, and HCl gas was passed through the solution. The semisolid precipitate was repeatedly triturated with small portions of CH_2Cl_2 and acetone until solidification.
Yield: 2.53 g (98 %)
^{1}H-NMR (DMSO-d_6, 300 MHz): δ 8.86 (m, 2H); 7.37 (s, 2H); 7.31 (d, *J*=8.1 Hz, 2H); 7.14 (d, *J*=8.1 Hz, 2H); 4.05 (q, *J*=7.1 Hz, 4H); 3.79 (d, *J*=5.7 Hz, 4H); 1.16 (t, *J*=7.1 Hz, 6H) ppm

Cleft-diethyl ester, 8.27

A solution of freshly prepared 4,4'-diaminobiphenyl-2,2'-bis(ethyl glycinato)dicarboxamide (0.25 mmol, 125 mg) in pyridine (20 ml) was added to 1-(N-imidazolo)-8-chlorocarbonyl-9,9-dimethyl-3,6-di(1,1-dimethylethyl)xanthene **8.26**, freshly prepared from carboxy-imidazolo-xanthene **8.20** (0.60 mmol, 260 mg). [The diamine was prepared by catalytic reduction of the dinitro compound **8.12** on Pd/C in $EtOH/C_6H_6$ in a Parr shaker at 50 psi. The carboxy-imidazolo-xanthene **8.20** was stirred at room temperature in CH_2Cl_2 with excess oxalyl chloride for 3 h, then evaporated to dryness and used without purification.] The mixture was heated to 60°C for 30 min, then stirred at room temperature over night. After evaporation of the solvent, the residue was dissolved in CH_2Cl_2 and washed with 2 N aq. HCl. The organic phase was dried over $MgSO_4$ and evaporated. The product was purified by column chromatography (silica gel; Hexanes/EtOAc 1:1, MeOH gradient 0→10%)
Yield: 176 mg (55 %)
^{1}H NMR ($CDCl_3$, 300 MHz): δ 9.81 (t, *J*=5.4 Hz, $2H_{NH}$); 8.33 (s, $2H_{NH}$); 7.19 (dd, J_1=8.3 Hz, J_2=2.0 Hz, $2H_{ar}$); 8.06 (d *J*=2.4 Hz, $2H_{ar}$); 7.96 (s, $2H_{Im}$); 7.62 (d, *J*=2.4 Hz, $2H_{ar}$); 7.57 (d, *J*=2.1 Hz, $2H_{ar}$); 7.35 (d, *J*=8.1 Hz, $2H_{ar}$); 7.18 (d, *J*=2.4 Hz, $2H_{ar}$); 7.15 (s,

$2H_{Im}$); 6.84 (s, $2H_{Im}$); 6.67 (d, *J*=1.8Hz, $2H_{ar}$); 4.35 (br, 2H); 4.16 (q, *J*=7.1 Hz, 4H); 4.08 (br, 2H); 1.77 (s, 12H); 1.38 (s, 18H); 1.37 (s, 18H); 1.23 (t, *J*=7.2 Hz, 6H) ppm

^{13}C NMR ($CDCl_3$, 75 MHz): δ 170.7; 169.9; 163.4; 158.1; 147.5; 147.2; 145.4; 142.1; 137.7; 136.8; 136.2; 135.7; 131.8; 131.1; 130.6; 130.1; 127.7; 126.6; 125.0; 123.5; 123.0; 122.3; 121.8; 121.1; 119.9; 61.1; 41.7; 35.2; 34.97; 34.95; 32.7; 31.6; 14.4

Notes: 1.) The triplet at 9.81 ppm disappears upon addition of D_2O.

2.) The singlet at 8.33 ppm disappears upon addition of D_2O with a trace of Et_3N and briefly heating the NMR tube.

HRMS calcd for M^+ $C_{76}H_{86}N_8O_{10}$ 1270.6467, found 1270.6485

Cleft-dicarboxylic acid, 8.28

To a solution of cleft-diethyl ester **8.27** (0.2 mmol, 254 mg) in a mixture of THF/MeOH/H_2O (20/3/1 ml) was added 100 mg finely powdered KOH. After stirring at room temperature over night, 20 ml brine and 25 ml water was added. The mixture was acidified with 1N aq. HCl and extracted with 3x30 ml CH_2Cl_2. The combined organic phases were dried over $MgSO_4$ and evaporated. The evaporation residue was purified by column chromatography (silica gel, CH_2Cl_2, 2 → 10 % MeOH).

Yield: 53 mg (22%)

^1H NMR (DMSO-d_6, 300 MHz): δ 10.39 (2H); 8.34 (2H); 8.01 ($2H_{ar}$); 7.79 (2H); 7.69 (H_{ar}); 7.65 (2H); 7.62 ($2H_{ar}$); 7.55 (2H); 7.45 ($2H_{ar}$); 7.37 ($2H_{ar}$); 7.27 (H_{ar}); 7.09 (H_{ar}); 6.50 (2H); 3.57 (4H); 1.74 (12H); 1.33 (36H) ppm

8.5
References

(1) Ibers, J. A.; Holm, R. H. *Science* **1980**, *209*, 223-235.

(2) Wieghardt, K.; Pohl, K.; Gebert, W. *Angew. Chem. Int Ed. Engl.* **1983**, *22*, 727.

(3) Wieghardt, K.; Pohl, K.; Ventur, D. *Angew. Chem. Int. Ed. Engl.* **1985**, *24*, 392-393.

(4) Armstrong, W. H.; Lippard, S. J. *J. Am. Chem. Soc.* **1983**, *105*, 4838-4839.

(5) Armstrong, W. H.; Spool, A.; Papaefthymiou, G. C.; Frankel, R. B.; Lippard, S. J. *J. Am. Chem. Soc.* **1984**, *106*, 3653-3667.

(6) Chaudhury, P.; Wieghardt, K. *Prog. Inorg. Chem.* **1986**, *35*, 329.

(7) Trofimenko, S. *Inorganic Syntheses* **1970**, *XII*, 99-109.

(8) Chaudhuri, P.; Wieghardt, K.; Nuber, B.; Weiss, J. *Angew. Chem. Int. Ed. Engl.* **1985**, *24*, 778-779.

(9) Hartman, J. R.; Rardin, R. L.; Chaudhury, P.; Pohl, K.; Wieghardt, K.; Nuber, B.; Weiss, J.; Papaefthymiou, G. C.; Frankel, R. B.; Lippard, S. J. *J. Am. Chem. Soc.* **1987**, *109*, 7387-7396.

(10) Bossek, U.; Hummel, H.; Weyherüller, T.; Bill, E.; Wieghardt, K. *Angew. Chem. Int. Ed. Engl.* **1995**, *34*, 2642-2645.

(11) Kurtz, D. M., Jr. *Chem. Rev.* **1990**, *90*, 585-606.

(12) Ménage, S.; Brennan, B.; Juarez-Garcia, C.; Münck, E.; Que, L., Jr. *J. Am. Chem. Soc.* **1990**, *112*, 6423-6425.

(13) Hayashi, Y.; Suzuki, M.; Uehara, A.; Mizutani, Y.; Kitagawa, T. *Chem. Lett.* **1992**, 91-94.

(14) Kitajima, N.; Fukui, H.; Moro-oka, Y.; Mizutani, Y.; Kitagawa, T. *J. Am. Chem. Soc.* **1990**, *112*, 6402-6403.

(15) Vincent, J. B.; Huffman, J. C.; Christou, G.; Li, Q.; Nanny, M. A.; Hendrickson, D. N.; Fong, R. H.; Fish, R. H. *J. Am. Chem. Soc.* **1988**, *110*, 6898-6900.

(16) Beer, R. H.; Tolman, W. B.; Bott, S. G.; Lippard, S. J. *Inorg. Chem.* **1989**, *28*, 4557-4559.

(17) Beer, R. H.; Tolman, W. B.; Bott, S. G.; Lippard, S. J. *Inorg. Chem.* **1991**, *30*, 2082-2092.

(18) Watton, S. P.; Masschelein, A.; Rebek, J., Jr.; Lippard, S. J. *J. Am. Chem. Soc.* **1994**, *116*, 5196-5205.

(19) Herold, S.; Pence, L. E.; Lippard, S. J. *J. Am. Chem. Soc.* **1995**, *117*, 6134-6135.

(20) Rebek, J., Jr.; Marshall, L.; Wolak, R.; Parris, K.; Killoran, M.; Askew, B.; Nemeth, D.; Islam, N. *J. Am. Chem. Soc.* **1985**, *107*, 7476-7481.

(21) Marshall, L.; Parris, K.; Rebek, J., Jr.; Luis, S. V.; Burguete, M. I. *J. Am. Chem. Soc.* **1988**, *110*, 5192-5193.

(22) Rebek, J., Jr. *Acc. Chem. Res.* **1990**, *23*, 399-404.

(23) Rebek, J., Jr. *Angew. Chem. Int. Ed. Engl.* **1990**, *29*, 245-255.

(24) Nowick, J. S.; Ballester, P.; Ebmeyer, F.; Rebek, J., Jr. *J. Am. Chem. Soc.* **1990**, *112*, 8902-8906.

(25) Sheriff, S.; Hendrickson, W. A.; Smith, J. L. *J. Mol. Biol.* **1987**, *197*, 273-296.

(26) Mohamadi, F.; Richards, N. G.; Guida, W. C.; Liskamp, R.; Lipton, M.; Caufield, C.; Chang, G.; Hendrickson, T.; Still, W. C. *J. Comput. Chem.* **1990**, *11*, 440-467.

(27) Jenny, T., unpublished results

(28) Cohen, T.; Lewarchik, R. J.; Tarino, J. Z. *J. Am. Chem. Soc.* **1974**, *96*, 7753-7760.

(29) Atkinson, E. R.; Lawler, H. J. *J. Am. Chem. Soc.* **1940**, *62*, 1704-1708.

(30) Atkinson, E. A.; Lawler, H. J. *Organic Syntheses*; Wiley: New York, 1941; Collect. Vol. I, pp 222-225.

(31) Atkinson, E. R.; Murphy, D. M.; Lufkin, J. E. *Organic Syntheses*; Wiley: New York, 1963; Collect. Vol. IV, pp 872-876.

(32) Underwood, H. W., Jr.; Kochmann, E. L. *J. Am. Chem. Soc.* **1924**, *46*, 2069-2078.

(33) Baglogh-Hergovich, É.; Speier, G.; Tyeklár, Z. *Synthesis* **1982**, 731-732.

(34) Fanta, P. E. *Synthesis* **1974**, 9-21.

(35) Fanta, P. E. *Chem. Rev.* **1964**, *64*, 613-632.

(36) Park, T. K.; Feng, Q.; Rebek, J., Jr. *J. Am. Chem. Soc.* **1992**, *114*, 4529-4532.

(37) Ellis, G. P.; Romney-Alexander, T. M. *Chem. Rev.* **1987**, *87*, 779-794.

(38) Autorenkollektiv *Organikum*; VEB Deutscher Verlag der Wissenschaften: Berlin, 1986.

Part III

Appendix

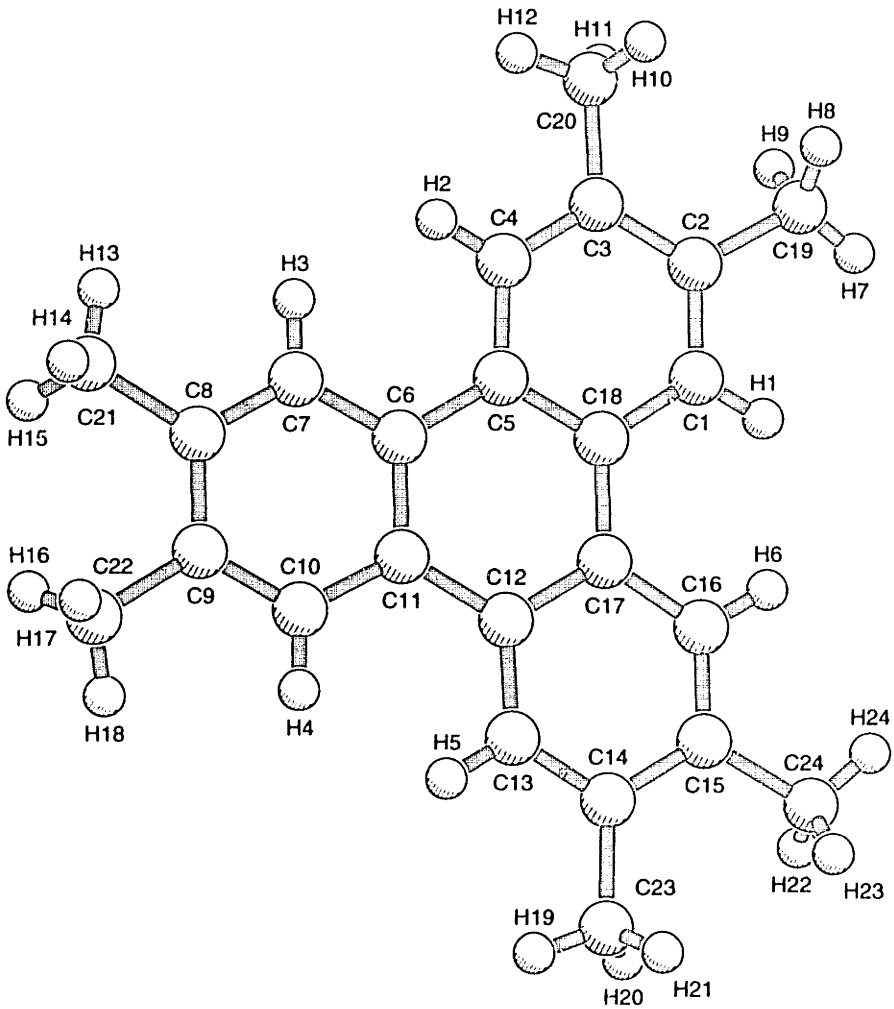
H12
H11
H10
C20
H8
H9
H2
C4
C3
C2
C19
H7
H13
H3
H14
C8
C7
C6
C5
C18
C1
H1
C21
H15
H16
C22
C10
C12
C16
H6
C9
C11
C17
H17
H18
H4
H5
C14
C24
H24
C13
C15
H22
H23
C23
H19
H20
H21

Crystallographic Parameters for 2,3,5,6,10,11-Hexamethyltriphenylene

Empirical Formula	$C_{24}H_{24}$
Formula Weight	312.45
Lattice Parameters	
a (Å)	8.4234(3)
b (Å)	20.7548(7)
c (Å)	10.1586(2)
β (°)	100.317(2)
Volume (Å^3)	1747.27(8)
Crystal Dimensions (mm)	0.4 x 0.3 x 0.2
Space Group	$P2_1/c$ (#14)
Crystal System	monoclinic
Lattice Type	Primitive
Z value	4
D_{calc} (g/cm^3)	1.188
F_{000}	672.00
μ(Mo K_α) (cm^{-1})	0.67
Radiation	Mo K_α (λ = 0.71069 Å)
$2\theta_{max}$	46.5°
Temperature	-66 °C
No. of Reflections Measured	Total: 7120
	Unique: 2582
No. Observations (I > 3.50σ (I), 2.8 > 2θ > 40.2°)	885
No. Variables	241
Residuals: R; R_w [a]	0.050; 0.054

[a] $R = \sum \| |Fo| - |Fc| \| / \sum |Fo|$, $R_w = \sqrt{\left(\sum_{\cdot} (|Fo| - |Fc|)^2 / \sum_{\cdot} Fo^2 \right)}$]

Table 1. Atomic coordinates and $\mathbb{B}_{iso}/\mathbb{B}_{eq}$

atom	x	y	z	$\mathbb{B}_{eq}$
C(1)	0.1773(5)	0.2023(3)	0.4487(4)	4.3(1)
C(2)	0.1670(5)	0.2683(3)	0.4533(4)	4.2(1)
C(3)	0.2608(5)	0.3007(2)	0.5619(5)	3.9(1)
C(4)	0.3574(5)	0.2648(3)	0.6578(4)	4.2(1)
C(5)	0.3686(5)	0.1973(2)	0.6547(4)	3.4(1)
C(6)	0.4713(5)	0.1617(2)	0.7602(4)	3.5(1)
C(7)	0.5674(6)	0.1923(2)	0.8720(5)	4.2(1)
C(8)	0.6667(5)	0.1601(3)	0.9719(4)	4.2(1)
C(9)	0.6735(5)	0.0928(3)	0.9647(4)	4.0(1)
C(10)	0.5818(6)	0.0619(2)	0.8583(5)	4.2(1)
C(11)	0.4792(5)	0.0939(2)	0.7544(4)	3.6(1)
C(12)	0.3808(5)	0.0592(2)	0.6425(4)	3.5(1)
C(13)	0.3804(5)	-0.0080(2)	0.6316(4)	4.0(1)
C(14)	0.2867(5)	-0.0417(2)	0.5304(5)	4.0(1)
C(15)	0.1876(5)	-0.0067(3)	0.4288(4)	3.9(1)
C(16)	0.1893(5)	0.0591(3)	0.4368(4)	4.1(1)
C(17)	0.2821(5)	0.0944(2)	0.5410(4)	3.6(1)
C(18)	0.2751(5)	0.1649(2)	0.5460(4)	3.3(1)
C(19)	0.0569(6)	0.3041(2)	0.3418(5)	5.9(1)
C(20)	0.2589(6)	0.3734(2)	0.5717(5)	5.8(1)
C(21)	0.7642(6)	0.1974(3)	1.0882(4)	6.2(2)
C(22)	0.7860(6)	0.0539(3)	1.0689(4)	6.0(2)
C(23)	0.2931(7)	-0.1145(2)	0.5288(5)	5.9(2)
C(24)	0.0803(6)	-0.0414(2)	0.3148(5)	5.7(1)

Table 1. Atomic coordinates and $\mathbb{B}_{iso}/\mathbb{B}_{eq}$ (continued)

atom	x	y	z	$\mathbb{B}_{eq}$
H(1)	0.112602003	0.179872006	0.375376999	3.8(9)
H(2)	0.417627990	0.287456006	0.730710030	5(1)
H(3)	0.563471973	0.237891003	0.876819015	4(1)
H(4)	0.588944018	0.016084000	0.855856001	2.6(9)
H(5)	0.449613988	-0.031869002	0.699231982	3.4(9)
H(6)	0.121619001	0.081327997	0.365927994	3.6(9)
H(7)	-0.007928000	0.279116988	0.285535008	17(1)
H(8)	0.112424999	0.336358011	0.305586010	9(1)
H(9)	-0.020532001	0.331149012	0.392816991	14(1)
H(10)	0.288560987	0.391698003	0.494563013	10(1)
H(11)	0.156179994	0.387652993	0.582562029	12(1)
H(12)	0.336995006	0.386067003	0.648819983	14(1)
H(13)	0.734149992	0.240143999	1.084903002	11(1)
H(14)	0.877897978	0.193902001	1.080870032	9(1)
H(15)	0.751824021	0.177643999	1.170037985	8(1)
H(16)	0.779459000	0.068882003	1.156149030	9(1)
H(17)	0.895460010	0.059974000	1.054906964	12(1)
H(18)	0.760058999	0.009940000	1.060698032	10(1)
H(19)	0.365972996	-0.129495993	0.604156971	7(1)
H(20)	0.187980995	-0.131174996	0.530547023	9(1)
H(21)	0.326934993	-0.128242001	0.449025989	13(1)
H(22)	-0.000643000	-0.065031998	0.348747998	13(1)
H(23)	0.143857002	-0.070464000	0.273757011	9(1)
H(24)	0.030575000	-0.011030000	0.250916004	14(1)

$$B_{eq} = 8/3\,\pi^2 [\, U_{11}(aa^*)^2 + U_{22}(bb^*)^2 + U_{33}(cc^*)^2 + 2U_{12}aa^*bb^* \cos\gamma + 2U_{13}aa^*cc^* \cos\beta + 2U_{23}bb^*cc^* \cos\alpha \,]$$

Table 2. Anisotropic Displacement Parameters

atom	U_{11}	U_{22}	U_{33}	U_{12}	U_{13}	U_{23}
C(1)	0.048(3)	0.063(4)	0.048(3)	0.002(3)	0.002(3)	0.002(3)
C(2)	0.052(3)	0.054(4)	0.057(4)	0.012(3)	0.017(3)	0.005(3)
C(3)	0.049(3)	0.041(3)	0.061(3)	0.003(3)	0.018(3)	0.000(3)
C(4)	0.050(3)	0.058(4)	0.051(3)	0.001(3)	0.005(3)	0.004(3)
C(5)	0.043(3)	0.043(4)	0.043(3)	0.004(3)	0.008(3)	0.004(3)
C(6)	0.043(3)	0.044(4)	0.048(4)	-0.005(3)	0.010(3)	-0.002(3)
C(7)	0.052(3)	0.050(4)	0.056(3)	-0.001(3)	0.007(3)	0.000(3)
C(8)	0.046(3)	0.062(4)	0.048(3)	-0.003(3)	0.002(3)	0.000(3)
C(9)	0.043(3)	0.064(4)	0.044(3)	-0.004(3)	0.002(3)	0.005(3)
C(10)	0.054(3)	0.047(4)	0.057(3)	0.001(3)	0.007(3)	0.007(3)
C(11)	0.040(3)	0.052(4)	0.042(3)	0.000(3)	0.005(3)	0.006(3)
C(12)	0.039(3)	0.048(4)	0.045(3)	-0.001(3)	0.005(3)	0.005(3)
C(13)	0.053(3)	0.044(4)	0.052(3)	-0.001(3)	0.002(3)	0.007(3)
C(14)	0.050(3)	0.047(3)	0.053(3)	-0.006(3)	0.010(3)	-0.005(3)
C(15)	0.044(3)	0.060(4)	0.043(3)	-0.003(3)	0.006(3)	-0.002(3)
C(16)	0.050(3)	0.055(4)	0.047(3)	0.002(3)	0.003(3)	0.008(3)
C(17)	0.044(3)	0.052(3)	0.042(3)	-0.009(3)	0.008(3)	-0.006(3)
C(18)	0.035(3)	0.049(3)	0.040(3)	-0.002(3)	0.001(2)	-0.001(3)
C(19)	0.077(3)	0.073(4)	0.070(3)	0.017(3)	0.000(3)	0.021(3)
C(20)	0.079(4)	0.047(3)	0.094(4)	0.005(3)	0.016(3)	0.006(3)
C(21)	0.076(5)	0.099(5)	0.054(4)	-0.008(3)	-0.009(3)	-0.012(3)
C(22)	0.070(4)	0.086(5)	0.063(4)	-0.005(3)	-0.015(3)	0.010(3)
C(23)	0.087(4)	0.051(4)	0.086(4)	-0.008(3)	0.015(4)	-0.002(3)
C(24)	0.068(3)	0.073(3)	0.067(3)	-0.012(3)	-0.005(3)	-0.020(3)

The general temperature factor expression:

$$\exp[\, -2\pi^2(a^{*2}U_{11}h^2 + b^{*2}U_{22}k^2 + c^{*2}U_{33}l^2 + 2a^*b^*U_{12}hk + 2a^*c^*U_{13}hl + 2b^*c^*U_{23}kl\,]$$

Table 3. Bond Lengths (Å)

atom	atom	distance	atom	atom	distance
C(1)	C(2)	1.373(5)	C(1)	C(18)	1.403(5)
C(2)	C(3)	1.408(5)	C(2)	C(19)	1.522(5)
C(3)	C(4)	1.373(5)	C(3)	C(20)	1.512(5)
C(4)	C(5)	1.404(5)	C(5)	C(6)	1.452(5)
C(5)	C(18)	1.408(4)	C(6)	C(7)	1.421(5)
C(6)	C(11)	1.411(5)	C(7)	C(8)	1.368(5)
C(8)	C(9)	1.399(5)	C(8)	C(21)	1.523(5)
C(9)	C(10)	1.370(5)	C(9)	C(22)	1.521(5)
C(10)	C(11)	1.405(5)	C(11)	C(12)	1.469(5)
C(12)	C(13)	1.399(5)	C(12)	C(17)	1.408(4)
C(13)	C(14)	1.370(5)	C(14)	C(15)	1.407(5)
C(14)	C(23)	1.512(5)	C(15)	C(16)	1.369(5)
C(15)	C(24)	1.517(4)	C(16)	C(17)	1.404(5)
C(17)	C(18)	1.464(5)			

Table 4. Bond Lengths (Å)

atom	atom	distance	atom	atom	distance
C(1)	H(1)	0.961(4)	C(4)	H(2)	0.944(4)
C(7)	H(3)	0.948(4)	C(10)	H(4)	0.954(4)
C(13)	H(5)	0.956(4)	C(16)	H(6)	0.954(4)
C(19)	H(7)	0.884(5)	C(19)	H(8)	0.930(5)
C(19)	H(9)	1.064(5)	C(20)	H(10)	0.943(5)
C(20)	H(11)	0.940(5)	C(20)	H(12)	0.965(5)
C(21)	H(13)	0.922(6)	C(21)	H(14)	0.977(5)
C(21)	H(15)	0.949(5)	C(22)	H(16)	0.950(5)
C(22)	H(17)	0.966(5)	C(22)	H(18)	0.939(5)
C(23)	H(19)	0.944(5)	C(23)	H(20)	0.954(5)
C(23)	H(21)	0.950(5)	C(24)	H(22)	0.953(5)
C(24)	H(23)	0.951(5)	C(24)	H(24)	0.947(5)

Table 5. Bond Angles (°)

atom	atom	atom	angle	atom	atom	atom	angle
C(2)	C(1)	C(18)	124.2(4)	C(1)	C(2)	C(3)	118.2(4)
C(1)	C(2)	C(19)	119.7(5)	C(3)	C(2)	C(19)	122.1(5)
C(2)	C(3)	C(4)	118.3(4)	C(2)	C(3)	C(20)	121.2(5)
C(4)	C(3)	C(20)	120.5(5)	C(3)	C(4)	C(5)	124.0(4)
C(4)	C(5)	C(6)	121.6(5)	C(4)	C(5)	C(18)	117.7(4)
C(6)	C(5)	C(18)	120.7(5)	C(5)	C(6)	C(7)	122.7(5)
C(5)	C(6)	C(11)	120.2(5)	C(7)	C(6)	C(11)	117.1(4)
C(6)	C(7)	C(8)	124.0(4)	C(7)	C(8)	C(9)	118.3(4)
C(7)	C(8)	C(21)	120.0(5)	C(9)	C(8)	C(21)	121.7(5)
C(8)	C(9)	C(10)	119.0(4)	C(8)	C(9)	C(22)	121.3(5)
C(10)	C(9)	C(22)	119.6(5)	C(9)	C(10)	C(11)	123.8(4)
C(6)	C(11)	C(10)	117.8(4)	C(6)	C(11)	C(12)	119.8(4)
C(10)	C(11)	C(12)	122.5(5)	C(11)	C(12)	C(13)	122.8(5)
C(11)	C(12)	C(17)	119.3(5)	C(13)	C(12)	C(17)	117.8(4)
C(12)	C(13)	C(14)	124.1(4)	C(13)	C(14)	C(15)	118.2(4)
C(13)	C(14)	C(23)	120.1(5)	C(15)	C(14)	C(23)	121.7(5)
C(14)	C(15)	C(16)	118.2(4)	C(14)	C(15)	C(24)	120.6(5)
C(16)	C(15)	C(24)	121.2(5)	C(15)	C(16)	C(17)	124.4(4)
C(12)	C(17)	C(16)	117.2(4)	C(12)	C(17)	C(18)	121.0(5)
C(16)	C(17)	C(18)	121.8(5)	C(1)	C(18)	C(5)	117.6(4)
C(1)	C(18)	C(17)	123.4(5)	C(5)	C(18)	C(17)	119.0(5)

Table 5. Bond Angles (°)

atom	atom	atom	angle	atom	atom	atom	angle
C(2)	C(1)	H(1)	119.1(6)	C(18)	C(1)	H(1)	117.9(6)
C(3)	C(4)	H(2)	118.4(6)	C(5)	C(4)	H(2)	118.0(6)
C(6)	C(7)	H(3)	118.2(6)	C(8)	C(7)	H(3)	118.9(6)
C(9)	C(10)	H(4)	117.7(6)	C(11)	C(10)	H(4)	119.0(6)
C(12)	C(13)	H(5)	118.3(5)	C(14)	C(13)	H(5)	118.1(6)
C(15)	C(16)	H(6)	117.9(5)	C(17)	C(16)	H(6)	118.4(6)
C(2)	C(19)	H(7)	115.0(6)	C(2)	C(19)	H(8)	112.0(6)
C(2)	C(19)	H(9)	104.4(5)	H(7)	C(19)	H(8)	116.9(7)
H(7)	C(19)	H(9)	104.6(6)	H(8)	C(19)	H(9)	101.7(6)
C(3)	C(20)	H(10)	110.0(6)	C(3)	C(20)	H(11)	110.0(6)
C(3)	C(20)	H(12)	108.6(6)	H(10)	C(20)	H(11)	110.9(6)
H(10)	C(20)	H(12)	108.6(6)	H(11)	C(20)	H(12)	108.7(6)
C(8)	C(21)	H(13)	110.9(6)	C(8)	C(21)	H(14)	108.3(5)
C(8)	C(21)	H(15)	109.6(6)	H(13)	C(21)	H(14)	109.1(6)
H(13)	C(21)	H(15)	111.1(7)	H(14)	C(21)	H(15)	107.7(6)
C(9)	C(22)	H(16)	110.2(6)	C(9)	C(22)	H(17)	109.4(5)
C(9)	C(22)	H(18)	110.7(6)	H(16)	C(22)	H(17)	107.9(6)
H(16)	C(22)	H(18)	109.8(6)	H(17)	C(22)	H(18)	108.8(6)
C(14)	C(23)	H(19)	110.1(6)	C(14)	C(23)	H(20)	109.3(6)
C(14)	C(23)	H(21)	109.3(6)	H(19)	C(23)	H(20)	109.5(7)
H(19)	C(23)	H(21)	109.7(7)	H(20)	C(23)	H(21)	108.9(7)
C(15)	C(24)	H(22)	109.6(6)	C(15)	C(24)	H(23)	110.1(6)
C(15)	C(24)	H(24)	109.8(6)	H(22)	C(24)	H(23)	109.2(7)
H(22)	C(24)	H(24)	108.6(6)	H(23)	C(24)	H(24)	109.5(6)

Table 6. Bond Angles (°)

atom	atom	atom	angle	atom	atom	atom	angle
C(2)	C(1)	H(1)	118.6(5)	C(18)	C(1)	H(1)	117.3(5)
C(3)	C(4)	H(2)	116.9(6)	C(5)	C(4)	H(2)	119.1(5)
C(6)	C(7)	H(3)	117.8(6)	C(8)	C(7)	H(3)	118.2(6)
C(9)	C(10)	H(4)	117.3(5)	C(11)	C(10)	H(4)	118.9(6)
C(12)	C(13)	H(5)	117.9(5)	C(14)	C(13)	H(5)	118.0(5)
C(15)	C(16)	H(6)	116.1(5)	C(17)	C(16)	H(6)	119.6(5)
C(2)	C(19)	H(7)	114.8(5)	C(2)	C(19)	H(8)	111.3(5)
C(2)	C(19)	H(9)	103.9(4)	H(7)	C(19)	H(8)	117.5(5)
H(7)	C(19)	H(9)	105.2(5)	H(8)	C(19)	H(9)	102.0(4)
C(3)	C(20)	H(10)	109.8(4)	C(3)	C(20)	H(11)	110.0(4)
C(3)	C(20)	H(12)	108.1(4)	H(10)	C(20)	H(11)	111.0(5)
H(10)	C(20)	H(12)	108.8(5)	H(11)	C(20)	H(12)	109.1(5)
C(8)	C(21)	H(13)	110.8(5)	C(8)	C(21)	H(14)	107.7(4)
C(8)	C(21)	H(15)	109.4(5)	H(13)	C(21)	H(14)	109.5(5)
H(13)	C(21)	H(15)	112.0(5)	H(14)	C(21)	H(15)	107.3(5)
C(9)	C(22)	H(16)	110.1(5)	C(9)	C(22)	H(17)	108.7(4)
C(9)	C(22)	H(18)	110.4(5)	H(16)	C(22)	H(17)	108.1(5)
H(16)	C(22)	H(18)	110.4(5)	H(17)	C(22)	H(18)	109.0(5)
C(14)	C(23)	H(19)	109.9(5)	C(14)	C(23)	H(20)	109.2(4)
C(14)	C(23)	H(21)	109.0(4)	H(19)	C(23)	H(20)	109.6(5)
H(19)	C(23)	H(21)	109.9(5)	H(20)	C(23)	H(21)	109.1(5)
C(15)	C(24)	H(22)	109.5(4)	C(15)	C(24)	H(23)	109.3(4)
C(15)	C(24)	H(24)	109.7(4)	H(22)	C(24)	H(23)	109.2(5)
H(22)	C(24)	H(24)	109.5(5)	H(23)	C(24)	H(24)	109.7(5)

Experimental

A crystal of about 0.4 x 0.3 x 0.2 mm was mounted on a fiber embedded in a matrix of Paraton N. Data were collected at -66 °C on a Siemens CCD diffractometer (equipped with an automated three-circle goniometer and a solid state generator) using graphite-monochromatized Mo-K_α radiation (0.710690 Å) by the ω scan method operating under the program SMART[1]. A total of 15 frames at 30 seconds measured at 0.3° increments of ω at three different values of 2θ and ϕ were collected, and after least squares, a preliminary unit cell was obtained. For data collection, three sets of frames of 30 seconds exposure were collected. Data were collected in three distinct shells. For the first shell, 606 frames were collected with values of $\phi = 0°$ and $\omega = -26°$, for the second shell, 435 were collected with $\phi = 88°$ and $\omega = -21°$ and for the third shell values of $\phi = 180°$ and $\omega = -23°$ were used to collect 230 frames. At the end of data collection the first 50 frames of the first shell were recollected to correct for any crystal decay, but no anomalies were observed. The data were integrated using the program SAINT[2]. The integrated intensities of the three shells were merged into one reflection file. The data were filtered to reject outliers based on the agreement of the intensity of the reflection and the average of the symmetry equivalents to which the reflection belongs. Of a total of 7120 reflections which were collected ($2\theta_{max} = 46.6°$), 2582 were unique ($R_{int} = 0.041$); equivalent reflections were merged.

The space group was determined to be monoclinic $P2_1/c$. The unit cell dimensions were a = 8.4234(3)Å, b = 20.7548(7)Å, c = 10.1586(2)Å, $\beta = 100.317(2)°$, V = 1747.27(8) $Å^3$ with Z = 4. The structure was solved using the direct methods program Sir92 of the TeXsan[3] (version 1.7-1) crystallographic package of Molecular Structure Corporation. The non-hydrogen atoms were refined anisotropically. Hydrogen atoms were included but not refined. The final cycle of full-matrix least-squares refinement was based on 885 reflections ($I > 3\sigma(I)$, $2.8 < 2\theta < 40.2°$) and 241 variables gave a final R = 0.050 ($1/\sigma^2$) and $R_w = 0.054$.

The structure was solved by Dr. Leticia Toledo.

---

1 SMART, V. 4.0; Siemens Industrial Automation, Inc.; Madison, WI, 1994.

2 SAINT, V. 4.0; Siemens Industrial Automation, Inc.; Madison, WI, 1995.

3 TeXsan: Single Crystal Analysis Package, V. 1.7-1; Molecular Structure Corporation; Woodlands, TX, 1995.